Summer 2021

Long-Term Hydrological Impacts of Historical Logging on Recent Hydro-Geomorphic Conditions, Big Barren Creek Watershed, Mark Twain National Forest

Shoukat Ahmed
Missouri State University, Shoukat009@live.missouristate.edu

LONG-TERM HYDROLOGICAL IMPACTS OF HISTORICAL LOGGING ON RECENT HYDRO-GEOMORPHIC CONDITIONS, BIG BARREN CREEK WATERSHED, MARK TWAIN NATIONAL FOREST

A Master's Thesis

Presented to

The Graduate College of

Missouri State University

In Partial Fulfillment

Of the Requirements for the Degree

Master of Science, Geography and Geology

By

Shoukat Ahmed

July 2021

LONG-TERM HYDROLOGICAL IMPACTS OF HISTORICAL LOGGING ON RECENT HYDRO-GEOMORPHIC CONDITIONS, BIG BARREN CREEK WATERSHED, MARK TWAIN NATIONAL FOREST

Geography, Geology, and Planning

Missouri State University, July 2021

Master of Science

Shoukat Ahmed

ABSTRACT

Despite their important role of headwater watersheds as a buffer for upland soil and vegetation disturbances, there has been little research about the effects of historical logging practices on present-day watershed hydrology and channel form. Middle Big Barren Creek (MBBC) watershed (48 km^2) drains Mark Twain National Forest in the Ozark Highlands and was heavily logged from 1880 to 1920, reducing native shortleaf pine forest by 90%. Additionally, the frequency of intense rainfall events has increased in the region over the past 30 years. In this study, field surveys and hydrologic/hydraulic modeling were used to evaluate the historical timber harvesting impacts on hydrology and channel hydraulics along a 4.5 km segment of MBBC. The models were accurately calibrated with actual gage discharge data and water surface elevations yielding a Nash-Sutcliffe coefficient value of 0.85 and $R^2 = 1$. Four different land use/cover scenarios were assessed to understand the history of hydrological alteration with five hydrologic parameters (flow duration, average discharge, runoff depth, peak discharge, and lag time) and three hydraulic parameters (shear stress, stream power, and velocity). Pine forest cover tended to reduce runoff with the present-day peak discharge predicted to be 23% higher than with 100% pine cover, but 3% lower with 100% hardwood forest cover. Change from pine to hardwood forest composition caused reduced canopy interception (-29%) and higher peak flow (+60%) during a modeled early spring rainstorm. Compared to the pre-settlement condition, present-day shear stress (SS) increased among channel types for a bank-full flood as follows: (i) multi-threaded, 29%; (ii) single-channel, 59% and (iii) channelized/leveed 19%. Therefore, the single-channel form probably indicates a geomorphic response to higher runoff rates in these forest streams including coarser substrates. In the study segment, artificial over-widening of the channel resulted in bed aggradation.

KEYWORDS: headwater streams, hydrologic and hydraulic modeling, shortleaf pine forest, historical logging effects, Ozark Highlands

LONG-TERM HYDROLOGICAL IMPACTS OF HISTORICAL LOGGING ON RECENT HYDRO-GEOMORPHIC CONDITIONS, BIG BARREN CREEK WATERSHED, MARK TWAIN NATIONAL FOREST

By

Shoukat Ahmed

A Master's Thesis
Submitted to the Graduate College
Of Missouri State University
In Partial Fulfillment of the Requirements
For the Degree of Master of Science, Geography and Geology

July 2021

Approved:

Robert T. Pavlowsky, PhD, Thesis Committee Chair

Matthew C. Pierson, PhD, Committee Member

Marc R. Owen, MSc, Committee Member

Julie Masterson, Ph.D., Dean of the Graduate College

ACKNOWLEDGEMENTS

I wish to express my sincere gratitude to my advisor Dr. Robert Pavlowsky for his continuous support during my MSc studies and for offering me an opportunity to work as a graduate research assistant at the Ozark Environmental and Water Resources Institute (OEWRI). In addition, his friendly guidance always helped me every time to complete my graduate research in an organizedand concise manner. I also thank my other thesis committee members, Dr. Matthew Pierson and Marc Owen, for their mentoring and technical support to complete my graduate thesis research.

When I first saw Marc's picture on the OEWRI website, I guessed to be an angry man. But my impression changed to 180º when I first met him on 2nd August 2019. I will never forget his support, guidance, friendly attitude, and all the cheerful times we spent during OEWRI field tours as well as in the office. His technical support was indispensable and helped me to complete my thesis analysis on time. I also would like to thank my fellow colleagues in OEWRI including Joshua Hess, Triston Rice, Kayla Coonen, Tyler Pursley, Sierra Casagrand, Michael Ferguson, Brendan Ryan, Teri Arceneaux, Hannah Eades, and Patrick Saulys for their help to complete my field works. I would like to thank the United States Forest Service for the partial funding of my thesis research under the agreement number FS CA# 20-CS 11090500-043. I am also grateful to OEWRI, the Graduate College, Department of Geography, Geology, and Planning for supporting my graduate research, field tour, and conference travel.

Lastly, I am thankful to my parents, sister, and special one Tania Islam, for providing me with continuous mental support to not be afraid of cultural changes and educational challenges while in the USA.

TABLE OF CONTENTS

LIST OF TABLES

LIST OF FIGURES

INTRODUCTION

A forested watershed is an essential component of the ecosystem that provides the basis for good water supply, habitat quality, and forest productivity in most developed and developing countries (Furniss et al., 2010; Sun and Vose, 2016). On a global scale, approximately 50% of the primary terrestrial production comes from forest resources (Bonan, 2008). Every year the tropical and temperate forests around the globe provide ecosystem goods and services that are over 23 trillion dollars (De Groot et al., 2012). In the United States, forested watersheds are essential for maintaining a sustainable freshwater supply (Furniss et al., 2010). For example, forested watersheds provide 60% of the water supply in the Western United States (Brown et al., 2008). In a forested watershed, the stream banks tend to be stable due to the lower runoff volume for a storm event (Brown et al., 2008). In addition, forest cover shades water surface, cycle nutrients, and filter pollutants that increase water quality (Brown et al., 2008). However, soil and vegetation disturbances in forests can cause serious environmental, social, and economic problems by negatively altering the overall hydrology, sediment regime, channel morphology, ecosystem, and forest production (Suryatmojo, 2015).

Forest disturbances can be human-induced (e.g., timber harvesting, road construction, poor soil conservation, and human modification) or climate change-driven (e.g., flood) (Figure 1) (Kochenderfer et al., 1997; Simon and Rinaldi, 2000; Suryatmojo, 2015). To assess the disturbance impacts on watershed hydrology, monitoring channel form, and sediment dynamics, headwater areas are often used since these geomorphic variables are responsive to hydrological disturbances (Figure 2) (MacDonald and Coe, 2007; Shepherd et al., 2010). Headwater streams are the small 1st and 2nd order streams that are more connected to the local factors and hill slope

characteristics than downstream segments and better indicators of watershed disturbances (Gomi et al., 2002; Whiting and Bradley, 1993). In response to the disturbances, channel adjustments occur upstream and downstream, consequently changing the channel morphology, sediment load, and hydraulic geometry of the stream (Simon and Rinaldi, 2000). Being the first source of aquatic life and clean water, headwater streams are a vital part of a forested watershed (MacDonald and Coe, 2007). However, these streams have been ignored from a governing perspective despite their potential downstream effects because they are so small or often unmapped (MacDonald and Coe, 2007; Richardson and Danehy, 2007). Further, it is challenging to evaluate the impact of anthropogenic activities on headwater streams due to the high degree of channel-hillslope complexity and temporal variability of in-channel processing and downstream conditions (MacDonald and Coe, 2007). In addition, the geographic extent of the headwater streams in the US is poorly documented due to mapping limitations and lack of identification in the National Hydrography Dataset (NHD) (Nadeau and Rains, 2007).

(A)

(B)

(C)

(D)

(E)

(F)

Figure 1: Forest disturbances. (A) timber harvesting; (B) logging road; (C) stream channelization; (D) logging railbeds; (E) flooding; (F) road crossing.

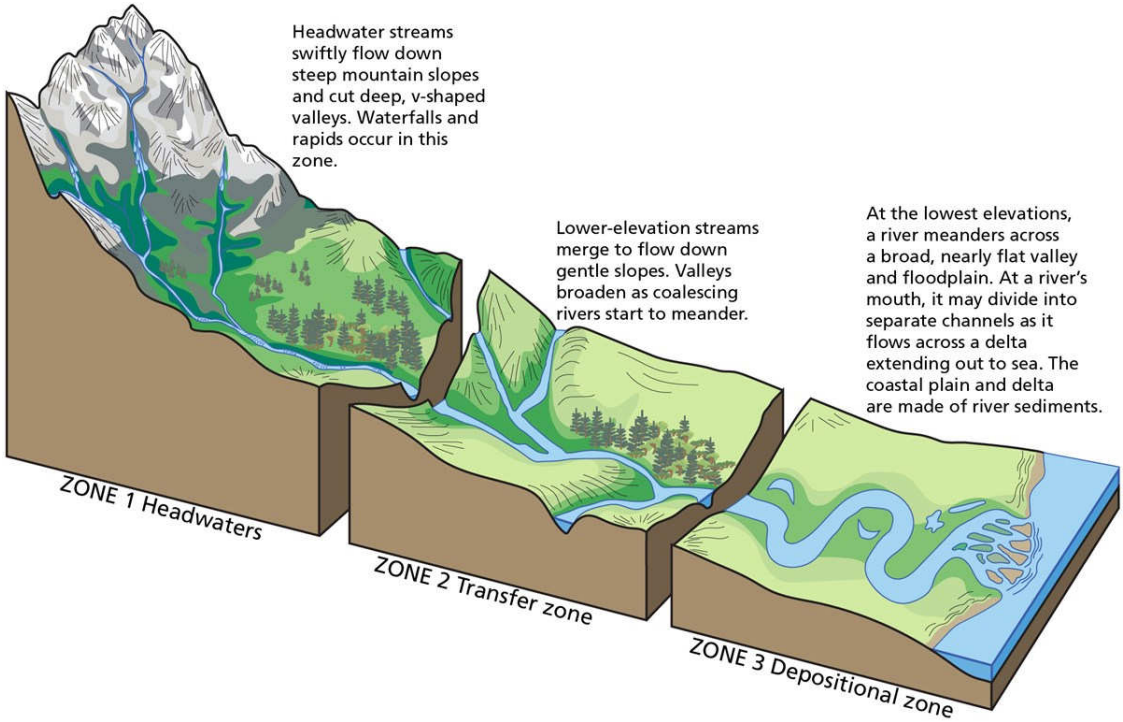

Figure 2. Headwater stream watershed. (Source: https://www.nps.gov/subjects/geology/fluvial-landforms.htm).

Forest Disturbances

Timber harvesting can alter the overall hydrology and forest species composition of a forested watershed (Mao and Cherkauer, 2009). Forest management and clearcutting is a common practice of timber harvesting around the globe that shrank the world's forest cover by 1.3 million square kilometers from 1990 to 2015 and show an increasing trend in the future (World Bank, 2016). It is one of the major human contributors to land-use change in the forested watershed. As a result, it imposes several environmental problems in the watershed by disturbing soil hydraulics, increasing the frequency and magnitude of surface runoff and soil erosion (Jacobson, 1995; Mohr et al., 2013; Restrepo et al., 2015). Typically, the pre and post timber harvesting activities increase the compactness that leads to an increase in surface runoff (Malmer and Grip, 1990; Safeeq et al., 2020). Timber harvesting can adversely affect the hillslope characteristics and processes that eventually affect the hydrology of the headwater streams (Gomi et al., 2002; Jacobson and Primm, 1997). Piest et al. (1976) found that due to the timber harvesting during the European settlement in Western Iowa, the surface runoff and peak flow increased 2-3 times and 10-50 times, respectively, compared to the pre-settlement condition. In northern hardwood forests draining to Hubbard Brook in central New Hampshire, Martin et al. (2000) found that the water yield of the watershed was increased more than 150 mm after the first year of clearcutting. Robles et al. (2014) found a 20% increment in annual runoff in a logged watershed compared to an unlogged forested watershed in a ponderosa pine forest in the southwest US.

Changes in forest species composition can significantly alter watershed hydrology. Mao and Cherkauer (2009) showed that the historical distribution of the forest tree species changed in the upper Midwest due to forest disturbances that ultimately changed the hydrologic balances of this region. The conversion of a deciduous forest to wooded grasslands and row crop in the central Midwest US resulted in a 5-15% decrease in evapotranspiration (ET) and a 10-30% increase in total runoff (Mao and Cherkauer, 2009). Likewise, in the northern Midwest US, the conversion of an evergreen forest to a one dominated by deciduous species resulted in a 20-40% increase in runoff and a 5-10% decrease in evapotranspiration (Mao and Cherkauer, 2009). The impact of timber harvesting on the water yield is unpredictable (Hibbert et al., 1967). However, Bosch and Hewlett (1982) found that a 10% decrease in pine forest type can cause an approximately + 40 mm change in annual water yield. In contrast, a 10% decrease in deciduous and scrub can increase around 25 mm and 10 mm annual water yield, respectively.

Timber harvesting can affect the hydrologic balance of the watershed enough to increase soil erosion and sediment supply to streams. In an undisturbed forest condition, the soil erosion rate is minimal because of having high soil infiltration of precipitation and impediment of generating Hortonian flow process (Hewlett et al., 1977; Leigh, 2016). However, removing forest cover reduces the canopy interception and storage capacity that increase soil erosion and surface runoff rate (Simon and Rinaldi, 2006). In North Fish Creek, Wisconsin, the timber harvesting during the European settlement in the 1870′s followed by extreme agricultural activities in the mid-1920′s to mid-1930′s significantly altered the hydrologic and geomorphic conditions of the watershed (Fitzpatrick et al., 1999). The floodplain and channel sedimentation rates of the North Fish Creek were 4 to 6 times higher than the pre-settlement rate (Fitzpatrick et al., 1999). In addition, modern flood peaks and sedimentation load of North Fish Creek were

twice the pre-settlement forest condition (Fitzpatrick et al., 1999). The dendrochronology study of the Drury Creek watershed, Southern Illinois, showed that the floodplain sedimentation (fine-grained) rate of this creek was 2.11 cm/year during the period 1890 to 1988 due to historical timber harvesting and settlement activities (Miller et al., 1993). Simmons (1993) showed that annually disturbed forest watersheds generate more sediment than the pristine forested watershed in Blue Ridge watersheds. In a natural forested condition, Blue Ridge watersheds caused 13,607 Mg/km^2 suspended sediment annually, whereas, with minor development, these watersheds generate 40.8 kg/km^2 sediment annually (Simmons, 1993). The post-settlement sedimentation rates and alluvium thickness of the seven small tributaries (< $65km^2$) and along the main channel of the upper Little Tennessee River showed a pronounced difference due to historical timber harvesting, land clearing for agriculture, and settlements (Leigh, 2016). The sedimentation rate in the seven tributaries was 2.9 mm/year, whereas, along the main channel, it was 9.4 mm/year (Leigh, 2016). The average post-settlement stratigraphic unit thickness of the small tributaries was 41 cm which found 134 cm along the main channel (Leigh, 2016). Lewis (1998) found that for a logging period between 1971-1973 for South creek and 1989-1992 for North Creek in California, the suspended loads increased by 212 percent in the North Creek and 89 percent in the South Creek compared to the undisturbed year.

Timber harvesting can also negatively alter the stream channel system. Disturbances increase the peak flow, total streamflow, and suspended sediment supply that make the channel unstable (Kochenderfer et al., 1997; Simon and Rinaldi, 2000). Peak discharge increases the unit stream power, channel shear stress, and velocity that increases the bed and bank erosion rate to alter channel form (Andrews and Nankervis, 1995; Magilligan, 1992; Merritt and Wohl, 2003; Ortega and Garzón Heydt, 2009; Simon, 1989; Surian and Cisotto, 2007; Yochum et al., 2017).

In a small headwater stream, Vanacker et al. (2005) found that historical upland forest clearing along the Deleg River in the Ecuadorian Andes caused channel narrowing and deposition of large gravel bars along 28.5 km river segment.

The channel geometry in the loess area of the Midwestern USA showed that logging resulted in a fourfold increase in channel depth and an around fivefold increase in channel width since the middle of the 19th century (Piest et al., 1976). Roberts and Church (1986) suggested that logging activities can trigger stream bank erosion and widen the channel width in the downstream segment. In Pine Creek, Idaho, the channel width increased by 50 m because of historical timber harvesting (Kondolf et al., 2002). A 25 km segment of Upper Middle Fork Willamette River, Oregon, showed that clearcutting and landslides from the forest roads caused the channel form to change from single-channel to a wider, multi-threaded form from 1969 to 1972 (Lyons and Beschta, 1983). However, historical poor land management, timber harvesting, dam construction, and agricultural activities converted the eastern and midwestern USA streams from stable multi-threaded channels to eroded single channels (Cluer and Thorne, 2014; Trimble and Lund, 1982; Walter and Merritts, 2008).

Logging roads can also negatively affect the forested watershed by changing the hydrology and sediment supply (N. S. Bradley, 2017; Carson, 2006; Mao and Cherkauer, 2009; Orndorff, 2017). The construction of logging roads decrease the infiltration rate, increase soil compaction, surface runoff and sediment supply (Reid and Dunne, 1984; Wemple et al., 2001; Sidle and Ochiai, 2006; Orndorff, 2017). Jones and Grant (1996) found that the hydrologic changes due to forest roads depend on the size of the watershed. Logging roads can increase the stream peak flow up to 100% in large watersheds (62-559 km^2) and 50% in small watersheds (< 1 km^2) (Jones and Grant, 1996). However, small watersheds may also respond significantly to

runoff from logging roads by peak streamflow increasing by 500% (Toman, 2004; Wigmosta and Perkins, 2011). In the Alsea Watershed, Harr et al. (1975) found that logging roads can increase the stream peak discharge by 30 percent if the road coverage is 12 percent of the whole watershed area. In Missouri, around 90 percent of soil erosion from timber harvesting comes from the gravel bed or paved haul roads system (MDC, 2020). In the Ouachita Mountains of Arkansas, nearly 70 percent of the total sediment supply comes from the logging roads during forest operation (Miller et al., 1985; Orndorff, 2017).

The channel morphology of a forest stream is also affected by the low water bridge and logging rail beds (Jones, 2000; Magilligan, 1992; Winterbottom, 2000). Sediment trapping along the logging rail bed can change the multi-threaded channel to a single-channel form (Gilvear and Winterbottom, 1992; Winterbottom, 2000). Rail bed embankments can cause channel incision by concentrating flow that was not present before (Florsheim et al., 2001). This incision can sometimes become extensive that can cause a series of head-cut and channel deepening and widening (Florsheim et al., 2001). Logging rail beds crossing any stream can constrict the channel flow and eventually affect the hydraulic geometry, shear stress, and velocity that affect the channel morphology and aquatic species (Krause, 2010). A low water bridge can also influence the local channel morphology by elevating the bed level and incision or scour downstream (Owen et al., 2018). Water flow is slowed upstream of a bridge that brings a drastic change in water surface elevation, and downstream expansion of the flow produces changes in velocity and stream power that can cause geomorphic changes (Krause, 2010).

Stream channelization or modification is a common practice by the private landowners or engineers to reduce the flood magnitude and frequency and control streambanks erosion (Simon and Rinaldi, 2006). In this process, the natural streams are modified by straightening, deepening,

and raising the bank height with levee construction (Brookes et al., 1983; Heine and Pinter, 2011). Improper design and channel modification adversely affect upstream hydrology and flood plain, physical damages to the channel geometry, and downstream flooding effects (Nunnally and Keller, 1979). At present, channel modification is one of the biggest threats to headwater stability (Elmore and Kaushal, 2008). Hupp and Bazemore (1993) found that channelization of the stream increases the velocity and turbulence that accelerates downstream sand deposition. Flood water can quickly pass through a channelized segment. However, having a low channel capacity, flooding occurs in the downstream portion of a stream (Nunnally and Keller, 1979). The construction of levee is another factor that adversely affects watershed hydrology (Tobin, 1995). Levees help to pass the flood water through a channel that restricts the floodwater from entering the flood plain, increasing the flood stage upstream and conveying the flood to the downstream (Tobin, 1995). The construction of the levee intensely changes the streamflow and sediment dynamics by reducing the connectivity between the stream and floodplain (Hupp et al., 2009).

Climate change is one of the natural factors that can change watershed hydrology. Climate change can directly alter the stream discharge and water budget by changing precipitation patterns (Hu et al., 2005). Historical rainfall trends in the Midwestern United States show that from the 1800′s to 1930′s, there was a decreasing precipitation trend; however, an increasing trend was observed until the present day (Groisman and Easterling, 1994; Winkler et al., 2014). Over the last century, extreme precipitation-induced flooding has increased in the Midwest region due to climate change, causing more stream erosion (Pryor et al., 2014a). The historical seasonal precipitation trend of the Midwest US shows that during the period 1890 to 2010, the maximum increase in precipitation occurred during spring, summer, and fall seasons

(Andresen et al., 2012; Pryor et al., 2014b; Winkler et al., 2014). However, most recent data exhibit a larger increase in winter precipitation in this region, with an annual average of 0.039 inches (Winkler et al., 2014). Overall, the precipitation throughout the Midwest increased 10% to 30% during the 21st century, increasing precipitation frequency and intensity (Easterling and Karl, 2000). This increasing precipitation can profoundly increase the peak discharge of the stream with an increase in soil loss and runoff (Easterling and Karl, 2000; O'Neal et al., 2005). Thus, considering climate change and increasing precipitation patterns, the forest area might be more vulnerable to hydrological disturbances in the future.

Modeling Approach to Forest Hydrology

The after-effects of forest disturbances on watershed hydrology can be analyzed effectively by using a spatially distributed rainfall-runoff-based hydrologic modeling approach (Hu and Shrestha, 2020; Storck et al., 1998). Hydrologic modeling of a watershed calculates the peak discharge and flow duration that are important to study flooding impact, stream instability, and stream ecology (McEnroe, 2010). On the other hand, by assessing different hydraulic parameters such as channel shear stress, hydraulic radius, velocity, water surface elevation, and stream power, hydraulic modeling technique can be used to quantify channel's geomorphic changes for different hydrologic settings (Abdelkarim et al., 2019; Johnson, 2015; Krause, 2010). The Hydrologic Engineering Center Hydrologic Modeling System (HEC-HMS) and HEC-RAS (River Analysis System) are two widely accepted hydrologic and hydraulic models that can be used for analyzing the flooding sedimentation and channel pattern changes due to historical land-cover changes (Carson, 2006; Dasanto et al., 2014; Fitzpatrick et al., 1999; Harvel, 2015; Krause, 2010; Storck et al., 1998), flood forecasting (Bhuiyan et al., 2017), and

post-fire analysis (Cydzik and Hogue, 2009). The earlier version of HEC-HMS was HEC-1 which has been regularly updated and is used for different watershed assessment-related research such as flood warning, stream restoration, stream discharge, and flood frequency analysis (James, 2020). On the other hand, HEC-RAS is the newest version of the early HEC-2 model that is now extensively being used for river hydraulics related analysis (FEMA, 2002)

Several studies have analyzed the historical forest destruction impact on forest hydrology using HEC-HMS or HEC-1 hydrologic modeling technique. North Fish Creek, Wisconsin, is one of the creeks that responded noticeably to the human disturbance since European settlement in the 1870′s (Fitzpatrick et al., 1999). Fitzpatrick et al. (1999) analyzed three land cover scenarios: pre-settlement condition with full forest cover, peak disturbance (agriculture), and current state in HEC-2 and HEC-1. The hydrologic and sediment transport modeling results demonstrated that recent flood peaks and sedimentation load in North Fish Creek are almost double compared to the pre-settlement forest cover (Fitzpatrick et al., 1999). The HEC-1 rainfall-runoff simulation showed that near the gaging station, the 2-year flood peak under the peak agricultural disturbance was three times higher than the pre-settlement forest condition. In contrast, in the present time, it was two times higher (Fitzpatrick et al., 1999). In addition, they assumed that flood peaks under the full forest cover could be smaller than the modeled discharge because of not accounting the decrease of the thickness of organic detritus layers on the forest ground after logging and burning in the modeling process (Fitzpatrick et al., 1999).

Geomorphic investigation and HEC-2 simulation showed that the North Fish Creek Basin faced 2.5 times more sediment load under peak disturbance than the modern land cover, which became five times greater than the pre-settlement condition (Fitzpatrick et al., 1999). The impact of timber harvesting on peak discharge and surface runoff was also analyzed by Sterling

and Schoenfelder (2010) using HEC-HMS single storm event simulation. Timber harvesting decreased the canopy interception rate, which increased peak discharge rates by about 30% in a forested watershed in Washington state (Sterling and Schoenfelder, 2010). Sterling and Schoenfelder (2010) also found that timber harvesting reduced the runoff generation by 3 hours compared to the unharvested condition. A similar type of study was also done by Magilligan and Stamp (1997) using the HEC-1 modeling technique at the Turner Creek watershed, Georgia. Due to the conversion of combined softwood and hardwood forest to cotton production land, the 2-year flood peak discharge increased more than two times. However, forest recovery already started to reduce runoff rates by 1937 (Magilligan and Stamp, 1997).

Field survey, geospatial analysis, and HEC-RAS hydraulic modeling techniques were adopted by Krause (2010) to evaluate the change from a hardwood and savanna forest to agriculture with channelized streams and railroad beds. A cross-section survey was conducted at twelve locations to get the current day channel geometry and run a present-day simulation (Krause, 2010). Later, several modifications such as widening the channel, increasing and dropping the bed elevation, and changing manning's n were performed to mimic the pre-settlement channel condition (Krause, 2010). The change in peak discharges due to the forest disturbances was represented using the PeakFQ analyzed flood recurrence intervals discharges (Krause, 2010). The 1-D steady-state HEC-RAS simulation of this watershed showed that the hydraulic radius, stream power, channel velocity, and water surface elevation differed considerably between the pre-settlement and current conditions (Krause, 2010). Modern-day shear stress was five to seven-time higher than the pre-settlement condition at some cross-sections closed to a bridge (Krause, 2010).

In response to large-scale timber harvesting and channelization, lateral connectivity between the channel and floodplain may change over time (Beck et al., 2019). Using 1-D steady-state HEC-RAS simulation, Beck et al. (2019) showed that due to historical channelization and increased channel cross-sectional area, the floodplain-channel connection has decreased in the present days. In addition, the threshold discharge for crossing the bank and entering the flood plain has increased by 15% from 1998 to 2014 because of channelization (Beck et al., 2019). Due to this increase in discharge threshold and channel cross-sectional area, the volume of the water during a storm event is confined within the channel that increases the stream power, and accelerates future channel bed and bank erosion (Beck et al., 2019). In Lower Minnesota, decreasing channel and floodplain connectivity and reduce woody riparian vegetation, the river has widened by 52% and shortened by 7% from 1938 to 2009 (Lenhart et al., 2013).

Forest Disturbance Histories in the Ozarks

The Ozark Highlands covers an area of 124,000 km^2, including northern Arkansas, Southeastern Kansas, Southern Missouri, and Northeastern Oklahoma (Davis et al., 1996; Dempsey, 2012). Geologically the Ozarks region is composed mainly of limestone and dolomite containing karst features such as sinkhole, losing, and stream-fed steams (Davis et al., 1996; Krause, 2010; Martin and Pavlowsky, 2011; MDC, 2020). The Euro-American settlement, generally beginning in the mid-1800s, was followed by various anthropogenic disturbances such as timber harvesting, logging rail bed/roads, channel modification, gravel mining, levee construction, and agricultural activities (Figure 3). Due to these disturbances, Ozarks forests and streams have undergone significant hydrological and geomorphic changes (Brown et al., 1998; Jacobson, 1995; Jacobson and Primm, 1997; Owen et al., 2011). In general, the disturbance

scenarios of the Ozarks can be divided into three parts: (a) before the 1880′s there were some rural settlements; (b) timber boom period from 1880 to 1920′s; and (c) a peak agricultural period from 1940 to early 1950′s (Jacobson, 1995).

Historical timber harvesting and settlement activities have changed the forest species composition of the Missouri Ozarks. In the Euro-American settlement period, shortleaf pine harvesting was only occurring in the North Fork, Gasconade, and Osage River valleys to support timber to the small village and railroad ties (Jacobson and Primm, 1997; Sauer, 1920; Hawker, 1992). Prior to 1880, no massive burning, timber harvesting, crops, and grazing were reported that contributed to the upland erosion in the Ozarks (Jacobson and Primm, 1997). However, this scenario significantly changed during the timber harvesting boom period 1880-1920′s (Jacobson and Primm, 1997). Shortleaf pine tree logging was so pervasive that the landscape changed from the shortleaf pine-dominated (covered around 6.6 million acres) forest to scrub oak and other hardwood forests (Jacobson and Primm, 1997). There were 26709 km^2 of pine at the time of settlement, but around 1700 km^2 remains today (Anderson et al., 2004; Cunningham, 2007).

During the transition of pre-settlement to the early-settlement period (around 1860-70s), Ozarks streams began to respond by incision and widening as riparian areas were cleared, cultivated, or grazed (Jacobson and Primm, 1997). In the post-timber boom period (1920′s), agricultural activities were widespread in the Ozarks region (Jacobson and Primm, 1997). These agricultural activities significantly increased the annual runoff, storm runoff, increased soil erosion producing long-lasting effects on the forest floor and probably nearby headwater streams (Jacobson and Primm, 1997). Annual burning grassland management, grazing, and plowing decreased the lag time, flow duration, and recession time of the hydrograph and generated higher peak discharge for a moderate frequency event (Jacobson and Primm, 1997). During the peak

disturbance period, peak discharge can be five times greater than the pre-settlement peak discharge (Knox, 1977). From the post-timber harvesting to the recent period (around the 1960s), land conversion practices were initiated and managed federal and state government-controlled land. However, some intense logging, agriculture, and grazing practices were still present in private lands (Jacobson and Primm, 1997). However, due to the overall decrease in croplands in the region, the bottomland erosional rate began to decrease after the 1950s (Jacobson and Primm, 1997).

Historically, alluvial streams in the Ozarks were subjected to different geomorphic disturbances such a bank erosion, channel aggradation, channel widening, incision, headcut migration, bed aggradation, and changes in channel pattern (Jacobson, 1995; Jacobson and Primm, 1997; Owen et al., 2011). Destruction of the riparian vegetation promoted the expansion of the first and second-order streams of the Ozarks (Jacobson and Primm, 1997). The morphology of the headwater streams in the Ozarks has high spatial variation, different geographic extent, and varied parameters for analysis (Shepherd et al., 2010). Remnants of logging tram are still be found in the headwater drainages of the Ozarks and were a source of stream disturbance (N. S. Bradley, 2017; Guyette and Larsen, 2000). Presence of confined and forced reaches of the Tram Hollow watershed that are directly related to the tram bed disturbances (N. S. Bradley, 2017). Channel instability caused by increased flood peaks or valley confinement often resulted in bed incision and the coarsening of bed substrates (N. S. Bradley, 2017; Montgomery and Buffington, 1993). Ozarks headwater streams have experienced excessive gravel aggradation in downstream of the main channels as a result of chert gravel erosion (Jacobson and Primm, 1997; Jacobson and Pugh, 1998). Despite the historical disturbances and impact on headwater streams in the Ozarks, the hydrological implications of

historical logging have not yet been evaluated, and the effects on headwater stream discharge and hydraulics are unclear (Kleekamp, 2016).

(A)

(B)

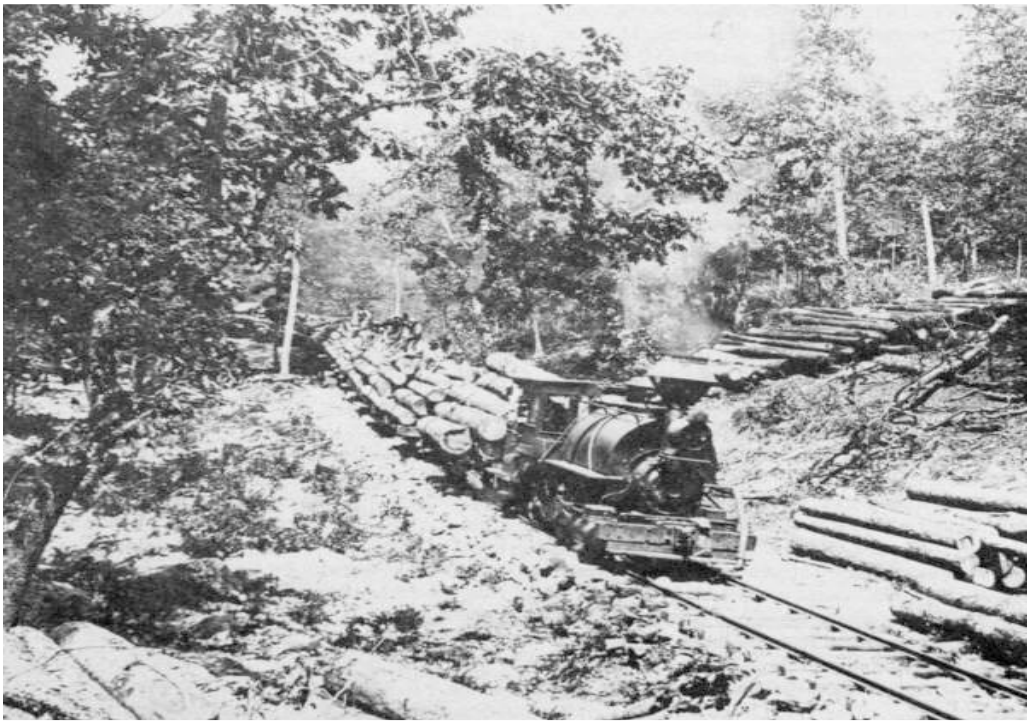

(C)

Figure 3. Logging history. (A) logging camps (1990); (B) logging railroad (1907); (C) pine logs at the mill (1900). (Source: https://www.nps.gov/parkhistory/online_books/ozar/hrs6a.htm)

Purpose and Objectives

Headwater streams are the vital part of a watershed that connects the upland hydrology to the channel system and convey the impacts of soil and vegetation disturbances downstream (MacDonald and Coe, 2007). However, in the Ozarks Highland, most channel disturbance studies have focused on the larger alluvial channels downstream, with few studies of smaller headwater streams (Kleekamp, 2016; Nickolotsky, 2005; Shepherd et al., 2010; Thies, 2017).

Despite their high importance, headwater streams have been neglected in many stream's sampling protocols, and there is a gap in knowledge regarding the effect of land disturbance on headwater streams in the Ozarks and their link to downstream main channel processes (Kleekamp, 2016).

Big Barren Creek watershed (191 km^2) is a headwater stream in the Ozarks Highlands and tributary of the Current River. The Current River and its adjacent lands are an important location to preserve Missouri's free-flowing streams, springs and caves, wildlife management, and outdoor recreation place that were designated as the Ozarks National Scenic Riverways in 1974 (Barks, 1978). Historically and in the present time, the BBC watershed has been affected by disturbances including historical logging, channel modifications, riparian forest clearing, gravel mining, road constructions, stream crossings, and land-use changes (N. Bradley, 2017; Owen et al., 2018; Thies, 2017). These disturbances have caused channel instability in BBC, such as channel enlargement, bed incision and head-cuts, excessive sedimentation and aggradation, and more variable and coarser bed substrate (Owen et al., 2018; Thies, 2017). In response to the historical disturbances, BBC has undergone a transition from form in many main channels and tributary segments (Reminga, 2019). In addition, bed elevations have risen above road crossings by aggradation and dropped through incision and head-cutting below them driven by local increases in bed slope (Owen et al., 2018). Hydrologic obstructions created by logging tram beds on valley floors built over 120 years ago have caused the progressive straightening and incision of stream systems (N. S. Bradley, 2017). Moreover, recent increases in rainfall intensity and flooding in BBC has increased the geomorphic activity in various locations throughout the drainage network (Pavlowsky et al., 2016; Thies, 2017).

Considering the historical impacts of land use and climate change on watershed and channel hydrology in the BBC, this study aims to use a modeling approach to assess historical hydrological changes in the BBC watershed to better understand the key factors influencing the present-day watershed and channel system. Field measurements and numerical modeling techniques have been used to assess hydrological variables and trends. Further, changes in channel form result from human disturbance and hydrological response to land-use changes are also evaluated. Importantly, hydrologic simulations have been calibrated using continuous discharge measurements from the gage network installed in 2016. The main objectives of this study are:

a) Hydrologic analysis was completed for four land-use scenarios reflecting the sequence of human disturbance and forest management: pre-settlement, post disturbances, and present condition. Five hydrologic parameters were estimated for a modern-day bankfull flood at several sites: flow duration, average discharge, runoff depth, peak discharge, and lag time.
b) The simulated peak discharges of the four HEC-HMS scenarios were used in a 1D HEC-RAS model to analyze the hydraulic impact on a channel segment in the lower portion of the watershed. Three important hydraulic parameters were estimated to evaluate the channel responses, such as channel velocity, shear stress, and stream power.
c) Simulated hydraulic parameters were compared to the channel substrate to develop shear stress and substrate relationships for different channel forms, for example, multi-threaded, single-channel, and channelized.

Benefits of the Study

This study will provide important insights to better understand the history of channel evolution and hydrologic factors affecting the BBC. A limited number of studies have been done to analyze the historical land-use change impact on the Big Barren Creek watershed. Previously, using aerial photographs and field observations, Bradley (2017) documented the influence of channelization on the channel system. Reminga (2019) analyzed the flood plain sediment trends in BBC. Guyette et al. (2007) evaluated the reduction of shortleaf pine forest in the Missouri Ozarks but overlooked the impact of this change on hydrology. Hu et al. (2005) addressed the land-use and climate change impact on the stream discharge from the Jack Fork River basin. Jacobson (2004, 1995) and Jacobson and Primm (1997) analyzed the land use and climate change impacts and downstream trend of disturbances on a basin-scale but did not directly study headwater streams. The spatial pattern of channel instability of the Little Piney Creek watershed was related to the distribution and disturbance of riparian vegetation (Jacobson and Pugh, 1998). However, little is known about the impacts of the historical timber harvesting and conversion of pine-dominated forest to an oak-dominated forest on the hydrology of the Big Barren Creek watershed and its subsequent effects on channel form. This study is the first to assess the hydrological impact of historical logging on headwater stream hydrology in the Ozarks. In addition, changes in the hydrological processes will be linked to the possible channel changes and disturbing channels.

STUDY AREA

This study focuses on understanding the hydrology and channel morphology of the headwater and middle portions of BBC with a drainage area of 48 km^2. The study area includes ten other small sub-basins with varying watershed areas (Figure 4). Streamflow gaging sites used to calibrate the HEC-HMS model for this study include the following: Upper Big Tributary (UBT), 4.18 km^2; Tram Hollow (TH), 1.59 km^2; Upper Big Barren (UBB), 2.51 km^2; Wolf Pond (WP), 5.12 km^2; Polecat (PC), 6.19 km^2; and Middle Big Barren Creek (MBBC), 48 km^2. The factors for selecting MBBC watershed for this study were: (1) availability of hydrologic monitoring data; (2) variety of channel types in one several km segments; and (3) previous research indicated changes in land use, runoff, and sediment load might have affected the channel form and processes.

In this study, using the MBBC gage as an outlet, around 48 km^2 watershed was generated using the HEC-HMS 4.4 tool, and this watershed boundary was then used for hydrologic simulation to reflect different land-use scenarios (Figure 5). In addition, a 4.5 km channel segment was selected for steady-state hydraulic simulation in the 1D HEC-RAS model (Figure 5). This segment was selected because it contained different types of channel forms, including multi-threaded, single-channel, stream crossing, incision, headcut, and channelized. Thus, this segment will be useful to evaluate the hydraulic channel responses for different channel types.

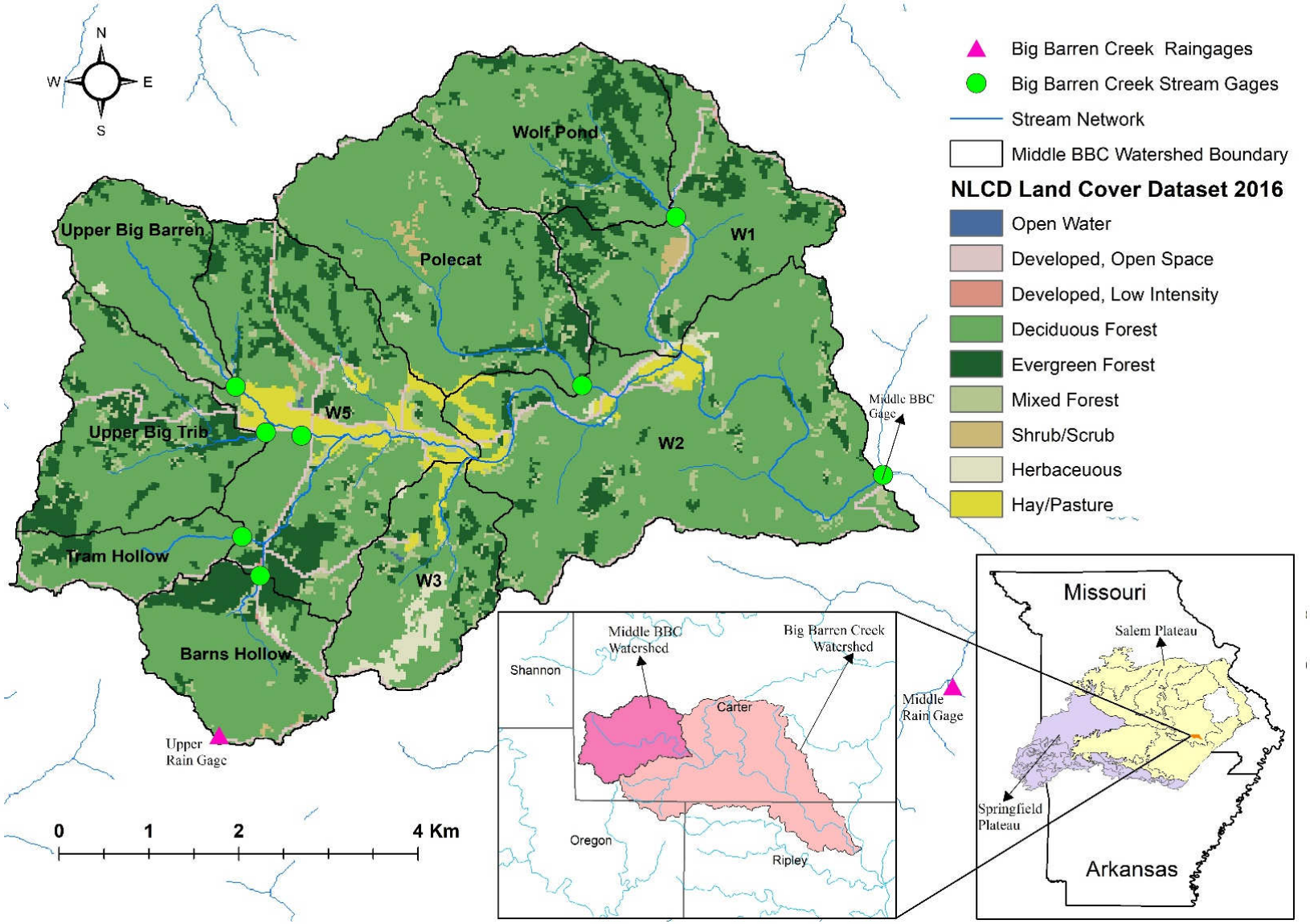

Figure 4. Land-use and location map of Middle BBC watershed.

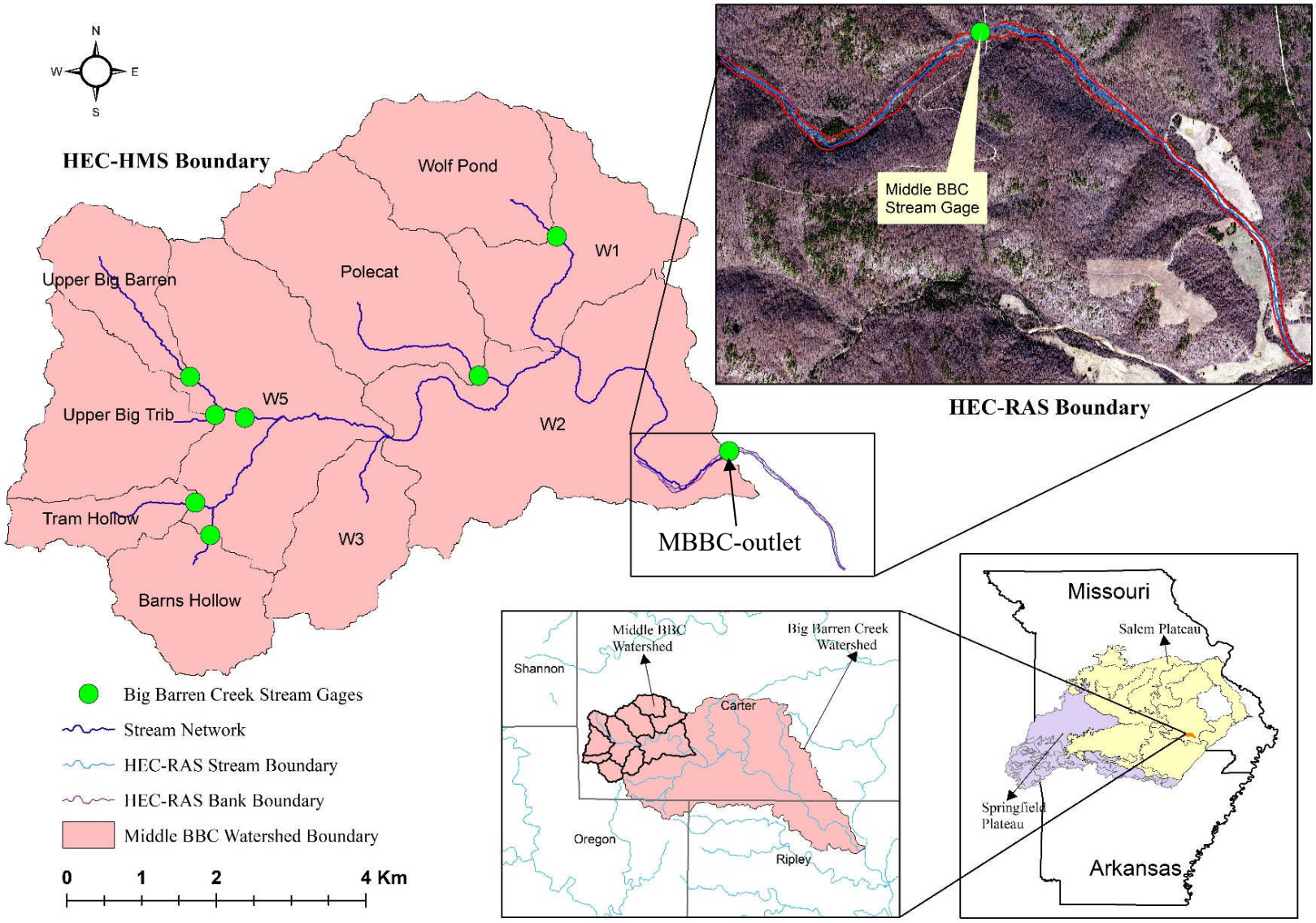

Figure 5. HEC-HMS and HEC-RAS model boundary of the study area

Geology and Soils

The MBBC watershed is underlain by Lower Ordovician-age starta that includes Gasconade Dolomite, Roubidoux Formation, and Jefferson City Dolomite (Weary et al., 2014) (Figure 6). The Gasconade Dolomite has a maximum exposed thickness of around 85 m and consists of dolomite, chert, sandstone, and orthoquartzite (Weary et al., 2014). The Jefferson City Dolomite is composed of dolomite, quartz, sandstone, and chert (Weary et al., 2014). The average thickness of Jefferson City Dolomite is 122 m (Weary et al., 2014). The Roubidoux Formation has a maximum thickness of 76 m and is composed of sandstone, orthoquartzite, cherty dolomite, and sandy dolomite (Weary et al., 2014; Weary and Schindler, 2004). This formation is considered the most extensive surface rock in the central Ozarks (Fletcher and McDermott, 1957). The Wilderness-Handy fault zone that passes through MBBC has a significant influence on the groundwater flow of this area (Weary et al., 2014) (Figure 6). There are 15 mapped sinkholes in this watershed, mainly in the Roubidoux Formation and Jefferson City Dolomite (Weary et al., 2014). The formation of these sinkholes is due to the dissolution of dolostone (Weary et al., 2014).

There are 28 soil series in the watershed (Figure 7). The Macedonia silt loam covers the largest area (18% of the watershed), occupying uplands covered by a thin layer of Pleistocene glacial loss overlying cherty dolomite residuum (Gott, 1975). The surface soil contains 0 – 15% Chert fragments (Gott, 1975). This soil is very important for the production of timber, hay, and pasture having medium surface runoff (Gott, 1975). The Clarksville very gravelly silt loam soil (15 to 35% slope) occupies around 12% of the watershed and covers 25 – 50% chert fragmentation (Gott, 1975). This site is also good for timber production and medium surface runoff; however, droughtiness, steepness, and high chert content limits productivity (Gott, 1975).

Coulstone very gravelly sandy loam (8 to 15 percent slopes) covers around 18% of the watershed and locates on the side slope of the watershed (Gott, 1975). Midco very gravelly loam soil occurs as excessively drained soil on narrow flood plains and is frequently flooded (Gott, 1975). The sandstone residuum over the Roubidoux formation was the most important factor associated with the extent of shortleaf pine during the pre-settlement condition (Fletcher and McDermott, 1957; Voelker, 2004). The soils of this formation contain higher sand content and low insoluble calcium and magnesium cations that increased the abundance of shortleaf pine in the pre-settlement condition (Voelker, 2004).

Climate and Hydrology

The study area occupies a temperate climate with an average mean temperature of 15^0C (Adamski et al., 1995). Annual high temperatures occur in July, and low yearly temperatures occur in January (Adamski et al., 1995). Precipitation patterns are influenced by moist air masses that originate in the Gulf of Mexico in the spring (Adamski et al., 1995). The southern region of the Ozark Plateau averages 120 cm of rainfall annually (Adamski et al., 1995). An increasing intense rainfall trend has affected the BBC watershed (Pavlowsky et al., 2016). High-intensity rainfall events (> 7.5 cm/day) only occurred six times from 1955 to 2005 (50 years) but occurred ten days from 2005 to 2015 (Pavlowsky et al., 2016). This increasing precipitation trend has increased flood frequency in the streams and increased channel erosion and instability in BBC (N. S. Bradley, 2017).

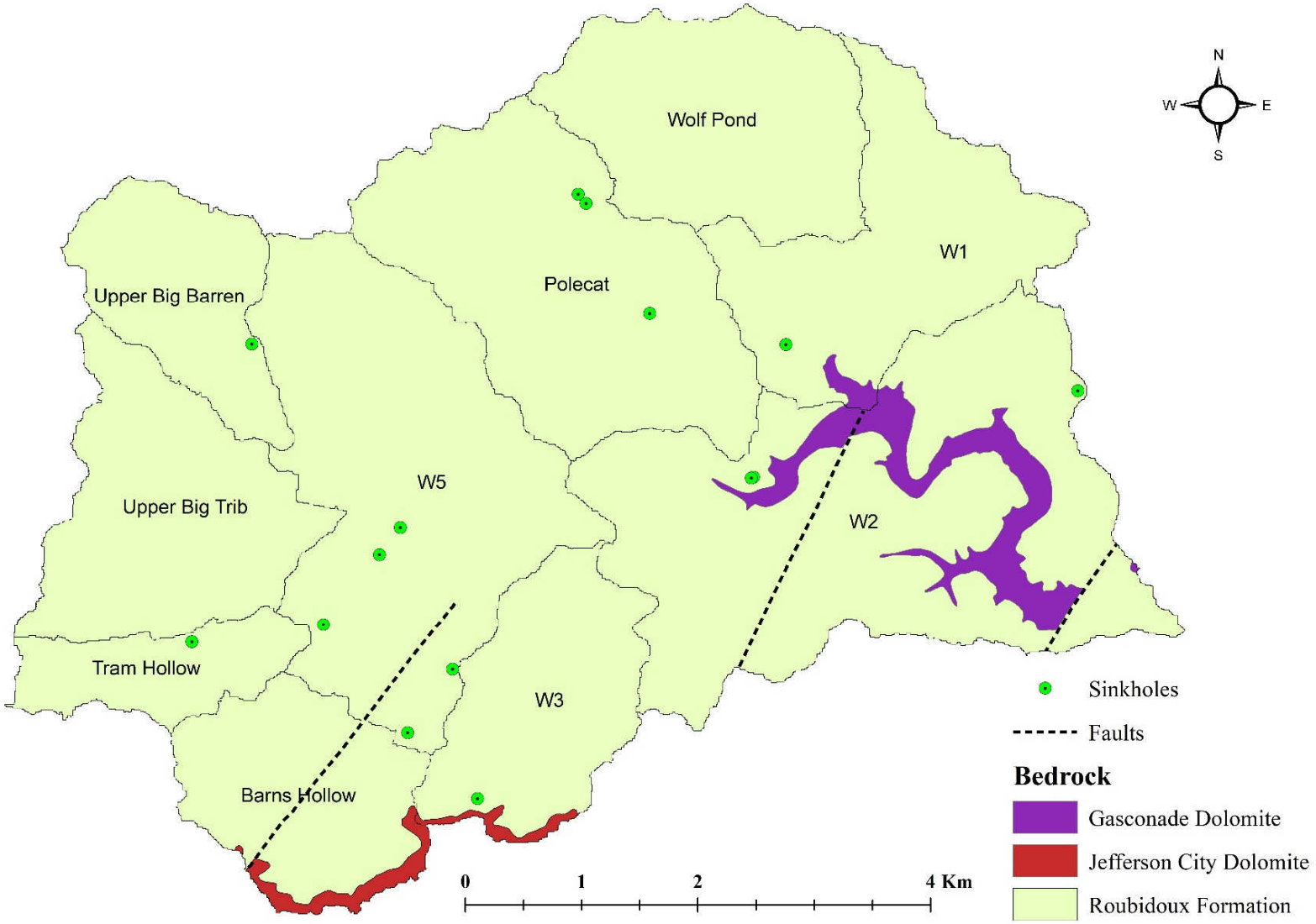

Figure 6. Bedrock geology map of the Middle Big Barren Creek watershed.

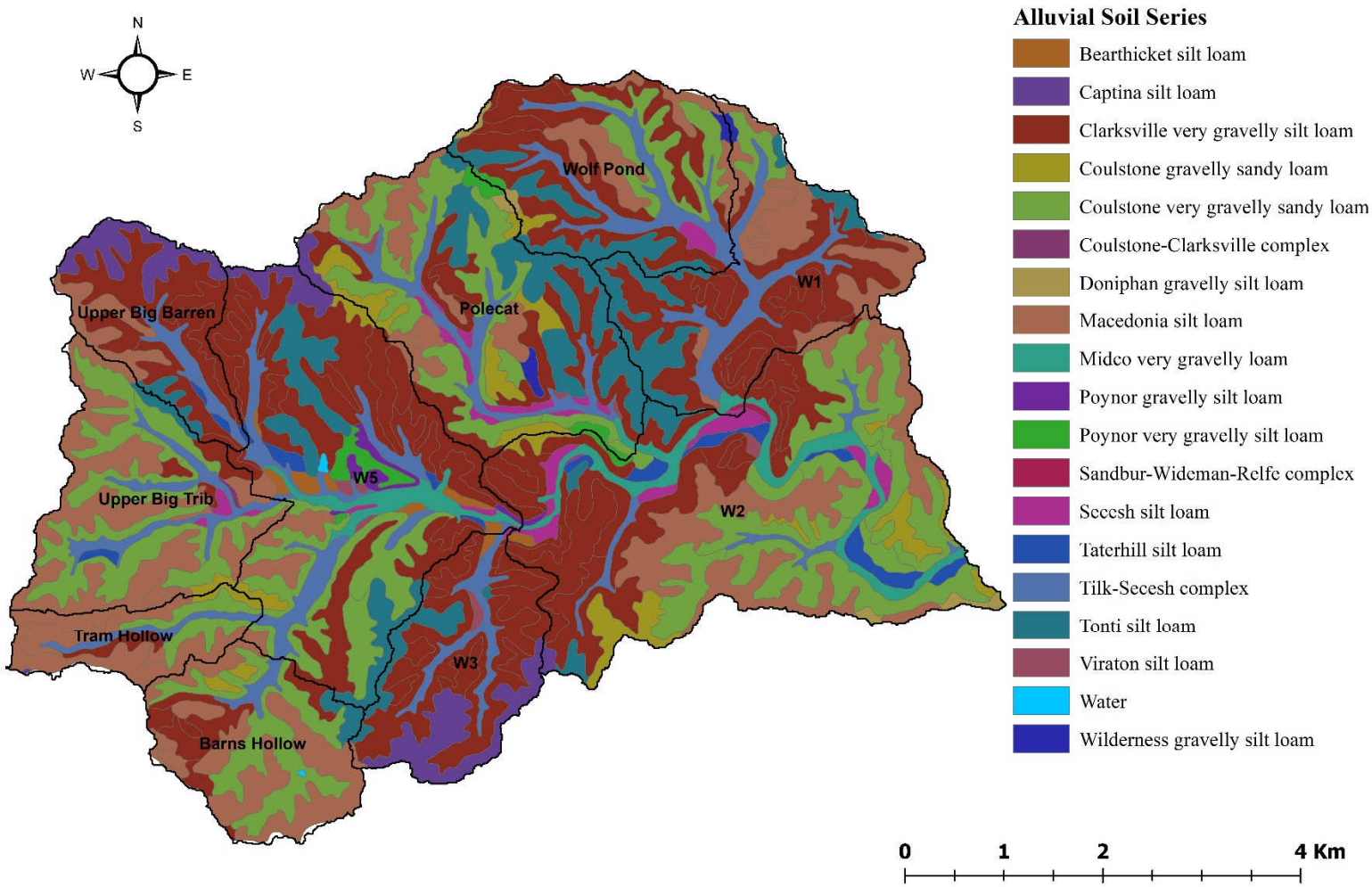

Figure 7. Alluvial soil map of the Middle Big Barren Creek watershed.

Channel Morphology

Different types of channels were observed in the study area, such as single-channel, transition channel, multi-threaded, headcut, incised channel, and channelized streams. Geographically these streams can be easily distinguishable.

Single-channel. According to Rosgen classification, a single-threaded stream has a width-depth ratio of less than 40 (w/d <40) (Rosgen, 1996). Bed material tends to be coarser along the thalweg and on riffles, typically in the cobble to boulder range (Rosgen, 1996).

Multi-threaded stream. In this stream, the width-depth ratio is greater than 40 (w/d >40) (Rosgen, 1996). Field inspection showed that several channels of the study area are stabilized by trees and vegetation. The channel bed is variable in texture, with patches of gravel overlying a cohesive soil material with a relatively dense root mat. Where channel threads flow near the valley sides, boulders and sometimes bedrock will be exposed along the bed.

Channelized stream. Channelized streams may have a similar width to a multi-threaded channel, are deeper and free from instream vegetation, and bank protected by artificial levees, with efforts to protect banks with gravelly loam materials scrapped from the bed or lower banks by machines (Thies, 2017). Field survey showed that the channel bed was mixed with gravel-cobble. As a result of high flow velocity and turbulence, incision and headcut formation were observed in the upstream segment of the channelized stream (Hupp et al., 2009).

Among the eight survey sites, the single-channel was found in site 4 (MBBC gage location). The multi-threaded channel was found at site-1, 2, 3, 5, and 6 (Figure 8). Sites 7 and 8 were characterized by a channelized stream, and a headcut was observed upstream of site 7 (Figure 8)

A) Site-1

Figure 8A. Site-1 covered by dense vegetation creating an impediment to flow.

B) Site-2

Figure 8B. Channel cross-section survey at site-2 using an auto-level.

C) Site-3

Figure 8C. Water flowing through the multiple channels at site-3.

D) Site-4

Figure 8D. Collecting discharge measurement with SonTek FlowTracker at the MBBC gage location (site-4).

E) Site-5

Figure 8E. Looking downstream at site-5 during a flow condition.

F) Site-6

Figure 8F. Channel bed of site-6 was covered by dense vegetation located upstream to the headcut.

G) Site-7

Figure 8G. Cross-section survey at site-7 located downstream to the headcut.

H) Site-8

Figure 8H. Looking downstream at site-8. Channel bed characterized by gravel-cobble.

I) Headcut

Figure 8I. Looking upstream to a 3 m headcut, located around 200 m upstream of site 7.

J) Incised Channel

Figure 8J. The incised channel looking downstream to the headcut.

Land-use and Vegetation Scenario

Pre-settlement condition. Historical analysis and archeological records indicate that during the pre-settlement period, different tribal groups lived in the Ozarks who relied on hunting for their livelihood (Jacobson and Primm, 1997). Native Americans used fire for the improvement of grassland, grazing, and hunting that played an important role in determining the vegetation distribution in this area (Jacobson and Primm, 1997; Ladd, 1991; Barrett, 1980). Historical accounts found that during the pre-settlement condition 50-80% of the Ozarks Highlands covered by shorleaf pine forest including MBBC watershed (Guyette et al., 2006). It was found that during the pre-settlement period, pine trees covered 6.6 million acres across the Ozarks region (Figure 9) (Liming, 1946). This vast amount of pine forest was distributed unevenly in the sandy land and portion of flint ridges. No logging road and stream channelization were found in the pre-settlement land cover of the MBBC watershed (Jacobson and Primm, 1997).

Early-settlement to post timber boom period. During the **e**arly settlement period (1800-80s), settlers cleared the valley bottom to facilitate grazing activities, row crop production, and small-scale timber harvesting (Jacobson and Primm, 1997). However, this scenario was radically changed during the timber boom period (the late 1880s to 1920) (Jacobson and Primm, 1997). By constructing high-capacity milling facilities, huge labor support, and railroad logging, the timber boom was started in the Ozarks region, including the Big Barren Creek watershed (Cunningham, 2007). During peak timber production, the shortleaf pine consumption rate was 70 acres per day in some Carter County where the BBC is located (Cunningham, 2007).

Present-day land-use. As a result of historical timber harvesting, at present, only 15-20 percent of the forest cover is occupied by shortleaf pine in the Ozarks that reduced the basal area

by 35 percent once dominated by shortleaf pine forest (Cunningham, 2007). Today the dominant forest species of the Ozarks are mixed oak, hickory, shortleaf pine, and grassland (USDA and NRCS, 2006). The Middle Big Barren Creek forest includes 75% deciduous, 13% evergreen, 4% mixed, and 8% others (Shrub/Scrub, Herbaceous, Hay/Pasture and developed open space/low intensity) (Table 1).

Table 1. National Land Cover Dataset (NCLD, 2016) land-use classification.

Land Use Class	Percent Cover (%)
Developed, Open Space	3.33
Developed, Low Intensity	0.10
Deciduous Forest	74.49
Evergreen Forest	13.22
Mixed Forest	4.21
Shrub/Scrub	0.40
Herbaceuous	1.21
Hay/Pasture	3.02
Open water	0.024

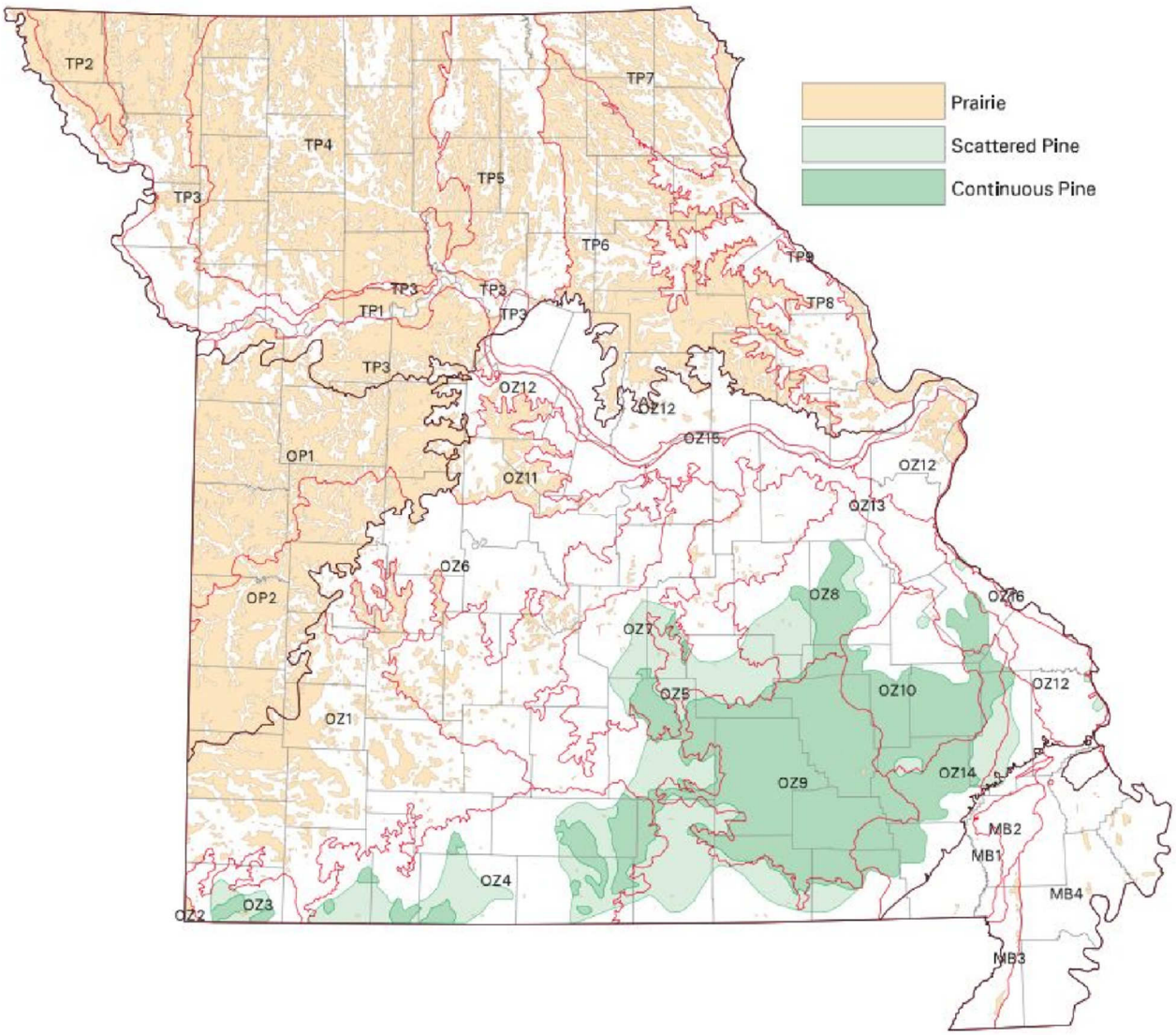

Figure 9. Pre-settlement of prairie and pine and ecological subsections of Missouri (Schroeder, 1981b; Liming, 1946).

METHODOLOGY

This chapter describes the methods used for field assessments, GIS analysis, watershed hydrological modeling, and channel hydraulics modeling. Field measurements were conducted to ground truth LiDAR imagery of the channel and flood plain of the MBBC watershed to determine channel substrate and roughness parameters. A 1-m resolution LiDAR-DEM (Digital Elevation Model) was used as the primary data of the modeling analysis. The study's main goal was to generate runoff hydrograph for pre-settlement, post-disturbance, and present-day scenarios using the HEC-HMS model using the best available data. After getting the HEC-HMS simulated discharges, a one-dimensional (1-D) HEC-RAS model was used to simulate channel flow conditions under the different land-use scenarios.

Field Survey

Field surveys were conducted on June 10 and 11, 2020. Eight sites were selected based on different geomorphic characteristics for cross-section, pebble count, and tree inventory surveys and numbered from one to eight in the downstream direction. The GPS locations of the sites were recorded using a Trimble GPS tool and TerraSync software. The GPS locations of the sites were used for further analysis in the HEC-RAS simulation. Pictures were taken to document the overall channel condition and validate the cross-section survey.

Cross-section surveys were conducted using an auto level, 100-meter tape, and stadia rod to evaluate the channel’s cross-sectional geometry. Cross-section length varied from 43 m to 126 m. The survey cross-sections were used to validate the appropriateness of the LiDAR DEM

extracted cross-section for HEC-RAS simulation. The LiDAR DEM of the study area was generated in 2016.

A pebble count survey was conducted for each site using the modified Wolman Pebble Count Survey technique (Rosgen, 1994). Substrate composition of the streambed, bank, and floodplain is an important factor in analyzing the stream character, form, channel hydraulics, and erosion rate of the channel (Harrelson et al., 1994). This survey was conducted at five evenly spaced transects of the upstream and downstream parts of each transect. As a result, a total of 99 pebbles were counted from 11 transects within pools and riffles at each survey site. This substrate collection technique was based on collecting various bed substrates on a proportional basis along the stream segment (Rosgen, 1994) The "blind-touch" method was used to grab the samples, and then a gravelometer was used to measure the pebble diameter. The minimum size of the gravelometer template was 2 mm. In addition, a ruler was used to measure the B-axis of the largest mobile clasts on the channel bed at each site. Pebble count survey was important to evaluate the shear stress and sediment movement of the channel.

Riparian zone large wood and tree inventory were performed to estimate the Manning's n value of the flood plain. A tree-caliper was used to measure the tree diameter at breast height (DBH). In this survey, the DBH of all the trees was measured within an area of 10-meter upstream and 10-meter downstream of each cross-section. Therefore, the width of the sample area was the same for all the sites (20 m or 65.6 ft). However, the cross-section length was ranged from 41 m to 111 m.

Stream Gage Network

A total of eight gaging stations were installed in the MBBC watershed. However, six of them (UBT, UBB, TH, WP, PC, and MBBC) were used in the model simulation validation procedure. The stage and discharge of each gage were recorded every 5-minutes intervals using Hobo U20L-04 Water Level Loggers (Figure 10a) (OEWRI, 2016). The data logger was installed inside a PVC pipe and attached firmly to a 1-2 m stuff gage that was installed at each site (Figure 10b). The level logger uses the change in pressure caused by increasing the water level in the pipe to measure the water surface level (Owen et al., 2021). The raw data is downloaded every ten weeks interval using the HObO Waterproof Shuttle (Figure 10a).

Figure 10. (a) HObO U20L-04 data logger, (b) gage installation.

Manning's n Value Estimation

The estimation of Manning's roughness coefficient (Manning's n) for the stream channels is well established; however, less in understood about how to estimate the Manning's roughness coefficient for the densely forested floodplain (FP) and the channel (Arcement and Schneider, 1993). In a forested watershed, the density of vegetation of the wooded flood plain is an important factor in determining Manning's roughness value (Arcement and Schneider, 1993). In this study, the vegetation-density method as described in Arcement and Schneider (1993) was used to estimate the Manning's n value of the flood plain. A tree count survey was conducted 10 m upstream and 10 m downstream of each cross-section line to estimate the vegetation density. All the trees in the sampling area were counted, and DBH (diameter at breast height) was measured that gave an average diameter for the expected flow depth of the sample area. Arcement and Schneider (1993) showed that a sample area along a 30 m long cross-section by 15 m wide in the flow direction is enough to determine the vegetation density of the flood plain. After collecting the tree DBH value, the vegetation density (Veg.d) of the flood plain was estimated using Equation 1 (Arcement and Schneider, 1993).

$$Veg.d = \frac{\sum A}{AL} = \frac{h\sum n_i d_i}{hwl} = \frac{\sum n_i d_i}{wl} \qquad \text{Equation 1}$$

Where, $\sum nidi$ is the summation of the number of trees multiplied by the diameter (ft); h is the height of the water depth on the flood plain (ft), w is the width of the sample area (ft), and l is the length of the sample area (ft)

Arcement and Schneider (1993) found that the flow depth of a sample area is equal to the hydraulic radius, R. In this study, the hydraulic radius of the eight surveyed sites (Figure 11) were calculated using xsecAnalyzer version 17 developed by the NRCS, an excel based software for determining the hydraulic parameters by using a single cross-section and relative roughness

(Moore, 2011). Using the hydraulic radius, the effective-drag coefficient (C_*) for each cross-section was calculated using the regression Equation 2. Finally, the Manning's n for the flood plain was estimated using Equation 3 (Arcement and Schneider, 1993).

$$C_* = -3.5157 * R + 21.367 \quad \text{Equation 2}$$

$$n = n_0 \sqrt{1 + Veg_d(C_*)\left(\frac{1.49}{n_0}\right)^2 (\frac{1}{2g})R^{4/3}} \quad \text{Equation 3}$$

Where n_0 is the Manning's boundary-roughness coefficient (omitting vegetation effect), determined using equation 4 (Arcement and Schneider, 1993), C_* is the effective drag coefficient, using equation 2, g is the gravitational constant (32.15 ft/s^2), R is the hydraulic radius (feet).

$$n_0 = n_b + n_1 + n_2 + n_3 + n_4 \quad \text{Equation 4}$$

Where, n_b is a base n value of the bare flood plain condition, n_1 is the surface irregularities, n_2 is a value representing the variation in shape and size of the flood plain, assumed equal to 0.0, n_3 is for obstructions, n_4' is for the vegetation type, all these values were determined based on the field observation (Arcement and Schneider, 1993).

The Manning's roughness coefficient for the channel was determined using Equation 5 (Limerinos, 1970). The estimated flood plain and channel Manning's roughness values are given in Table 2.

$$n = \frac{0.0926R^{1/6}}{1.16 + 2.0\log(\frac{R}{d_{84}})} \quad \text{Equation 5}$$

Where n is the Manning's n value of the channel, R is the hydraulic radius (ft), d_{84} is the bed substrate diameter (ft) of the 84th percentile.

Model Selection

In this study, the HEC-HMS (Hydrologic Engineering Center-Hydrologic Modeling System) and HEC-RAS (River Analysis System) were used for hydrologic and hydraulic simulation successively. Both were developed by the HEC of the U.S. Army Corps of Engineers (http://www.hec.usace.army.mil/software/hec-hms/). Compared to the other available hydrological models, HEC-HMS is well suited for this study as it can analyze the spatially distributed rainfall and consider the topography, soil, and LULC (Land Use Land Cover) (Hu and Shrestha, 2020). Therefore, this model is appropriate for analyzing the historical land-use change impact on hydrology in forested watersheds (Beck et al., 2019; Fitzpatrick et al., 1999; Krause, 2010; Magilligan and Stamp, 1997).

The impact of the hydrological changes on the channel morphology can effectively be analyzed using the hydraulic models (Johnson, 2015). One-dimensional (1-D) HEC-RAS model is very useful to analyze the connectivity between channel and flood plain using a series of cross-sections for different flood discharges (Beck et al., 2019). This model gives different hydraulic parameters such as inundation depth, velocity, shear stress, and stream power at each cross-section that are critical to analyzing the channel geomorphic changes for varying flood discharges (Beck et al., 2019).

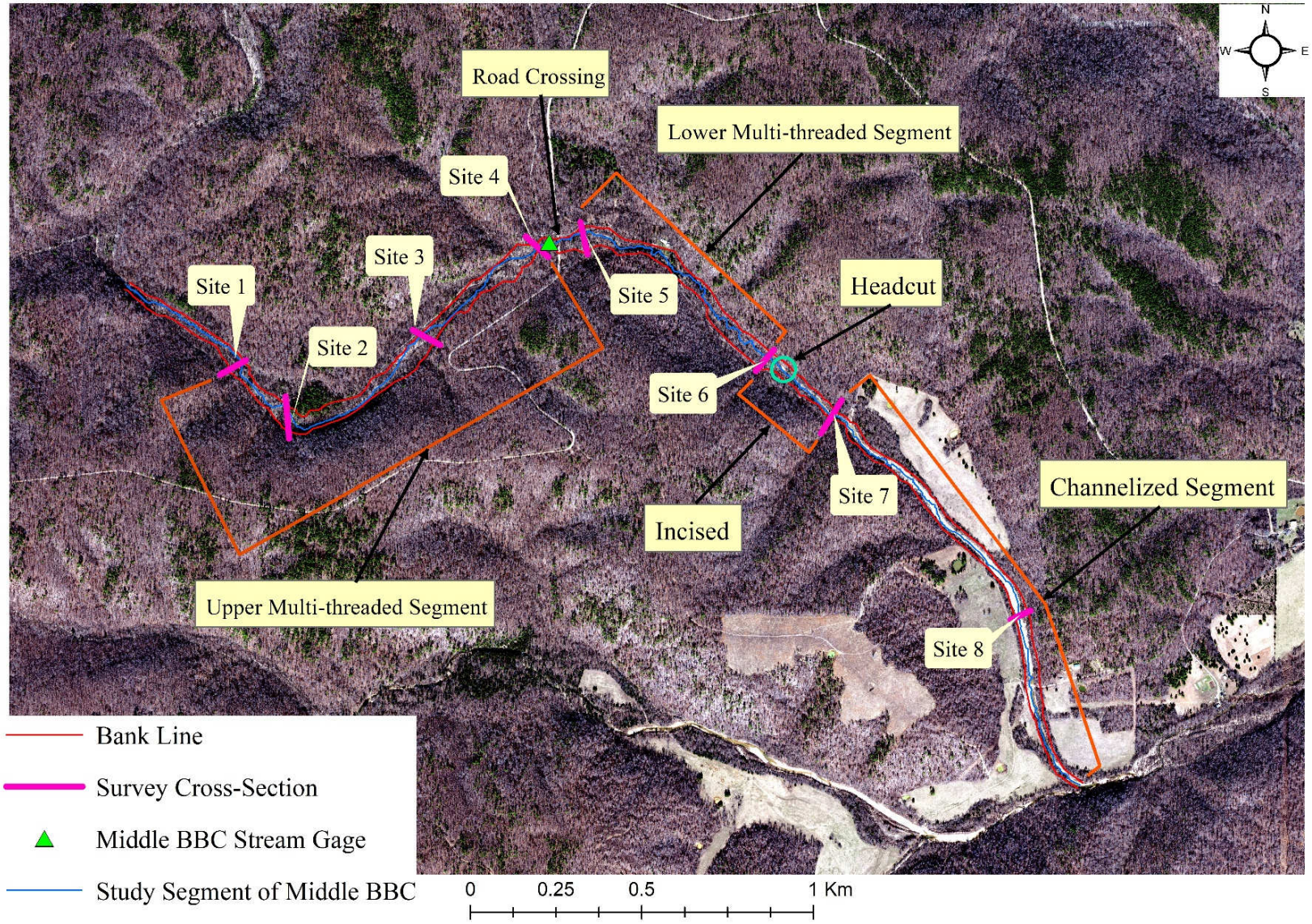

Figure 11. Field survey sites location and channel types.

Table 2. The adjustment factors and Manning's N value for the channel and flood plain of the study sites.

Location	Width (w), feet	length (l), feet	n_1	n_3	n_4	n_b	n_0	$Veg.d$	R	C_*	Channel Manning's n	Flood plain Manning's n	Channel Type*
Site 1	65.6	137.76	0.01	0.025	0.10	0.032	0.167	0.002	1.68	15.46	0.10	0.17	Multi-threaded
Site 2	65.6	144.32	0.011	0.030	0.10	0.032	0.173	0.002	1.17	17.26	0.07	0.18	Multi-threaded
Site 3	65.6	170.56	0.011	0.030	0.10	0.030	0.171	0.002	1.00	17.85	0.06	0.18	Multi-threaded
Site 4 (MBBC gage)	65.6	364.08	0.011	0.030	0.10	0.030	0.171	0.003	3.30	9.76	0.13	0.19	Multi-threaded
Site 5	65.6	364.08	0.011	0.030	0.10	0.030	0.171	0.004	1.16	17.28	0.10	0.18	Multi-threaded
Site 6	65.6	85.28	0.011	0.030	0.10	0.030	0.171	0.005	1.80	16.60	0.09	0.19	Multi-threaded
Site 7	65.6	186.96	0.007	0.019	0.06	0.030	0.116	0.003	1.35	15.04	0.05	0.12	Single-channel (Incised)
Site 8	65.6	134.48	0.007	0.019	0.06	0.030	0.116	0.003	2.20	13.63	0.08	0.14	(Channelized)

*Channel classification based on the w/d ratio of Rosgen channel classification (Rosgen, 1996).

HEC-HMS Modeling Approach

Terrain processing. The first step of HEC-HMS simulation is to divide the whole watershed into several sub-basins and their associated reaches (Scharffenberg, 2016). In this study, a 1-m LiDAR-DEM (Digital Elevation Model) was used for watershed processing and catchment delineation using the GIS menu of the HEC-HMS 4.4. This DEM is a combination of a ½ m DEM from the Forest Service and a 1-m DEM of Ripley County from MSDIS. These two DEMs were merged and reclassified to 1-m, so there would be one resolution for the entire watershed (Roman, 2019). The watershed processing consists of several successive steps: selecting the coordinate system (NAD_1983_UTM_Zone_15N), preprocessing sinks, processing drainage, identify streams, breakpoint manager, and delineate elements (Scharffenberg, 2016). In the identify stream step, a threshold value is used for a grid cell within the catchment that helps to delineate the stream link more precisely. An iterative process determined the minimum watershed area for stream network delineation, and a drainage area of 0.26 km^2 was eventually chosen as the best option to run the model efficiently. For the breakpoint manager, an outlet was set in the Middle Big Barren Creek stream gage location that divided the whole watershed area of 48 km^2 into ten sub-basins and 31 reaches (Figure 12). Two models are required for completing HEC-HMS simulations: the basin model and a meteorological model. After preparing all the respective parameters for these models, a simulation time from 27 March 2018 to 30 March 2018 at 15-minute intervals was set to analyze the hydrologic process.

Basin Model. The basin model contains all of the delineated sub-basins, reaches, and junctions. It also accommodates all the hydrologic components for the sub-basins and reaches. In this study, the canopy, surface, loss, and transform methods were used for each sub-basin element, and the Muskingum-Cunge method was used for the reach routing method (Table 3).

Table 3. Dataset for the HEC-HMS basin model of Middle BBC watershed.

Component	Calculation Method	Dataset/Method
Canopy	Simple Canopy	NLCD land cover dataset 2016
Surface	Simple Surface	Fleming, 2002
Loss	SCS Curve number	Literature review, NLCD 2016, and Web Soil Survey (WSS)
Transform	SCS Unit Hydrograph	Lag time estimation using NRCS part 630 hydrology National Engineering Handbook
Reach routing	Muskingum-Cunge	1-m LiDAR DEM and field survey
Loss/Gain	Percolation	Calibration

Canopy Method. The Canopy method was used to represent plants' presence in the landscape (Scharffenberg, 2016). In a forested watershed, rainfall first comes in contact with the tree leaves and branches, and when the maximum canopy interception is obtained, the remaining rainfall creates through-fall (Scharffenberg, 2016; Ward and Trimble, 1995). This method has three data requirements: initial storage (%), maximum canopy storage (in), crop coefficient. In this study, the initial storage was set to zero, which meant no water remained in the canopy prior to the simulation event, and only a dry period was selected for evapotranspiration. Maximum canopy interception or canopy storage amount varies with tree canopy types or vegetation types (deciduous or evergreen) and meteorological factors (rain intensity and wind speed) (Scharffenberg, 2016; Ward and Trimble, 1995). According to the National Land Cover Dataset 2016, the vegetation type and its associated maximum canopy interception are given in Table 4.

Table 4. Maximum canopy intercept and crop coefficient of fully developed canopies (Ward and Trimble, 1995, Allen, R. G. et al., 1998; Corbari et al., 2017).

	Leaf on condition		Leaf off Condition	
	Intercept capacity, mm	Crop coefficient	Intercept capacity, mm	Crop coefficient
Evergreen Forest (Shortleaf pine)	0.14	1.00	0.14	1.00
Deciduous Forest-Hardwoods	0.10	0.91	0.05	0.15
Mixed Forest	0.12	0.95	0.10	0.58
Shrubs/Scrub	0.10	0.91	0.05	0.15
Herbaceuous	0.05	0.80	0.05	0.35
Hay/Pasture	0.05	0.80	0.05	0.35

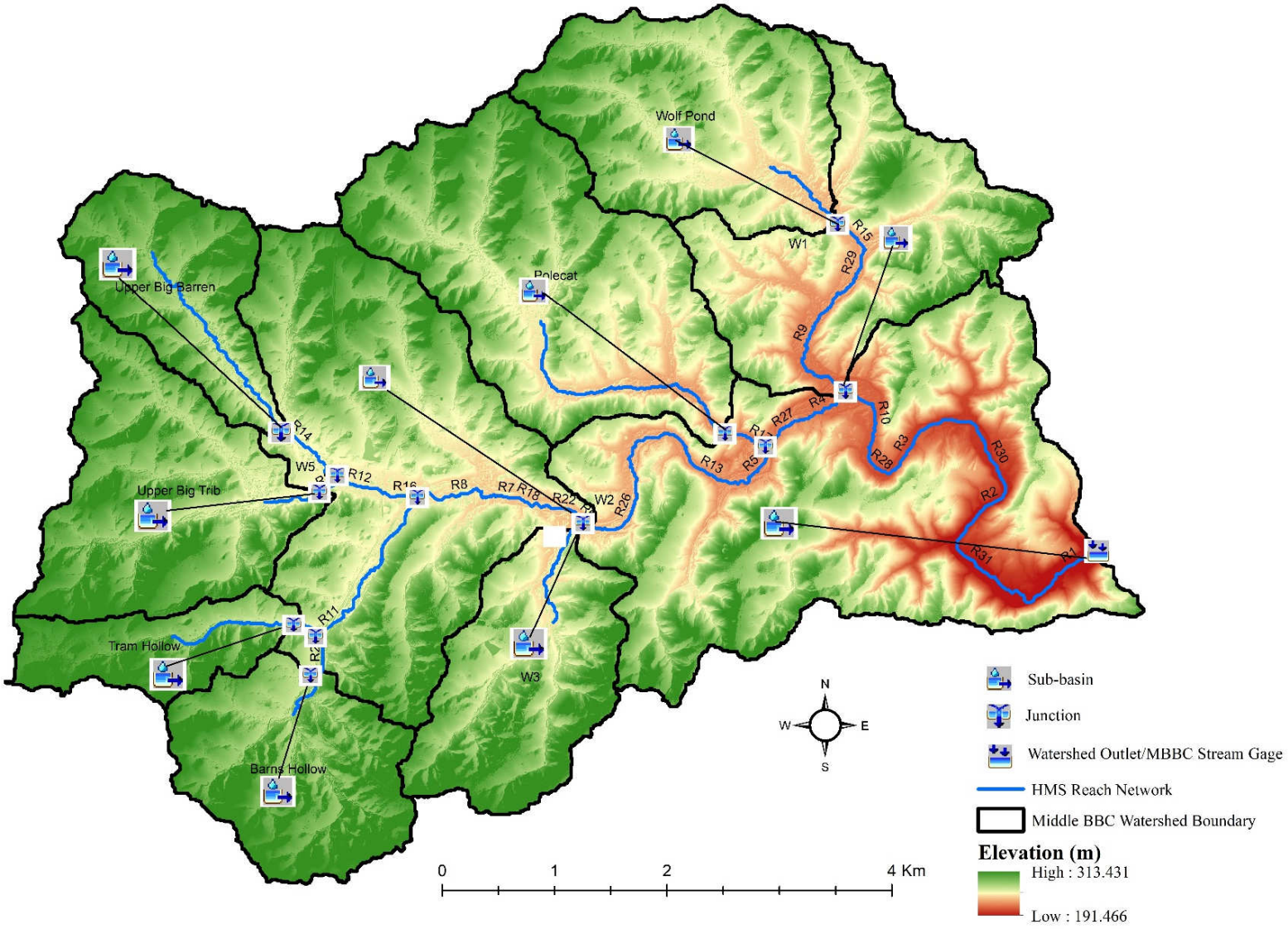

Figure 12. HEC-HMS model setup.

The crop coefficient (CC) is the ratio of a reference potential evapotranspiration (ETo) and generic potential evapotranspiration (ETP) (Allen, R. G. et al., 1998). In the meteorological model, the exact amount of extracted water from the soil is calculated by multiplying the crop coefficient value with the potential evapotranspiration (Allen, R. G. et al., 1998). In this study, a higher crop coefficient value was selected for the evergreen forest in a leaf on condition (Table 4). After determining the maximum canopy storage and crop coefficient for each type of vegetation, an area-weighted average was used to estimate the crop coefficient values for each sub-basin in a leaf off condition to represent the dormant scenario since the model simulation period was in March (Table 5; Equation 6; Hu & Shrestha, 2020). These values were then used for generating the land-use scenarios.

$$W_{composite} = \sum A_i \times X_i / \sum A_i \quad \text{Equation 6}$$

Where, $W_{composite}$ is the weighted average of maximum CS or CC or maximum SS or CN, A_i is the drainage area covered for the land use or soil type i, and X_i is the respected value for the i-type land used or soil or canopy.

Surface Method. When the maximum canopy coverage is exceeded, the precipitation through-fall starts that arrives at the soil surface (Scharffenberg, 2016). Initial storage (%) and maximum surface water storage (in) (SS) are the primary data requirements in this surface method. Surface storage represents the maximum water depth that can be accumulated on the soil surface before starting surface runoff (Scharffenberg, 2016). In this study, initial storage was set to zero (no water in the soil surface), and the maximum surface storage data of each sub-basin was estimated based on the topographic slope of the sub-basins (Fleming, 2002) (Table 6, 7).

Table 5. Sub-basin-wise canopy storage and crop coefficient value in a leaf-off condition.

Sub-basin	Area, Km^2	Weighted max. canopy storage, in	Crop coefficient
Polecat	6.19	0.059	0.244
Tram Hollow	1.59	0.059	0.248
Upper BB	2.51	0.056	0.211
Upper BT	4.18	0.070	0.348
Wolf Pond	5.12	0.070	0.347
Barnes Hollow	3.13	0.066	0.314
W1	4.58	0.064	0.302
W2	10.49	0.055	0.219
W3	3.24	0.060	0.287
W5	7.67	0.060	0.338

Table 6. Surface storage (SS) value based on the topographic slope (Fleming, 2002).

Description	Slope (%)	Surface Storage (SS)	
		in.	mm
Paved Impervious Areas	NA	0.125-0.25	3.18-6.35
Flat, Furrowed Land	0-5	2.00	50.80
Moderate to Gentle Slopes	5-30	0.25-0.50	6.35-12.70
Steep, Smooth Slopes	>30	0.04	1.02

Table 7. Sub-basin-wise surface storage (SS) value.

Sub-basin	Slope (%)	SS, mm	SS, in
Polecat	13.42	8.49	0.340
Tram Hollow	10.01	7.62	0.305
Upper Big Barren	11.79	8.07	0.323
Upper Big Trib	11.55	8.01	0.321
Wolf Pond	11.84	8.09	0.323
Barns Hollow	10.37	7.71	0.309
W1	14.50	8.76	0.351
W2	18.09	9.67	0.387
W3	12.56	8.27	0.331
W5	12.08	8.15	0.326

Loss Method. The Soil Conservation Service (SCS)-Curve Number (CN) and percentage of imperviousness-based loss method were used in HEC-HMS for the specific rainfall event simulation. The significant factors of estimating SCS-CN are the hydrologic soil group (HSG), land cover type, treatment, hydrologic condition, and antecedent runoff condition (ARC) (NRCS, 1986). Based on the minimum infiltration capacity, soils are classified into four groups (A, B, C, and D) (NRCS, 1986). The hydrologic soil group (HSG) distribution of the MBBC watershed shows that around 68% of the soils are HSG-B (Figure 13). This soil group has a moderate infiltration rate when thoroughly wet (NRCS, 1986). In this study, hydrologic soil group and

land-use data were collected from the web soil survey and National Land Cover Dataset 2016 (NLCD-2016) (Figure 7, 10).

The CN value for each watershed was determined primarily for woodland use, hydrologic soil group (according to each sub-basin), and fair hydrologic condition (Table 8). In this study, the fair soil condition was used to represent the average baseline land where grazing was not allowed, some areas were burned seasonally, and some never burned. Each sub-basin of the study area covers multiple hydrologic soil groups; thus, an area-weighted average was used to estimate the final curve number for the sub-basin (Equation 5, Table 9).

Table 8. Curve number for woods with different hydrologic conditions by soil group (NRCS, 1986).

	Hydrologic soil group			
Hydrologic Condition	A	B	C	D
Poor	45	66	77	83
Fair	36	60	73	79
Good	30	55	70	77

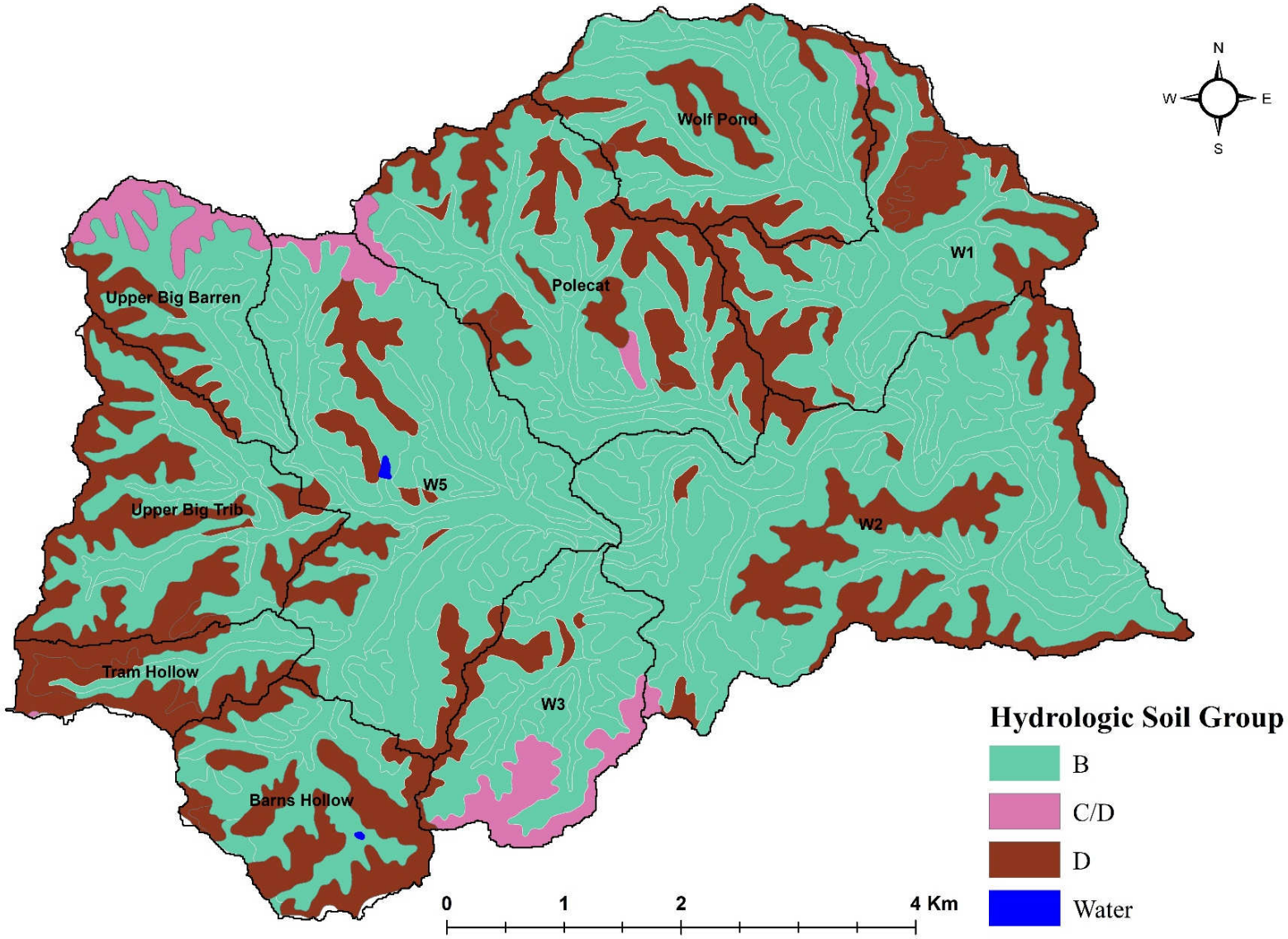

Figure 13. Hydrologic Soil Group (HSG) of the MBBC watershed .

Table 9. Estimated curve number (CN) for each sub-basin.

Catchments	Weighted CN value	Impervious (%)
Polecat	66.19	0.45
Tram Hollow	71.36	0.80
Upper BB	65.71	0.56
Upper BT	68.35	0.91
Wolf Pond	65.15	0.45
Barnes Hollow	68.88	1.13
W1	67.14	1.12
W2	64.12	0.57
W3	64.54	0.05
W5	63.26	1.30

Transform Method. In a watershed, the transform method calculates the direct runoff from the excess precipitation (Hu and Shrestha, 2020). The SCS unit hydrograph option in the transform method requires a watershed lag time (minute) and a peak rate factor that defines the percentage of unit runoff before the peak discharge. The watershed lag time covers a broad range of conditions ranging from heavily forested watersheds with a steep channel to meadows (NRCS, 2010). The watershed lag time usually defines the time duration (hour/minute) between the centroid of excess rainfall and peak discharge (Figure 14) (NRCS, 2010).

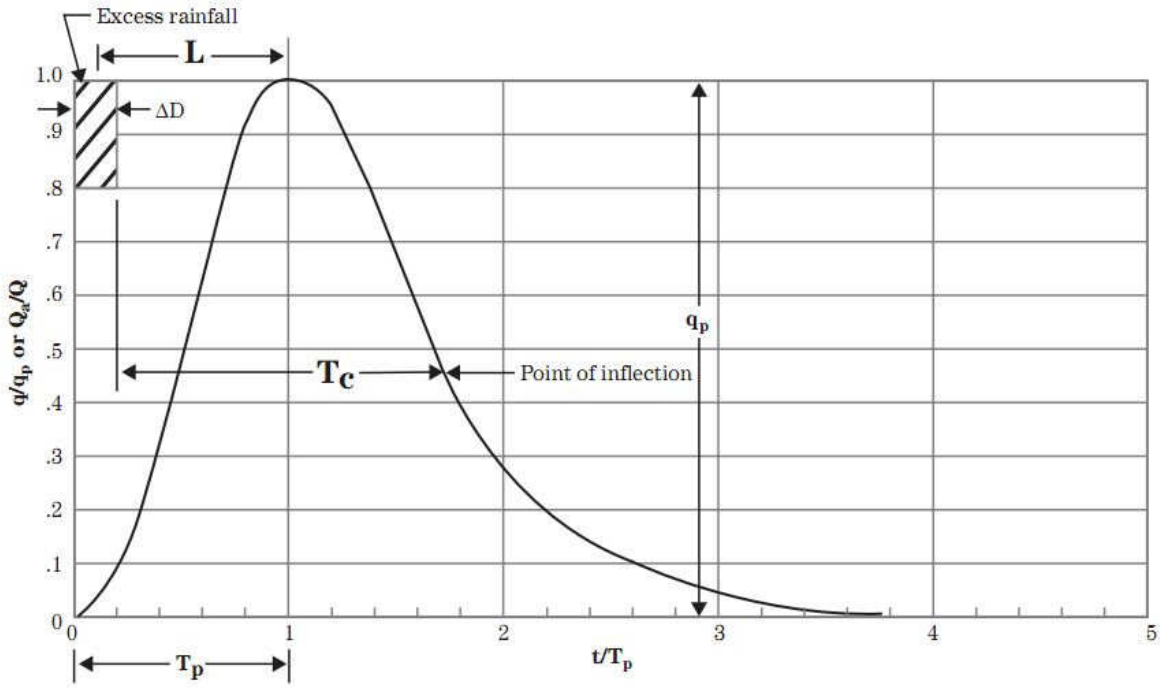

Figure 14. Watershed lag time (L) and time of concentration (Tc) to a dimensionless unit hydrograph.

Where L is the lag time, Tc is the time of concentration, Tp is the time to peak, ΔD is the duration of excess rainfall, t/Tp is the dimensionless ratio of any time to time to peak, q is the discharge rate at time t (m^3/s), q_p is the peak discharge rate at time Tp, Qa is the runoff volume (cm) up to t, and Q is the total runoff volume (cm).

The calculation of watershed lag time requires estimating the flow length, average watershed slope, and maximum potential retention (NRCS, 2010).

$$L = \frac{l^{0.8}(S+1)^{0.7}}{1900Y^{0.6}}$$

Equation 7

Where L is the lag time (hour), l is the flow length (feet), Y is the average watershed land slope (%) calculated using 1-m LiDAR DEM in GIS environment, and S is the maximum potential retention (in)

$$S = \frac{1000}{CN} - 10$$

Equation 8

Where S is the maximum potential retention (in), and CN is the watershed curve number.

$$l = 209A^{0.6}$$

Equation 9

Where l is the flow length (feet), and A is the drainage area (acres)

After calculating all the parameters for the lag time, the final lag time (minute) of each sub-basin is given in Table 10. The peak rate factor (PRF) of the transform method defines the percentage of unit runoff that occurs before the peak discharge. The PRF depends on the topography of the watershed. For example, a flat watershed has a lower PRF near 100, and a steep watershed can have a value of up to 600 (NRCS, 2007). In this study, the PRF was selected in the model calibration process, where the simulated peak-discharge and lag time were matched well with the observed data. The highest PRF (600) was observed in the Barnes hollow, W3, and W5, whereas the lowest PRK (150) was in Upper Big Barren (Table 10).

Reach Routing. In this study, the Muskingum-Cunge and percolation method was used for the reach routing and loss method. For the initial flow type, the inflow was selected equal to the outflow. The length and slope of each reach were collected from the 1-m LiDAR DEM. The Manning's n value of each reach was estimated based on the channel types of the eight study sites (Table 2, Appendix A). Flow technique was used as the index method, whereas this reference flow depends on the average value of the hydrograph (the midway between the base flow and peak flow) (Scharffenberg, 2016). The Eight-point cross-section technique was used for specifying the cross-section of each reach. In this configuration, the main channel and the left

and right bank were defined using the eight points (Scharffenberg, 2016). Using the calibration process, 0.15 to 0.42 cms/hactare of loss value was selected for the specified reaches.

Table 10. Lag time and peak rate factor of each sub-basin.

Sub-basin	Lag time (min)	Peak rate factor
Polecat	74.61	250
Tram Hollow	39.24	200
Upper BB	51.72	150
Upper BT	63.31	200
Wolf Pond	68.57	250
Barnes Hollow	58.25	600
W1	64.79	300
W2	96.98	300
W3	48.95	600
W5	93.71	600

Meteorological Model

The meteorological model is an important component of HEC-HMS simulations that sets the meteorological boundary conditions of each sub-basin (Scharffenberg, 2016). Five different components were selected for creating the meteorological model (Table 11). Short-wave radiation defines the sun's radiant energy with a wavelength ranging from infrared through visible to ultraviolet (Scharffenberg, 2016). In the Hargreaves short-wave method, the geographic coordinate of the centroid of the sub-basin was used to calculate the solar declination and solar angle for each time interval (Scharffenberg, 2016). A daily air temperature gage was selected for the maximum, and minimum temperature was used as a proxy of cloud (Scharffenberg, 2016). The Satterlund method was used for long-wave estimation that uses the temperature and vapor pressure to estimate long-wave radiation (Scharffenberg, 2016). The dew point temperature was used as the vapor pressure type in the HEC-HMS simulation. Air temperature and wind speed gage located in the Alley Spring, Shannon County, were also selected to estimate long-wave radiation from the meteorological components bar (Table 11).

Table 11. Components of the meteorological model.

Component	Method
Short-wave Radiation	Hargreaves
Long-wave Radiation	Satterlund
Precipitation	Specified hyetograph
Evapotranspiration	Penman-Monteith

The precipitation data for the simulation period was collected from the two rain gages in the watershed. The Upper rain gage and the basin centroid of Barnes Hollow, Tram Hollow, W3, W5, and Upper Big Trib (UBT) are considerably lower than the Middle Rain gage (Table 12). Thus, during the simulation, only the Upper rain gage data was used for these sub-basins. The observed upper rain gage (URG) rainfall amount was 12.5 cm for the simulation duration from 27 March 2018 to 30 March 2018. An inverse distance weighted (IDW) method was used to estimate the rainfall amount of the remaining sub-basins (Chen and Liu, 2012; Equation 10).

$$R_p = \sum_{i=1}^{n} w_i R_i$$

$$w_i = \frac{1/d^2}{\sum_{i=1}^{n} 1/d^2} \qquad \text{Equation 10}$$

Where, R_p is the unknown precipitation (cm) at the location of interest; R_i is the known precipitation (cm) at the weather stations; n is the number of stations used in the analysis; w_i is the weighting of each station, and di is the distance (km) from each rain gage.

Evapotranspiration is the process that combines evaporation from the ground and transpiration from the vegetation (Scharffenberg, 2016). The Penman-Monteith method was used in this study to estimate evapotranspiration. This method requires selecting an air temperature gage (dew point temperature) and a wind speed gage (Table 13). A reference default albedo 0.23 was used to compute the energy balance in the ground surface (Scharffenberg, 2016).

Table 12. Distance between the sub-basin centroid and rain gages.

Sub-basin	Distance (km)		Used Rain gage	Rainfall (cm)
	Upper BB Rain Gage	Middle BB Rain Gage		
Polecat	5.85	7.42	IDW	12.48
Tram hollow	2.22	9.32	URG	12.5
Upper BB	5.25	10.14	URG	12.5
Upper BT	3.43	9.55	URG	12.5
Wolf Pond	7.70	7.57	IDW	12.47
Barnes Hollow	0.94	7.94	URG	12.5
W1	7.67	5.83	IDW	12.46
W2	6.09	4.09	IDW	12.46
W3	2.87	5.99	URG	12.5
W5	3.75	7.73	URG	12.5

Time Series Data

Hydrologic modeling requires time-series data to incorporate the analysis process in the meteorological model (Scharffenberg, 2016). Different types of time series data were used in this study (Table 13). Generally, time-series data contains the value of a selected parameter according to the same model simulation period.

Table 13. Time series database for model simulation.

Data	Purpose	Data Source
Observed discharge data at six gage sites	Model calibration	Field data collection (primary data source)
Precipitation gage (15 min interval)	Meteorological model	Upper and Middle BBC rain gage (primary data source)
Air temperature gage (minimum)	Meteorological model	Missouri historical agricultural weather Database. http://agebb.missouri.edu/weather/history/index.asp
Dew point temperature	Meteorological model	Missouri historical agricultural weather Database. (Shannon County gage station). http://agebb.missouri.edu/weather/history/index.asp
Maximum wind speed	Meteorological model	Missouri historical agricultural weather Database (Shannon County gage station). http://agebb.missouri.edu/weather/history/index.asp

Scenario Generation Using HEC-HMS Simulation

In this study, one of the primary objectives was to evaluate the impact of timber harvesting and tree species changes on the hydrology of the MBBC watershed using the HEC-HMS simulation. Three different scenarios were considered in the HEC-HMS simulations to analyze the hydrologic changes such as present-day calibrated, pre-settlement, and post-disturbance scenarios. The differences between these simulations were evaluated by comparing flow duration, runoff depth, peak discharge, and lag time. Before starting the scenario generation, the model was calibrated and validated with the present-day data with considerable accuracy. The present-day calibration was performed based on the canopy, surface storage, transform, and loss method (Table 5, 7, 9, 10).

Pre-settlement Condition. Historical analysis showed that prior to pre-settlement, shortleaf pine forest covered 50-80% of the Ozarks, which is currently dominated by hardwood forest due to historical timber harvesting (Cunningham, 2007; Guyette et al., 2007). Today the number of pine trees in the region is only 20-50% compared to presettlement estimates (Guyette et al., 2007). In this study, the hydrological impact of this change was analyzed in HEC-HMS simulation by changing the present-day forest canopy cover to the pre-settlement canopy and decreasing the SCS-Curve Number for representing a good soil condition (Table 14, 15). In general, two types of forest covers were selected for generating pre-settlement scenario generation (Table 15). Different studies evaluated the impact of timber harvesting on SCS-CN value. For example, a study of four watersheds with basin areas ranging from 2,313 to 1,1419 km^2 in Iowa found that for a forest disturbance history of above 132 years, the curve number increased from 61.4 in pre-settlement conditions to 77.8 during the first 30 years of settlement period (Wehmeyer et al., 2011). Thus, in the pre-settlement forest condition, the SCS-CN value was 16.4 units lower than the present day. This study also found that after the state-wide forest

regeneration, the curve number dropped to 76.7 (Wehmeyer et al., 2011). Another study in a comparatively small watershed (0.14 km^2) located in the Appalachian Mountains of the eastern United States found that the runoff curve number in an undisturbed forest cover was 8.1 units lower than a fixed diameter limited timber harvesting (Tedela et al., 2012). Taking this into consideration, in this study, the following two scenarios were selected to represent the pre-settlement condition.

1) Changed the forest species from the current condition to the pre-settlement condition by multiplying the present-day pine forest cover by three (Table 14, 15). This was based on taking the halfway (33.33% or three times) of the pre-settlement shortleaf pine cover range 20 – 50% (Guyette et al., 2006). In addition, all other land uses were omitted, for example, roads and stream channelization. All the channelized streams were converted to the natural streams by increasing the Manning's n value according to Table 2.
2) Keeping the pre-settlement forest cover and the SCS-CN value was reduced by 1 CN unit. All other parameters were kept the same as scenario 1.

Table 14. Pre-settlement forest species (leaf-off condition) and SCS-CN value.

	Pre-settlement evergreen forest = current	Changes in CN

	(2016) amount * 3		value	
Sub-basin	Weighted Max. Storage, in	Weighted Crop Coefficient	Calibrated	Drop 1
Polecat	0.077	0.402	71	70
Upper Big Barren	0.065	0.293	76	75
Upper Big Trib	0.109	0.704	74	73
Wolf Pond	0.109	0.707	71	70
Barnes Hollow	0.099	0.384	70	69
Tram Hollow	0.081	0.439	75	74
W1	0.096	0.581	71	70
W2	0.064	0.279	69	68
W3	0.078	0.413	70	69
W5	0.097	0.592	70	69

Table 15. Current and pre-settlement land-use database (Guyette et al., 2006; NLCD, 2016).

		Present Condition (2016)				Pre-Settlement Condition [b] (< 1820)	
sub-basin	Area (km^2)	Deciduous (%)	Evergreen (%)	Mixed forest (%)	Others [a]	Deciduous (%)	Evergreen (%)
TH	1.6	81	11	2	5	66	34
UBB	2.5	88	6	4	3	83	17
UBT	4.2	70	22	0	8	35	65
WP	4.3	73	22	3	2	34	66
PC	6.2	84	10	3	4	70	30
BH	3.2	72	18	3	6	45	55
W1	4.6	73	17	3	7	49	51
W2	10.5	82	5	5	8	85	15
W3	3.3	66	10	5	18	69	31
W5	7.7	59	17	6	17	48	52
Total	47.8	75	13	4	8	61	39

[a] Others = developed open space, developed low intensity, shrub/Scrub, herbaceous, hay/pasture
[b] The pre-settlement evergreen forest was estimated by taking three times the current amount (Guyette et al., 2006).

Post-disturbance scenario. In this scenario, the canopy coverage was changed to a shrubs cover to represent the loss of forest species during the timber boom period 1880-1920. All the streams remained natural as the channel modification had not been started in this period. However, to represent the post-disturbance scenario, the curve number was increased based on the literature reviews (Tedela et al., 2012; Wehmeyer et al., 2011). In this technique, to represent the poor soil condition and comparatively higher runoff scenario, an extra 3 CN-unit were added to the present-day calibrated curve number (Table 16).

Table 16. Post disturbance scenario generation.

Sub-basin	Max canopy storage	Crop coefficient	Post disturbance CN
Polecat	0.05	0.15	74
Upper Big Barren	0.05	0.15	79
Upper Big Trib	0.05	0.15	77
Wolf Pond	0.05	0.15	74
Barnes Hollow	0.05	0.15	73
Tram Hollow	0.05	0.15	78
W1	0.05	0.15	74
W2	0.05	0.15	72
W3	0.05	0.15	73
W5	0.05	0.15	73

HEC-RAS Modeling

The HEC-HMS simulated peak discharge of each scenario was used in the one-dimensional HEC-RAS 5.07 to evaluate the channel response of these scenarios. In this study, a 4.5 km segment of the Middle Big Barren Creek was selected to analyze the impact of the simulated discharges on the current day channel form (Figure 15). Different hydraulic parameters were generated in this steady-state simulation, for example, channel velocity, shear stress, and stream power.

The delineations of the 4.5 km segment HEC-RAS boundary parameters such as stream centerline, banks (left and right), flow path centerline, and cross-sectional cut lines were completed in the RAS Mapper option of the HEC-RAS 5.07. A 1-m LiDAR DEM was used to extract cross-sections to the study channel. A total of 78 cross-sections were extracted to represent the channel geometry and one-dimensional steady-state simulation in HEC-RAS. The spacing of the cross-sections (around 50 m) was selected based on Samuel's equation (Equation 11) (Gary W Brunner, 2016).

$$\Delta x \leq \frac{0.15D}{S_0}$$ Equation 11

Where D is the average bank full depth of main channel (ft), and S_0 is the average bed slope (ft/ft).

The appropriateness of the DEM extracted cross-sections was then evaluated by comparing these cross-sections with the eight field-surveyed cross-sections. Survey and LiDAR cross-sections of sites 4, 6, 7, and 8 were matched very well (Appendix B). Overall, because of the good representation of the cross-section geometry, the LiDAR cross-sections were then used

for the HEC-RAS simulation. A few modifications were performed for cross-sections 7 and 8 to make the LiDAR cross-section deeper to match the surveyed cross-section (Appendix B).

Manning's n is another important parameter for HEC-RAS simulation. In this study, the selection of the Manning's n values (bank and channel) for each cross-section were based on the field estimated Manning's n and channel type (Table 1; Figure 14). Then, the Manning's n of these eight surveyed cross-sections were distributed among the LiDAR cross-section with the same channel type and proximity to the study sites. The longitudinal bed slope of the study stream was 0.004 m/m. For the HEC-RAS simulation, as a boundary condition, the simulated peak discharges, field estimated Manning's n, and the channel bed slope were used to perform the 1-D steady-state simulation. The observed water surface level of the cross-section located near the Middle BBC gage (site 4) was used to calibrate the model by changing Manning's n value.

Stream power. The stream power is an essential hydraulic parameter for assessing the channel's sediment transport capacity, stability, and deposition pattern (Bizzi and Lerner, 2015). The total stream power calculation in HEC-RAS is governed by Equation 12 (Gary W. Brunner, 2016).

$$\Omega = \gamma Q S_e \qquad \text{Equation 12}$$

Where Ω is the total stream power (W/m), γ is the specific weight of water (N), Q is the discharge, S_e is the energy gradient slope (m/m).

The extent of geomorphic changes generally increased with the unit stream power (Yochum et al., 2017). The unit stream power can be computed by Equation 13.

$$Unit\ Stream\ Power = \frac{Total\ Stream\ Power}{Channel\ Bankfull\ Width\ (m)} \qquad \text{Equation 13}$$

Channel shear stress. This is another important hydraulic parameter responsible for bedload transport that acts parallel to the channel bed (Hodges, 2015). Estimating channel' shear stress is essential for assessing the critical shear stress of a specific sediment size (Jhonson and Heil, 1996). In HEC-RAS, the shear stress is calculated by Equation 14 (Gary W. Brunner, 2016).

$$\tau_0 = \gamma R S_e \qquad \text{Equation 14}$$

Where τ_0 is shear stress (N/m^2), γ is the specific weight of water (N), R is the hydraulic radius (m) of the cross-section, S_e is the energy gradient or channel slope (m/m).

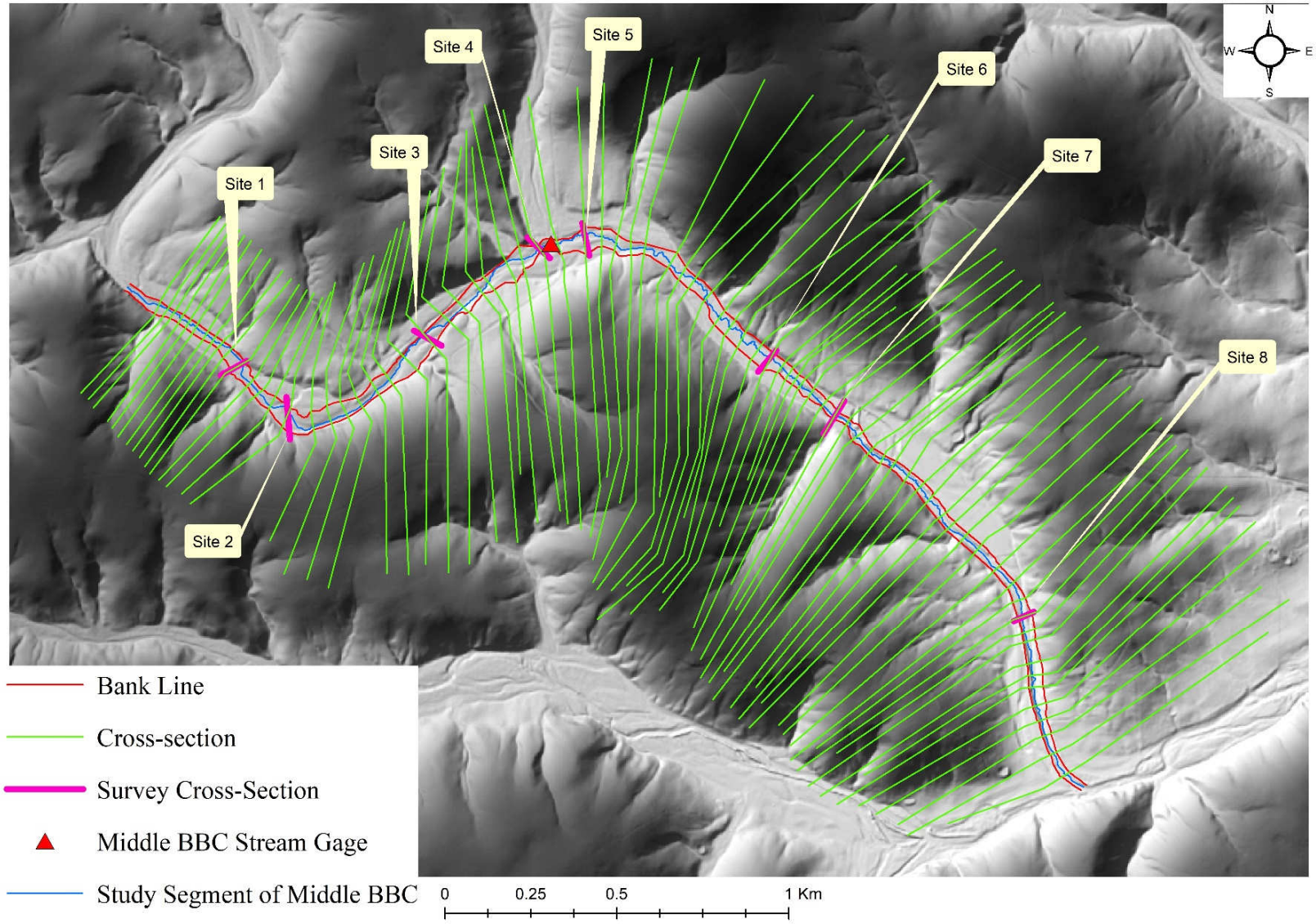

Figure 15. HEC-RAS model boundary parameters.

RESULTS AND DISCUSSION

The purpose of this chapter is to describe model calibration and validation. First, the calibration and validation procedures are described to show the accuracy of the modeling results. Second, using the calibrated HEC-HMS watershed model, the history of the hydrological alterations in the MBBC watershed are evaluated for four scenarios as follows: pre-settlement forest condition, pre-settlement forest cover with SCS CN-1 soil condition, post-disturbance, and present-period. For each scenario, five hydrologic parameters were used to evaluate the hydrologic alteration: flow duration, average discharge, runoff depth, peak discharge, and lag time. Third, field survey and channel modeling results are reported and discussed. Relationships between channel form and hydraulics were evaluated for each scenario using HEC-RAS study-state modeling. Three hydraulic parameters were selected to study the effect of varying discharges on channel form: channel shear stress, stream power, and velocity. Modeling results are related to field data obtained from channel, substrate, and vegetation surveys to evaluate channel response to floods hydrographs generated under different land-use scenarios.

Hydrologic Modeling of Land Use and Soil Scenarios

Hydrological modeling is an effective way to analyze the impacts of historical timber harvesting or other forest disturbance on watershed hydrology using spatially distributed rainfall and other meteorological data (Storck et al., 1998; Hu and Shrestha, 2020). The models can estimate the peak discharge and flow duration that are important to study flooding impact, stream instability, and stream ecology (McEnroe, 2010). The evaluation of the modeling results is based on calibration and validation to ensure the acceptability of the simulation results (Hu and

Shrestha, 2020). The HEC-HMS model was calibrated using flow data from six gages network with calibrated rating curves located in MBBC. However, most analysis focuses on the lower MBBC gage segment at the outlet of the watershed.

HEC-HMS Model Calibration and Validation. Model calibration involves several steps, including simulation with the measured or primary database, comparing the observed and simulated data, and changing the model parameters to get a good match between the observed and simulated results (Hu and Shrestha, 2020). Model calibration was performed by comparing the simulated and observed hydrograph of the six gages (UBB, UBT, TH, PC, WP, and MBBC). First, a simulation was performed for a rainfall event of 12.48 cm (from 27 to 29 March 2018) at 15 minutes intervals, and then the simulated peak discharge and lag time were matched with the observed data. Second, following the simulation, model parameters were adjusted to match the simulated peak discharge and lag time with the observed data. The Nash-Sutcliffe Efficiency (NSE) coefficient value was used to evaluate the model performance. In the model calibration process, the SCS-CN value, peak rate factor, and maximum surface storage were adjusted to ensure a good match (NSE > 0.5) between the simulated peak discharge and lag time to the observed data. By a trial-and-error process, model calibration estimated the best-fitted parameters for model simulation. Because of poor performance (NSE < 0.5) in the model optimization step, manual calibration was adopted for changing the model calibration parameters (Table 16). The high NSE (NSE = 0.85) value at MBBC watershed outlet showed the sufficient acceptability of the model results (Appendix C, Table 17).

Table 17. Model calibration parameters.

Parameters	PC	TH	UBB	UBT	WP	MBBC
Weighted CN value	66.19	71.36	65.71	68.35	65.14	----
CN Calibrated	71	75	76	74	71	----
Base value of max. surface storage, in	0.340	0.305	0.323	0.321	0.323	----
Calibrated value of max. surface storage, in	0.291	0.160	0.180	0.270	0.370	----
Peak rate factor	250	200	150	200	250	----
NSE Coefficient	0.91	0.70	0.71	0.64	0.94	0.85

The validation of the model was performed using the same calibrated parameters but a different rainfall event to test the acceptability of calibrated parameters (Hu and Shrestha, 2020). In this study, a rainfall event of 12.5 cm (from 9 to 11 January 2020) was selected for model validation, similar to the model rainfall event (12.48 cm). In the first trial, model validation showed poor performance of the model yielding a Nash-Sutcliffe Efficiency (NSE) coefficient of 0.328. The seasonal variation of the SCS-CN value was responsible for the poor performance in the validation period. Tedela et al. (2012) found that the SCS-CN value can vary between 3 to 14

CN units because of seasonal effects (dormant or growing). Additionally, in the dormant season, the SCS-CN value tended to be higher than the growing season (Price, 1998; Tedela et al., 2012). In our study, the SCS-CN values were calibrated at the end of the dormant season scenario (leaf-off) (end of March). However, the validation rainfall duration was in January or the mid of the dormant season. Therefore, an extra one CN unit was added to the calibrated CN value that showed a good performance of the model yielding a NSE value of 0.642.

HEC-HMS Model Performance Evaluation. The Nash-Sutcliffe Efficiency (NSE) coefficient of the HEC-HMS simulation is generally used to evaluate model performance and evaluate the similarity of observed and similarted values (Humphrey et al., 2012). NSE coefficient values can range between 0 to 1, where 1 means a perfect model performance (Moriasi et al., 2007; Nash and Sutcliffe, 1970). Studies have found that an NSE coefficient value greater than 0.5 represents a reliable acceptance of the model simulation (Ali et al., 2011; Chen et al., 2009; Zhang et al., 2013). In this study, among the five sub-basins, the calibration was excellent for the gages located in PC and WP yielding a NSE value around 0.9 (Table 17). The simulated hydrograph of these sub-basins was well-matched with the observed hydrograph (Figure 16). The simulated peak discharge and lag time of PC and WP were almost identical to the field gage data (Figure 16). In addition, the flow duration was also close to the observed data that was responsible for the excellent NSE coefficient value (Figure 16).

The simulated hydrograph of the TH, UBB, and UBT was also matched with the observed data (Figure 16). However, errors were observed in the simulated peak discharge and flow duration (Figure 16). The simulated peak discharge of these sub-basins was lower than the observed data that caused a low NSE value compared to the PC and WP (Table 17). In general, the model performance was excellent at the MBBC gage location that was the outlet of the entire

watershed for model calibration and validation. The simulated peak discharge, lag time, and flow duration were matched significantly with the observed data that yielded an excellent NSE value of 0.85 and 0.642 for model validation (Table 17, Figure 17, 18).

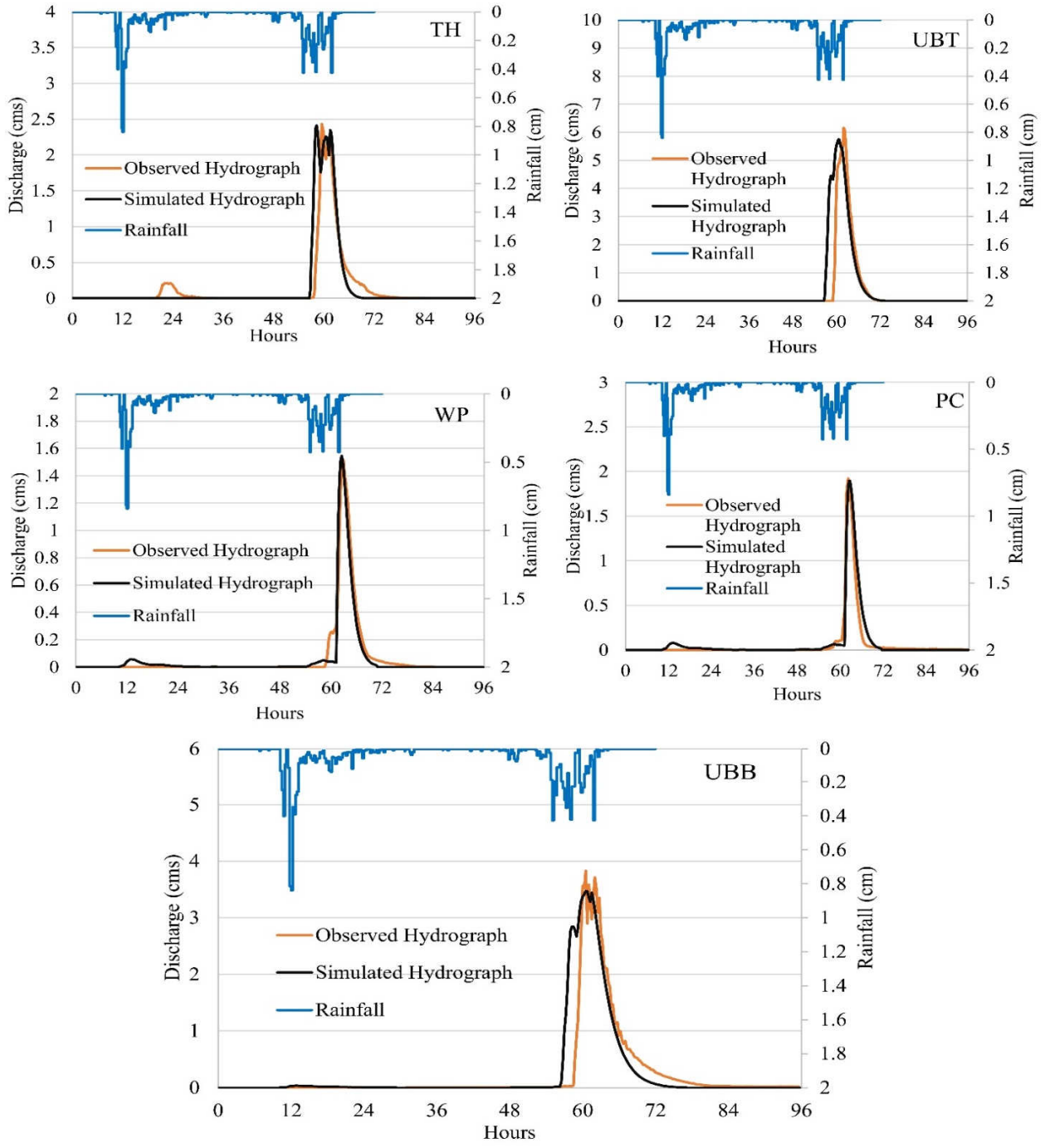

Figure 16. Calibrated hydrographs of the five sub-basins gage locations.

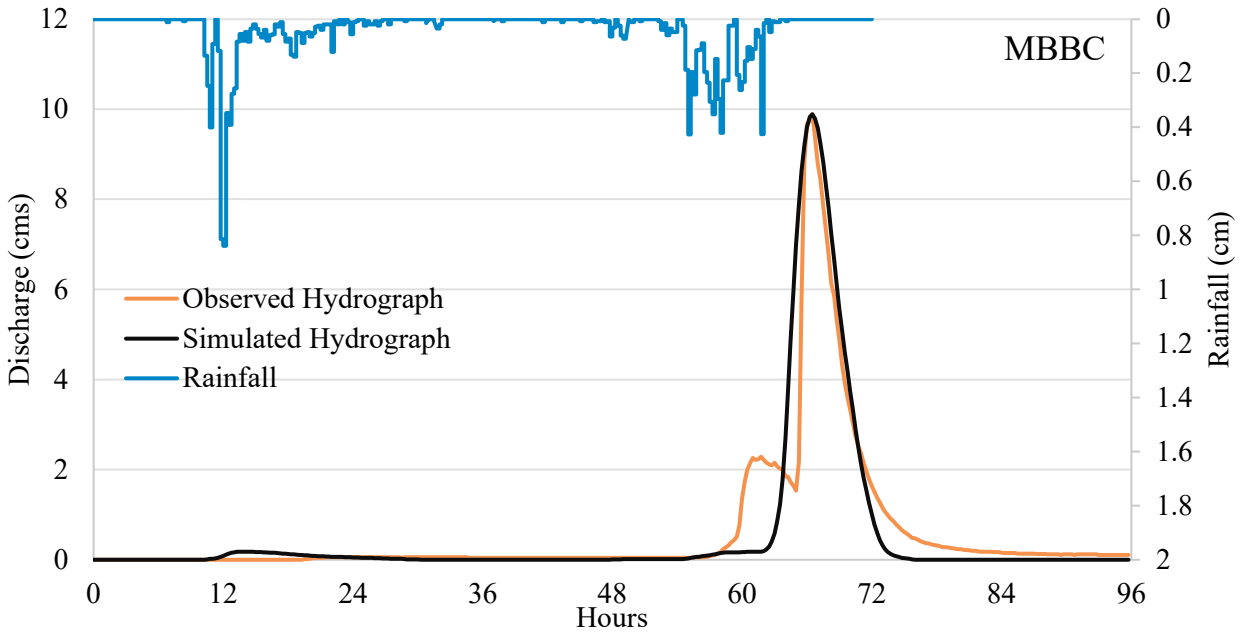

Figure 17. Calibrated hydrograph at MBBC gage location.

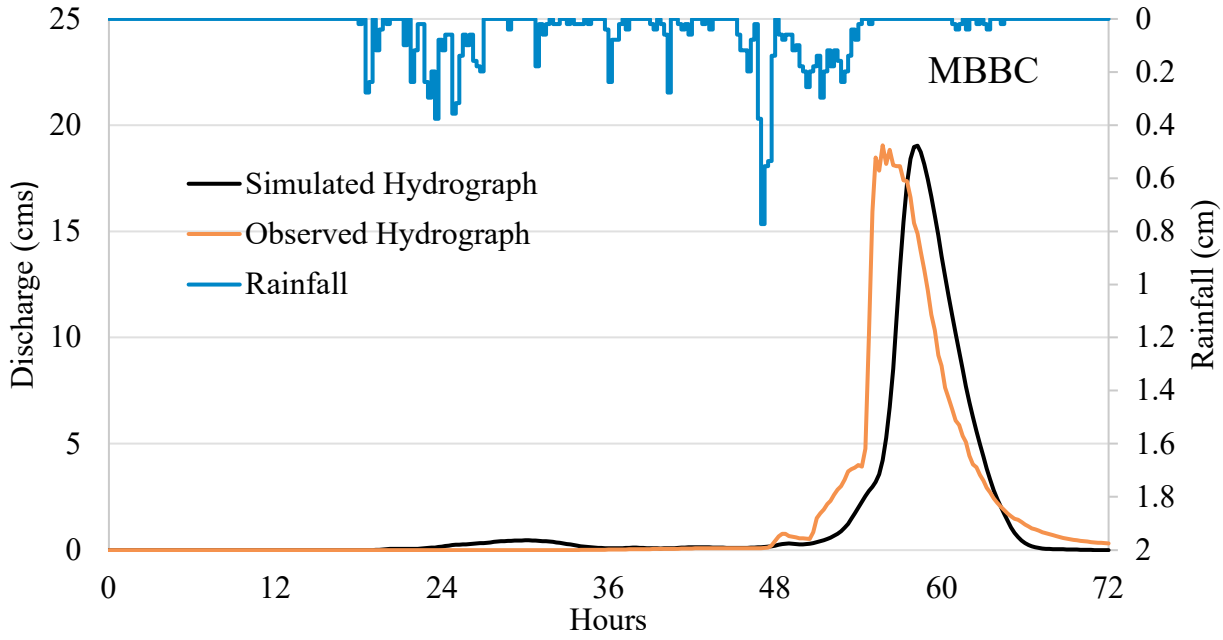

Figure 18. Validated hydrograph at MBBC gage location.

HEC-RAS Model Calibration and Validation. Changing the Manning's n value is an effective way of model calibration in HEC-RAS simulation (Jobe et al., 2018). In this study, the estimation of Manning's n was accomplished by the field survey and flood plain vegetation method (Table 2). The water surface elevation (WSE) in the HEC-RAS simulation was used to evaluate the model performance. Using the estimated Manning's n value, the simulated WSE of the MBBC gage site closely matched with the gage recorded WES for the peak discharge of 9.34 m^3/s (Table 18). Therefore, field-based Manning's n values were used for model calibration and further simulations. For validation, the model was also tested for a different peak discharge of 17.53 m^3/s, and the simulated WSE showed a similar result as the observed data (Table 18).

Table 18. HEC-RAS model performance at Middle Big Barren gage cross-section.

Rainfall Duration	Peak discharge (m^3/s)	Simulated WSE (m)	Observed WSE (m)
27th March 2018 to 29th March 2018	9.34	1.03	1.01
9th January 2020 to 11th January 2020	17.53	1.26	1.22

Present Day (2016) Hydrology of Middle BBC Watershed. Analyzing the present-day hydrologic scenario was the first step of the watershed modeling of the MBBC watershed. It was essential to evaluate the extent of hydrologic alteration in the present-day to assess the long-term effects of historical logging and past and present land use changes. This study evaluated present-day watershed hydrology by assessing the flow duration, average discharge, runoff depth, peak discharge, and lag time (Appendix C). The peak discharge of this rainfall event was 9.34 m^3/s that was considered as a bankfull discharge for the selected channel segment of the MBBC. The relative percent difference (RPD) was used to analyze the difference between the simulated and observed data.

In the present-day scenario, simulated flow duration values of four sub-basins were lower than the observed data (Appendix C). The RPD of these sub-basins was ranged from around 19% in WP to the highest 47% in TH (Appendix C). The observed hydrograph of these sub-basins was flashy than the simulated hydrograph that was responsible for this disagreement (Figure 16). In contrast, the simulated flow duration of UBT was 1.3 times higher than the observed flow duration (12.75 hours) (Appendix C). The simulated average discharge was higher for all the sub-basins except UBB. The RPD of average discharge was ranged from a maximum of 52% in TH to 2.5 % in UBT (Appendix C). The runoff depth of WP was simulated (0.4 cm) lower than the observed data (0.48 cm), with an RPD of 18.18% (Appendix C). However, the simulated runoff depth of the other four sub-basins was higher than the observed data. For runoff depth, the TH and UBB occupied an RPD lower than 10%, whereas UBT and PC occupied an RPD value lower than 30%. The peak discharge of all the sub-basins was simulated well with an RDP of less than 10% (Appendix C). The simulated lag time was lower than the observed data for the sub-basin TH, UBT, and WP. In contrast, the simulated lag time of UBB was matched perfectly

with the observed data (Appendix C). The Middle Big Barren Creek watershed outlet showed excellent results despite having greater variability in the five sub-basins (Figure 19). The RPD of average discharge, runoff depth, and lag time were zero (Figure 19, Appendix C). In contrast, the simulated flow duration was 2.42 hours higher than the observed data (22.83 hours). However, the RPD was around only 10%. The NSE coefficient value of this outlet was 0.85. Thus, it can be concluded that the HEC-HMS simulation accurately represented the present-day overall hydrology and rainfall-runoff scenarios of the MBBC watershed (Figure 19).

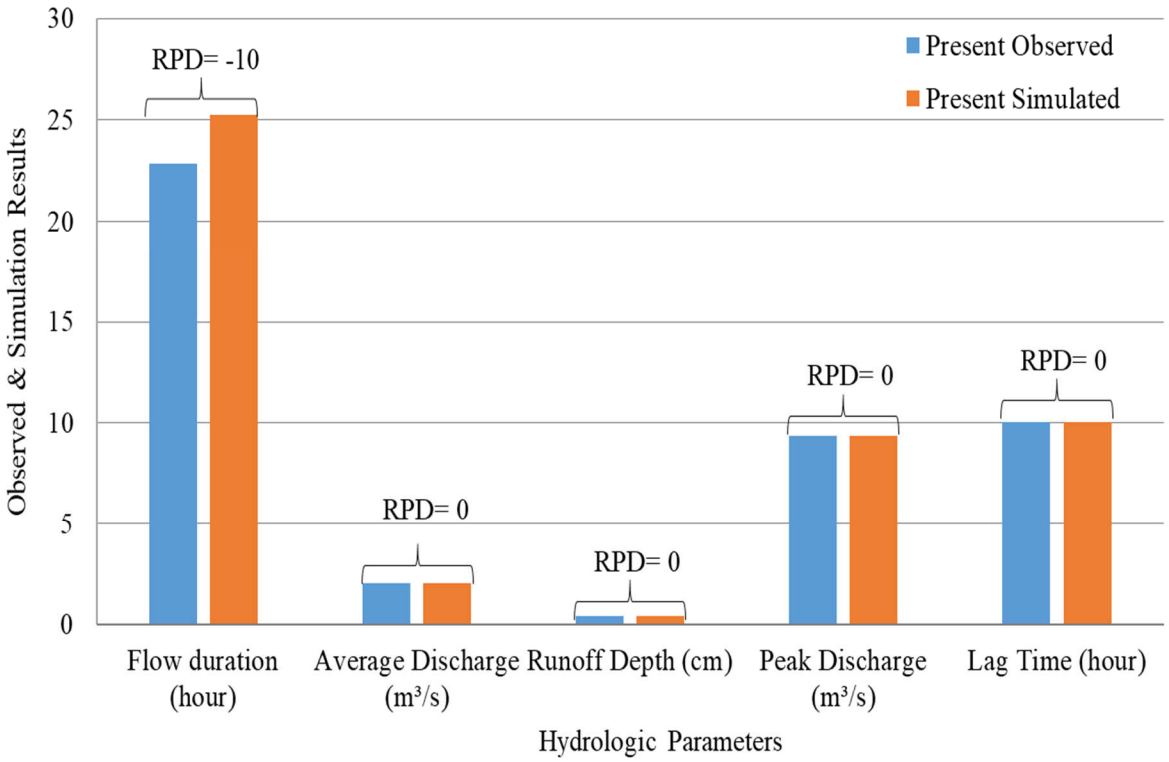

Figure 19. Present-day (2016) HEC-HMS simulation results at MBBC watershed outlet.

Pre-Settlement Scenario Generation in HMS-HMS. The analysis of the hydrology of the MBBC watershed in the pre-settlement forest cover was one of the primary objectives of this study. This analysis helped to evaluate the hydrology MBBC watershed during the pre-settlement shortleaf pine-dominated forest condition. The calibrated present-day HEC-HMS model was used to generate the pre-settlement hydrology of the MBBC watershed. Two different techniques were used to evaluate the pre-settlement hydrological condition of the MBBC watershed. First, a simulation was performed to test the impact of forest species change on watershed hydrology. Shortleaf pine was the dominant forest species during the pre-settlement condition, which is currently dominating by hardwood forest (Guyette et al., 2006). According to the pre-settlement scenario, forest species and land use were changed to analyze the pre-settlement watershed hydrology (Table 15). Second, simulation was performed in the shortleaf pine-dominated condition and reduced the calibrated SCS-CN by 1 to represent a good soil condition.

The simulated hydrographs showed variability of the hydrologic parameters in different scenarios (Figure 20, 21). In the first trial of the pre-settlement scenario, the flow duration was 8% lower in the present-day hardwood-dominated forest cover compared to the shortleaf pine-dominated forest condition for a 12.48 cm rainfall event (Table 19; Appendix D). The present-day flow duration was 25.25 hours, which was simulated at 27.50 hours during the shortleaf pine-dominated forest condition (Figure 20a). The present-day average discharge was 21% higher than the shortleaf pine-dominated forest condition (Table 19). In the pre-settlement forest cover, the average discharge was 1.68 m^3/s, which increased to 2.03 m^3/s in the present-day condition (Figure 20b). The runoff depth under the current hardwood-dominated forest condition (0.41 cm) was 17% higher than the pre-settlement runoff depth (0.35 cm) (Table 19; Figure 20c).

The minimum change was found in the watershed's peak discharge (Table 19; Figure 20d). It was found that in the present-day hardwood forest-dominated watershed, the peak discharge (9.34 m^3/s) was only 7% higher than the shortleaf pine-dominated forest (8.7 m^3/s) (Table 19; Figure 20d). No change was observed in the watershed lag time (Figure 20e, Table 19). In addition to the pre-settlement forest cover scenario, the simulation was also performed for 100% shortleaf pine and 100% hardwood forest cover conditions. Results showed that the present-day runoff depth (0.41 cm) and peak discharge was predicted 31% and 23% higher, respectively compared to the 100% pine cover condition. On the other hand, in the 100% hardwood forest condition, the runoff depth was predicted 8% lower, but peak discharge was simulated 3% higher than the present-day forest condition.

Table 19. Percent difference of the hydrologic parameters in present-day (2016).

Parameters	Present-day Simulated	Pre-settlement shortleaf pine forest cover	Pre-settlement forest cover and CN reduced by 1	Post-disturbance (shrubs cover and CN increased by 3)
Flow duration (hour)	25.25	-8% (-9%)	84% (59%)	-8% (8%)
Average Discharge (m^3/s)	2.03	21% (19%)	37% (31%)	-199% (100%)
Runoff Depth (cm)	0.41	17% (16%)	173% (93%)	-202% (100%)
Peak Discharge (m^3/s)	9.34	7% (7%)	140% (82%)	-245% (110%)
Lag Time (hour)	10.05	0% (0%)	-9% (10%)	17% (19%)

( ) = Relative Percentage Difference (RPD)

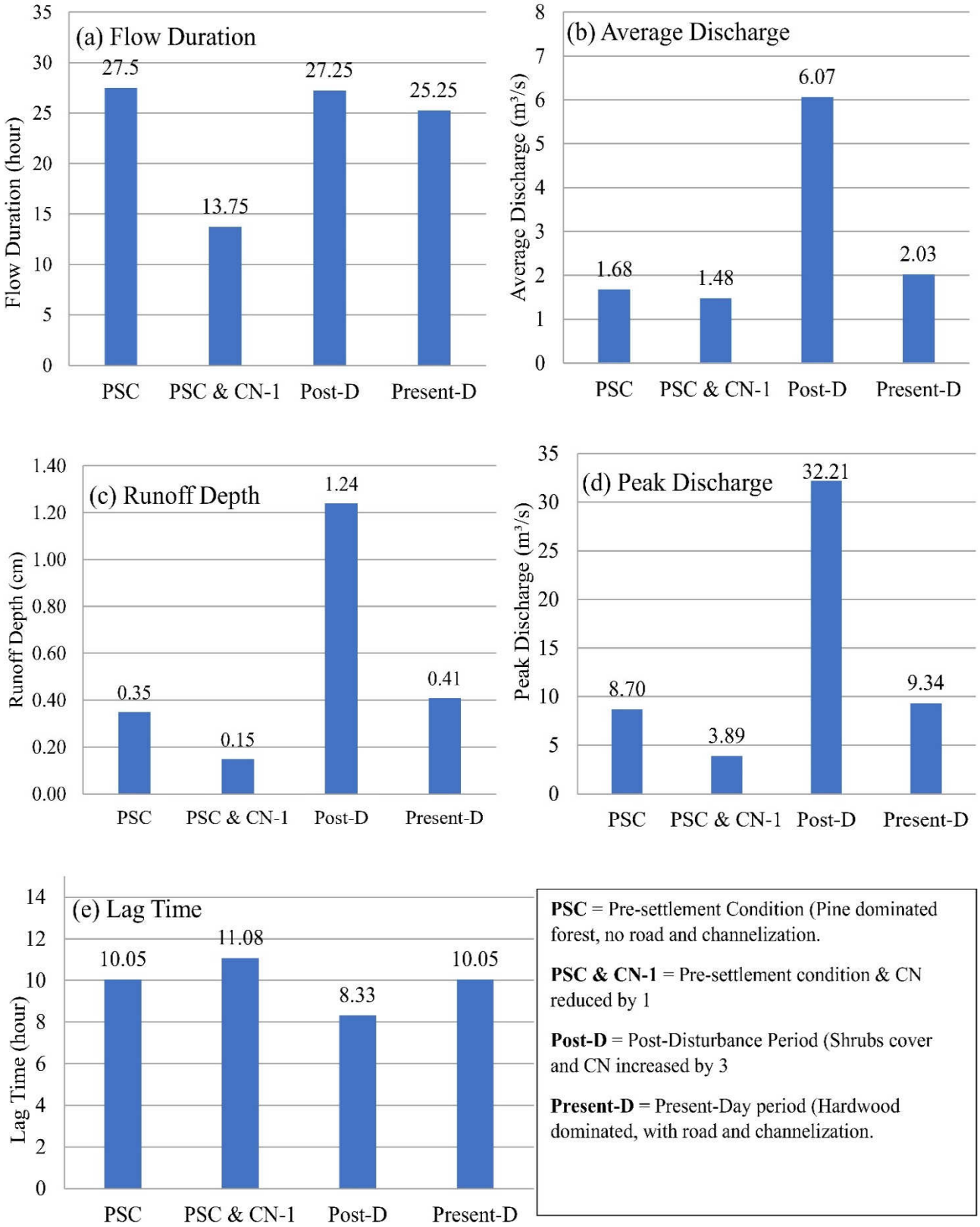

Figure 20. Hydrologic parameters at MBBC gage location for different scenarios.

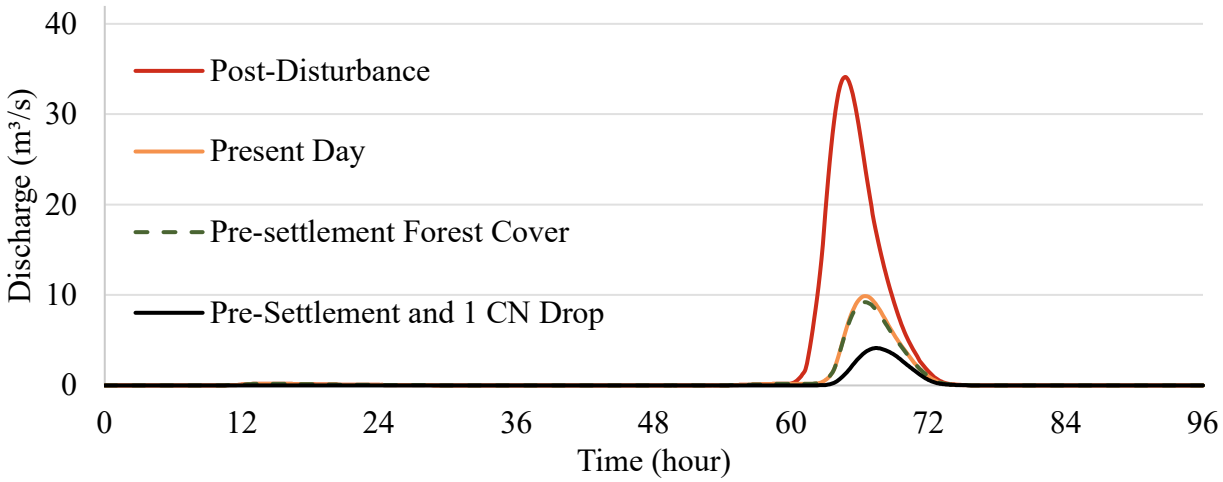

Figure 21. Hydrograph of the four different scenarios.

The simulated hydrographs showed variability of the hydrologic parameters in different scenarios (Figure 21). In the first trial of the pre-settlement scenario, the flow duration was 8% lower in the present-day hardwood-dominated forest cover compared to the shortleaf pine-dominated forest condition for a 12.48 cm rainfall event (Table 19; Appendix D). The present-day flow duration was 25.25 hours, which was simulated at 27.50 hours during the shortleaf pine-dominated forest condition (Figure 20a, 21). The present-day average discharge was 21% higher than the shortleaf pine-dominated forest condition (Table 19). In the pre-settlement forest cover, the average discharge was 1.68 m^3/s, which increased to 2.03 m^3/s in the present-day condition (Figure 20b, 21). The runoff depth under the current hardwood-dominated forest condition (0.41 cm) was 17% higher than the pre-settlement runoff depth (0.35 cm) (Table 19; Figure 20c, 21). The minimum change was found in the watershed's peak discharge (Table 19; Figure 20d, 21). It was found that in the present-day hardwood forest-dominated watershed, the peak discharge (9.34 m^3/s) was only 7% higher than the shortleaf pine-dominated forest (8.7 m^3/s) (Table 19, Figure 20d, 21). No change was observed in the watershed lag time (Figure 20e,

21; Table 19). In addition to the pre-settlement forest cover scenario, the simulation was also performed for 100% shortleaf pine and 100% hardwood forest cover conditions. Results showed that the present-day runoff depth (0.41 cm) and peak discharge was predicted 31% and 23% higher, respectively compared to the 100% pine cover condition. On the other hand, in the 100% hardwood forest condition, the runoff depth was predicted 8% lower, but peak discharge was simulated 3% higher than the present-day forest condition.

In the second trial, the pre-settlement forest cover and SCS CN-1 soil condition significantly changed all the hydrologic parameters (Appendix E). At present, the flow duration (25.25 hours) was 84% higher than the shortleaf pine forest and good soil condition (13.75 hours) (Table 19, Figure 20a, 21). The average discharge in the present-day forest condition (2.03 m^3/s) was 37% higher than the pre-settlement forest and SCS CN-1 soil condition (1.48 m^3/s) (Table 19). The runoff depth and peak discharge under the current forest condition were 173% and 140% higher, respectively, compared to the pre-settlement forest cover and SCS CN-1 soil conditions (Table 19). At present, the lag time (10.05 hours) was 9% shorter than the pre-settlement forest cover and good soil condition (11.08 hours) (Table 19, Figure 20e, 21). Due to an increase in the channel bed and floodplain roughness, the watershed lag time in the pre-settlement condition was higher compared to the present condition.

Sub-basin-wise analysis of the MBBC watershed showed that the impact of CN value reduction was different from sub-basin to sub-basin. Results showed that WP and PC were very sensitive to the CN value change. The decline of the flow was 100% for only one CN value change at WP (Appendix E). Pre-settlement forest composition showed that a maximum of 66% evergreen forest (shortleaf pine) was found in the WP watershed. This high percentage of shortleaf pine cover increased the canopy interception, and when this high canopy interception

interacted with the good soil condition (decreasing CN value), it drastically reduced the runoff depth the WP watershed (Appendix E). On the other hand, the PC watershed contained only 30% shortleaf pine forest cover, but around 24% and 18% of the watershed area is covered by excessively drained and moderately well drained Coulstone very gravelly sandy loam and Tonti silt loam soil cover (Figure 7) (Gott, 1975). These well-drained soils could be resposible for the significant decrease in runoff when coinciding with the reduced CN value (Appendix E). However, the upstream sub-basins faced a substantial reduction in all the hydrologic parameters except lag time in the CN value reduction scenarios (Appendix E). Decreasing CN value represented the pre-settlement forest condition where forest floor adequately covered by bursh and forest litter. In addition, increased in canopy incercept decreased the rain fall throughfall. These conditions increased the surface roughness and obstructed the watershed runoff that increased the lag time in all the sub-basins.

Post-Disturbance Scenario Generation in HEC-HMS. The disturbances in the post-disturbance period increased the average discharge, runoff depth, and peak discharge considerably compared to the present condition (Figure 20, 21; Table 19; Appendix F). At present, the flow duration was 8% lower than the post-disturbance period (Table 19). The maximum percentage change was observed in the average discharge due to the maximum soil disturbance and shortleaf pine forest cover losses. Currently, the observed peak discharge was 245% shorter than the post-disturbance period (Table 19). The simulated peak discharge in the post-disturbance period and shrubs cover was 32.21 m^3/s, whereas, in the preset-day forest cover, the peak discharge was 9.34 m^3/s (Figure 20d, 21). The average discharge in the current forest condition was 2.03 m^3/s which estimated at 6.07 m^3/s during the post-disturbance period (Figure 20b, 21). A reduction of 202% was observed in the runoff depth (Table 19). In the post-

disturbance period, the runoff depth was significantly higher (1.24 cm) than in the present-day condition (0.41 cm) (Figure 20c, 21). Because of increased watershed forest cover and channel roughness, the watershed lag time is 17% higher at the present day compared to the post-disturbance period (Table 19). During the post-disturbance condition, the reduction of forest cover and disturbed soil increased the rainfall-runoff, reducing the watershed lag time.

Watershed hydrology and channel form influence on hydraulic variables

This section aims to evaluate channel responses to the HEC-HMS simulated peak discharges under different land-use and disturbances scenarios. Three hydraulic parameters were estimated including channel shear stress, stream power, and velocity through 1-D HEC-RAS steady-state simulation using the HEC-HMS simulated peak discharges to access the channel response (Table 20). The hydraulic analysis of a channel is a valuable tool to understand the channel response to disturbance and process to obtain a quasi-equilibrium state that combines the impact of flow regime and channel boundary condition (Knighton, 1984; Singh, 2004). The present-day channel and floodplain conditions are discussed in the first part of this section by analyzing the pebble and tree count survey results. Later, HEC-RAS simulation results and related discussions are presented.

Table 20. HEC-HMS simulated discharges.

Scenarios	Simulated peak discharge (m^3/s)
Pre-settlement condition and CN drop 1	3.89
Pre-settlement condition (shortleaf pine-dominated forest)	8.70
Post-disturbance (shrubs cover and CN increased up to 3)	32.21
Present-day (hardwood dominated forest condition)	9.34

Channel Substrate Characteristics. The composition of the stream's bed and bank materials is one of the critical geomorphic variables that help to understand the channel form, erosion rate, hydraulics, and sediment supply (Rosgen, 1996). The pebble count survey is typically conducted using a gravelometer to assess the sediment size distribution of a stream (Rosgen, 1996). In this study, the pebble count survey showed that the upstream multi-threaded channels (sites 1-6) are shallow and mixed with lots of soil and fines (>50% fines and sand) and heavily covered by trees and vegetation. On the other hand, the downstream single-channel (Site 7, 8) were gravel-cobble-dominated, deep, and free of instream vegetation with relatively low flow resistance. Channel incision and a headcut were observed in the upstream part of site-7 (Figure 11). The grain size distribution of the study sites varied based on the channel form. A higher percentage of sandy soil was observed in the multi-threaded channel's bed, whereas mostly gravel-cobble size pebbles were found in the channelized segments (Table 21). In general, the pebble size of the study stream ranged from fine gravel to large cobble with an average substrate size of 22 mm, and the pebbles were ranging from 11 – 45 mm (Table 22). The D84 particle size of the eight survey sites was coarse gravel type with a range from 18– 64 mm (Table 22). The largest mobile clast size was ranged from the coarse gravel to boulder (32 – 450 mm) (Table 22). During the geomorphic assessment, a potential source of channel instability (headcut) was found upstream of site-7. The sediment supply in the channel increases because of the vertical incision of the headcut. Due to the increased sediment supply, this location acted as a sediment deposition zone. No fine sediments were found in the channelized segments (site-7 and 8) because of the higher velocity and shear stress. All the fine sediments were transported to the more downstream area due to the higher transport capacity of these sites. The largest mobile clast (450 mm), D50 (45 mm), and D84 (64 mm) were found in site-7 (Table 22).

Table 21. Percent distribution of the collected pebbles.

Site Number	Percent Fines (%)	Percent Sand (%)	Percent Pebble (%)
Site 1	28	37	35
Site 2	16	18	65
Site 3	17	27	56
Site 4	2	5	94
Site 5	17	0	83
Site 6	4	6	90
Site 7	0	2	98
Site 8	0	0	100

Table 22. Pebble size distribution at study sites.

Site	Number of Pebbles	Minimum (mm)	D25 (mm)	D50 (mm)	D84 (mm)	Largest Mobile Clast Size (mm)
Site 1	32	2.8	8	11	18.6	32
Site 2	64	4	10	16	35	172
Site 3	55	4	11	16	22.6	130
Site 4	92	5.6	11	22.6	32	160
Site 5	82	8	16	22.6	45	130
Site 6	89	5.6	11	22.6	64	160
Site 7	97	8	22.6	45	64	450
Site 8	99	8	22.6	32	45	160
Average	76	5.4	13.2	22.1	40	167
Minimum	32	2	8	11	18.6	32
Maximum	99	8	22.6	45	64	450

Channelization may be linked to the incision of the upstream of site-7. In addition, the higher velosity and shear stress increased the transport capacity of site-7 and site-8 and made the channel unstable (Simon and Rinaldi, 2006). The in-stream and flood plain trees and dense vegetation have increased the hydraulic roughness and dissipated the flow energy facilitated sediment deposition in the multi-threaded streams (McKenney et al., 1995). The higher percentage of the fine sediment and sand represented the lower sediment transport capacity of the natural multi-threaded streams (site 1-6).

Tree Count Survey Findings. The tree count survey was conducted to analyze the roughness coefficient of the in-stream and flood plain (FP) of the eight study sites. The total number active-channel tree counts ranged from 0 to 208 within the surveyed area of the sites, with an average count of 64 (Table 23). An average of 177 trees was found in the flood plain, ranging from 52 to 241 (Table 23). The multi-threaded channels covered the maximum number of tree counts in the flood plain and channel. A total of 68 trees were found in the point bar of channelized site-8, whereas no tree was found in site 7 (Table 23). The in-channel tree's average diameter was 6 cm which was found 9 cm in the flood plain (Table 23). The distribution of the basal area also high in the multi-threaded segments among the eight study sites (Figure 22). The maximum channel basal area was found in site-1 (around 6 m^2/ha), and the maximum flood plain basal area was found in site-8 (approximately 9 m^2/ha). The channelized segments (sites-7, 8) were covered by a minimum basal area (Figure 22). In the Big Barren Creek watershed Roman (2019) found that the basal area decrease with the increase in the drainage area. In addition, Roman (2019) found in-channel basal area of 87.6 m^2/ha and 9.0 m^2/ha for the drainage area less than 1.0 ha and greater than 10 ha., respectively. In another study on the Missouri Ozarks,

Hanberry et al. (2014) found that the basal area of Oak/Pine forest cover was 35 m^2/ha, Oak/Pine open woodland was 21 m^2/ha, and Oak/Pine closed woodland was 25 m^2/ha.

Table 23. Tree counts of study sites.

Location	Width of the cross-section (m)	Length of the cross-section (m)	Channel Tree Count	FP Tree Count	Avg. tree diameter (Channel)	Avg. tree diameter (Floodplain)
Site 1	20	42	44	68	10	10
Site 2	20	44	23	52	6	10
Site 3	20	52	26	63	8	12
Site 4	20	111	53	126	12	12
Site 5	20	111	118	241	4	8
Site 6	20	26	208	119	5	7
Site 7	20	57	0	175	0	5
Site 8	20	41	68	126	5	7
Average	20	61	64	177	6	9
Minimum	20	26	0	52	12	12
Maximum	20	111	208	241	0	5

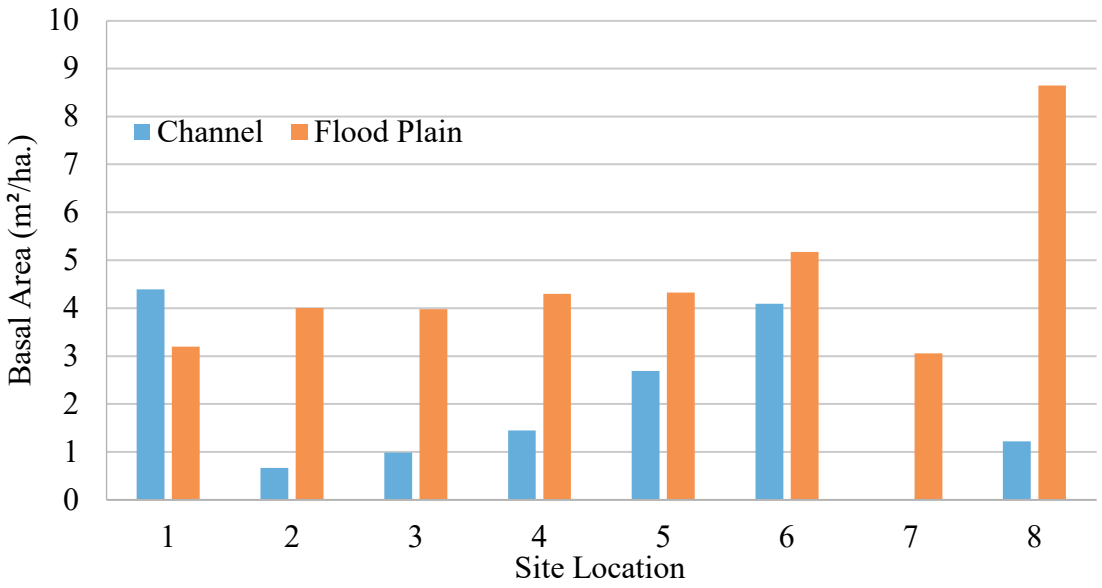

Figure 22. Estimated basal area of the study sites.

HEC-RAS Modeling Results

Width-Depth Ratio (W/D). The width-depth ratio is one of the crucial parameters to understand the stability of the channel that shows the distribution of energy within the channel and channel sediment movement for different discharges (Rosgen, 1996). This ratio is defined as the ratio of the bankfull surface width to the mean bankfull depth of the cross-section (Rosgen, 1996). The comparison between the channel shape and the width-depth ratio is vital to understand the disturbance impact on channel stability, pattern, and stream type (Rosgen, 1996). In the Rosgen classification, the width-depth ratio of multi-threaded channels is greater than 40, and single channels are lower than 40 (Rosgen, 1996). According to this range, among the eight study cross-sections, six are multi-threaded and stream type D4, where the W/D ratio ranged from around 91 to 138 (Table 24). This width-depth ratio was calculated for the bankfull discharge of 9.34 m^3/s.

Table 24. Width-Depth ratio of the eight study sites.

Location	Flow Area (m^2)	Top Width (W) (m)	Mean Depth (D) (m)	W/D Ratio
Site 1	25	50	0.50	101
Site 2	35	70	0.50	138
Site 3	34	57	0.60	96
Site 4	28	55	0.50	111
Site 5	22	53	0.41	131
Site 6	20	42	0.47	91
Site 7	26	16	1.57	10
Site 8	20	26	0.79	32

The increased slope and low width-depth ratio can increase the shear stress and stream power, causing erosion and increasing channel erosion (Hadadin, 2010). Generally, channel incision occurs when the width-depth ratio is less than ten, corresponding to the high unit stream power (Rosgen, 2001). In this study, the incision was observed in the upstream portion of site-7. Results showed that the w/d ratio of this site was 10 (Table 24). Thus, the lower w/d ratio of this site and the upstream segment is responsible for the channel incision. Rosgen (2001) found that the wider channel (high w/d ratio) bed occupies a higher percentage of sand contents for a given bankfull discharge but then decreases, and as a result, the channel bed will be dominated by gravel and cobbles. In this study, a higher percentage of sand components (37%) and fine sediments (28%) were found in the most upstream site-1 with a w/d ratio of 101 (Table 21, 24). However, this scenario was changed in the downstream sites with an increased percentage in the gravel and cobble (Table 21). Rosgen (1996) showed that D4 stream types are characterized by

high bank erosion. However, field investigation found that the multi-threaded D4 stream type of the study area has high bank stability with in-stream and flood plain trees and vegetation, low sediment load, and infrequent flow.

Channel Velocity. Channel velocity is an important hydraulic parameter that is essential for controlling the bedload transport rate (Wilcock et al., 2009). In addition, flow velocity and hydraulic depth are important factors for estimating the stream power or the erosion potential of a stream. (Naiman et al., 2005; Yang and Stall, 1974). The changes in channel velocity-depth relation can significantly alter the channel form by making it broader and deeper (Mosley, 1982). For a constant discharge, channel cross-sectional area (m^2) and mean flow velocity (m/s) are highly correlated with each other (Naiman et al., 2005). A narrow shape channel causes a deeper and faster flow, whereas an increase in width causes shallow depth and slow flow (Naiman et al., 2005). Channel velocity for the pre-settlement forest cover and good soil condition (SCS CN – 1) discharge (3.89 m^3/s) varied between 0.19 to 0.36 m/s. In this scenario, a maximum velocity of 0.36 m/s was found at site-6 (just above the headcut), and the minimum velocity was found at site-7 (Figure 23a). The conversion of shortleaf pine-dominated forest cover to hardwood-dominated forest cover did not change the channel velocity of the study sites. In this scenario, the channel velocity ranged from 0.28 to 0.46 m/s (Figure 23a). However, in the post-disturbance period, channel velocity was increased to a range from 0.34 to 0.82 m/s (Figure 23a). The relation among the channel velocity, hydraulic depth, and top width showed that in the post-disturbance discharge (32.21 m^3/s), the channelized segments (site-7 & 8) were undergone an increase in the hydraulic depth and decrease in top width that caused higher channel velocity in these segments (Figure 23a, 24, 25). However, despite having low hydraulic depth and high top width, the maximum channel velocity (0.82 m/s) was observed at site-4 (Figure 23a, 24, 25).

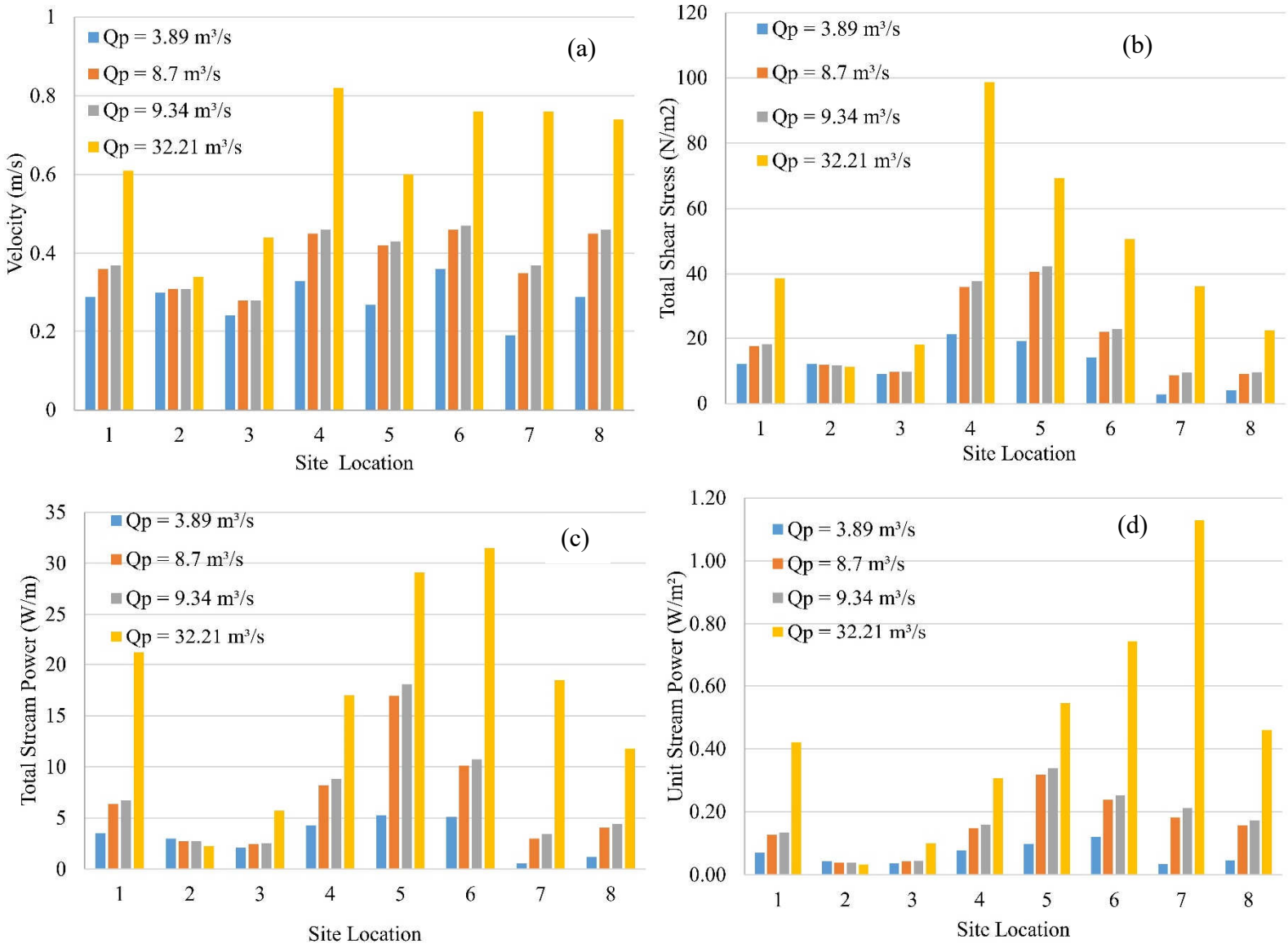

Figure 23. HEC-RAS simulation results of the study sites.

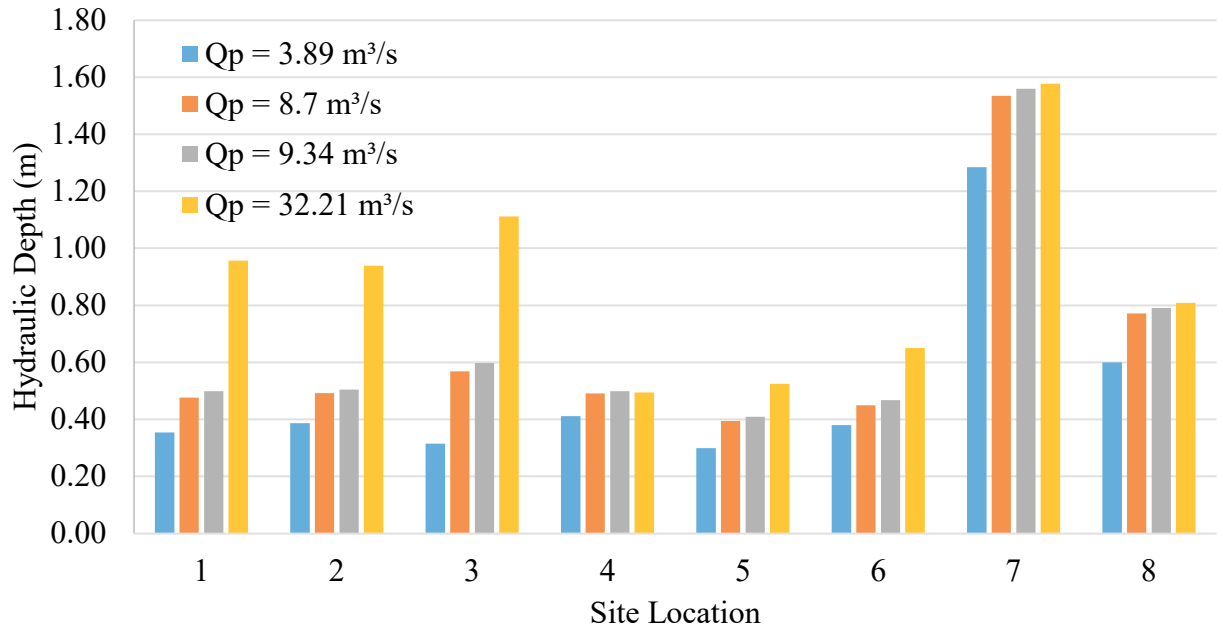

Figure 24. Hydraulic depth of the study sites.

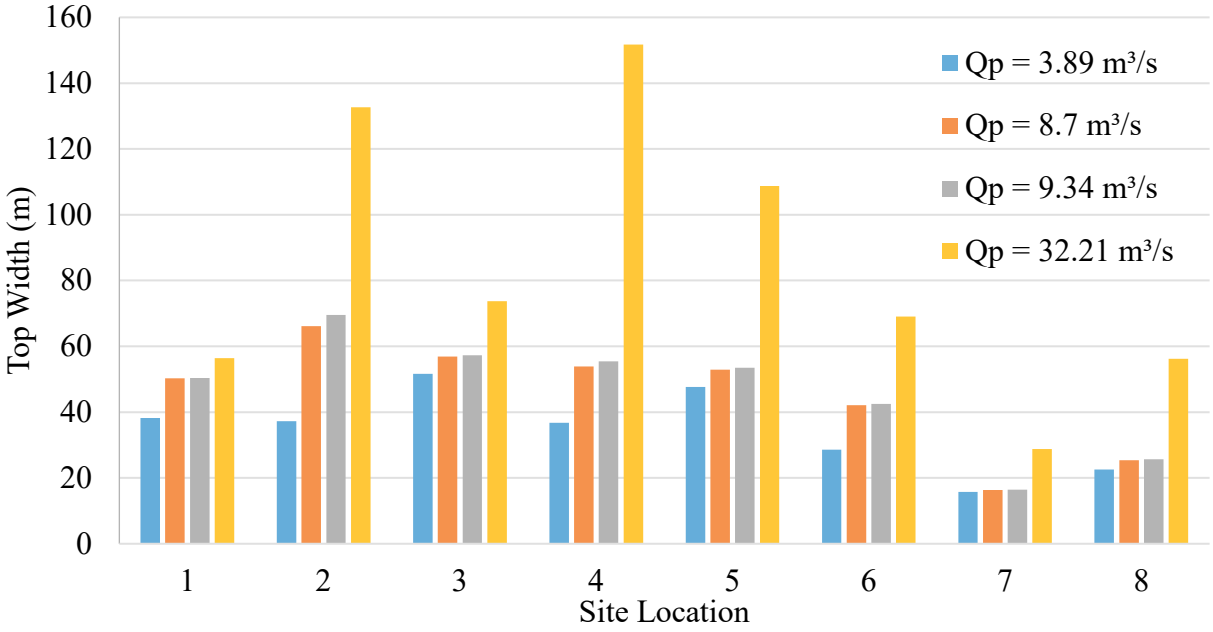

Figure 25. Top width of the study sites.

The Froude numbers in all simulations were relatively low throughout the entire channel segment except the headcut location (Figure 26, 27). The Froude number is a function of channel velocity, hydraulic depth, and gravitational acceleration that can be expressed as $F = V/\sqrt{(gd)}$ where V is velocity, g is the acceleration due to gravity, and d is hydraulic depth (Krause, 2010). For the pre-settlement forest cover to present-day scenario discharges, the multi-threaded segments (site-1 to 6) experiences a lower Froude number (< 0.4) since the channel slope of this segment was gentle (0.004) (Figure 26, 27). In contrast, this scenario changed to the single-channel and channelized segments (Figure 26). In the headcut location, the Froude number was estimated above one that caused a super-critical flow in this segment (Figure 26, 27).

Overall stream velocity showed higher velocity in the segment from the headcut to the channelized segment (Appendix G). Changing flow patterns from sub-critical to supercritical due to headcut and low stream bed resistance was responsible for the increased velocity of this segment. On average, during the post-disturbance period, the average velocity of the multi-threaded segment was increased by two times compared to the pre-settlement forest cover and good soil condition (Appendix G-1, G-4). A higher velocity was found near the bank of the multi-threaded segment that caused stream bank erosion during the post-disturbance period (Appendix G-4). In the post-disturbance scenario (32.21 m^3/s), the average velocity of the single-channel was ranged from 0.71 to 1.11 m/s that was found from 0.49 to 1.55 m/s in the channelized segment (Appendix G-4). No significant change was observed in the average velocity due to converting presettlement shortleaf pine-dominated forest cover to the present-day hardwood-dominated forest.

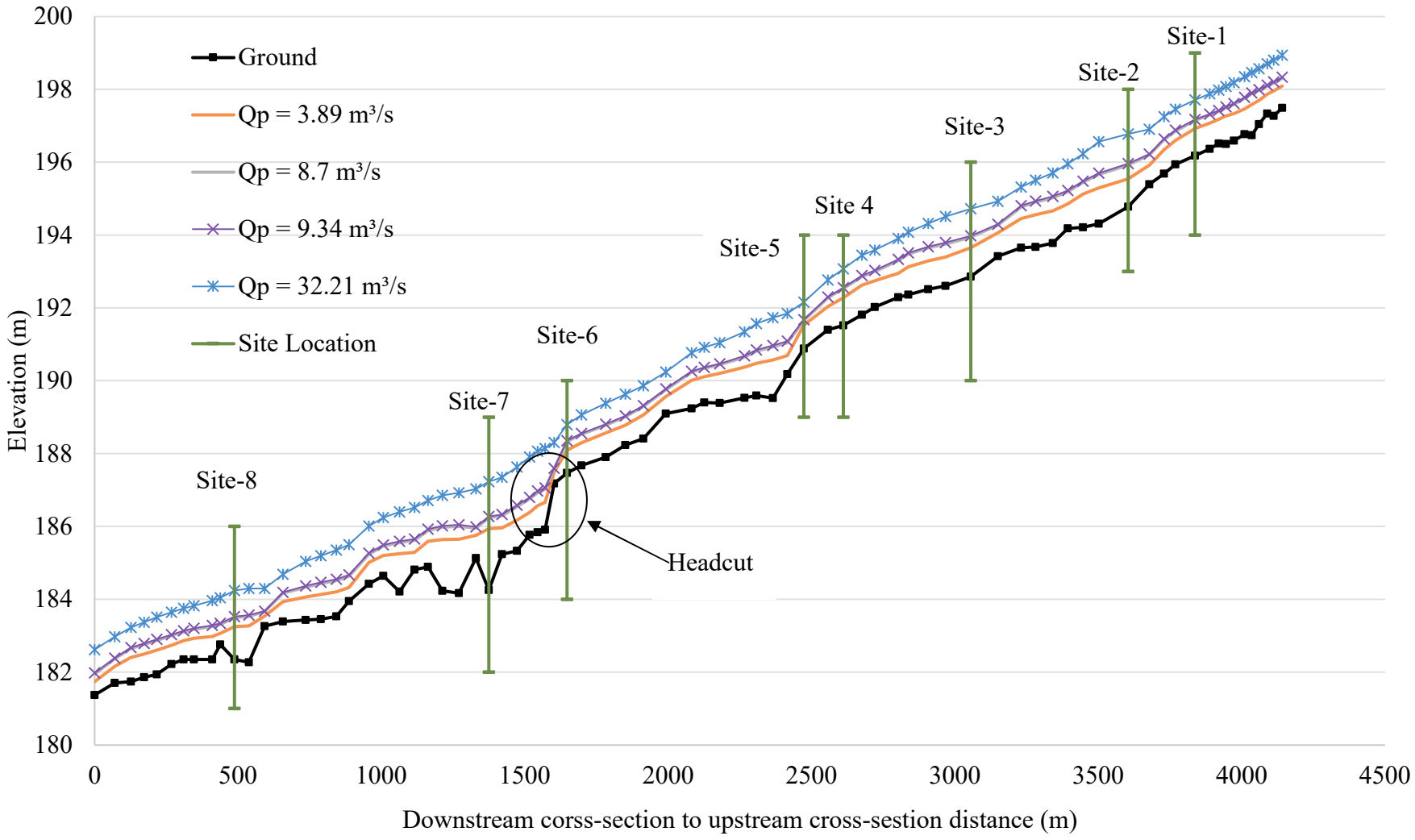

Figure 26. Longitudinal profile of the study stream and water surface elevations.

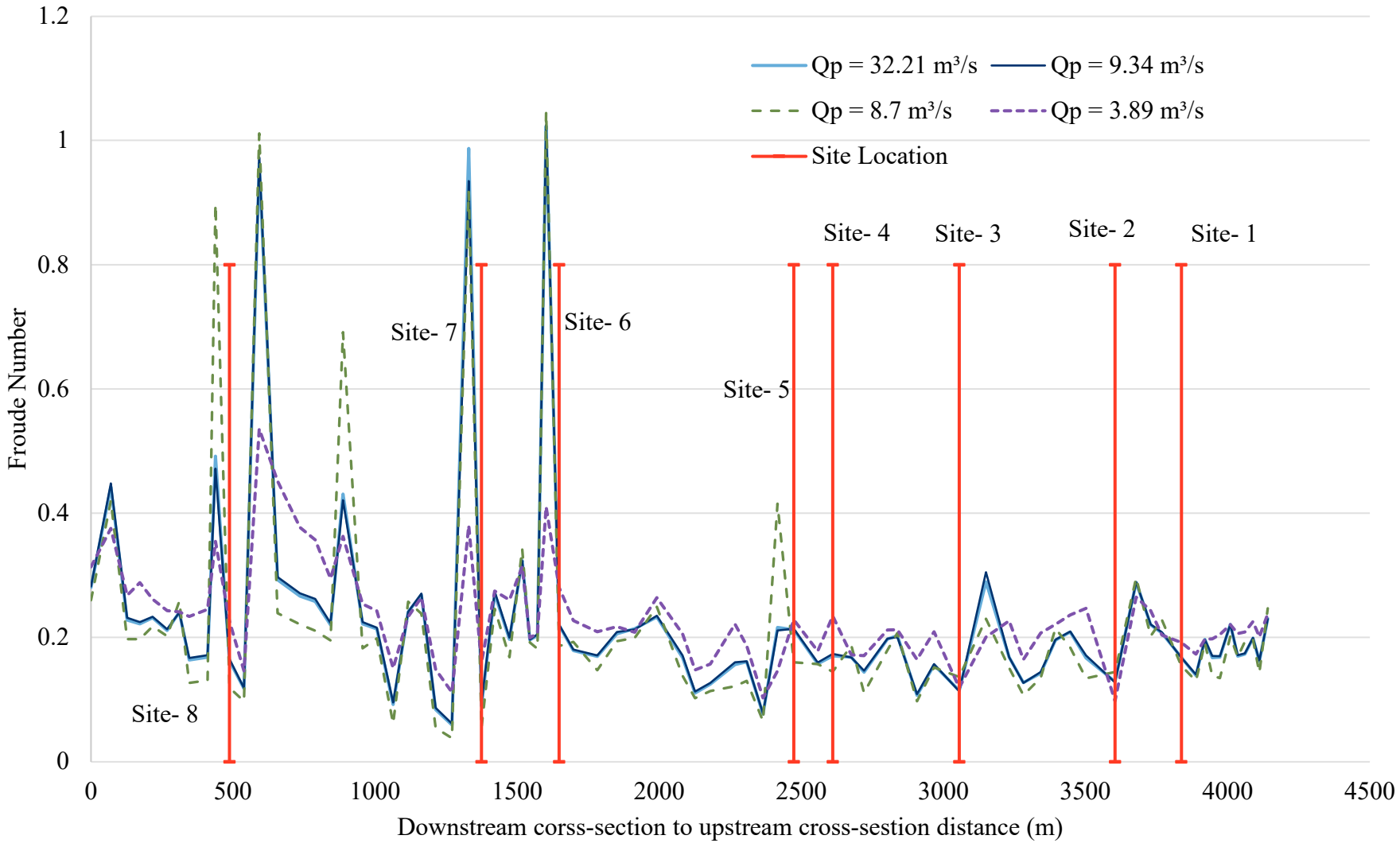

Figure 27. Channel Froude number along with the longitudinal profile.

Channel Shear Stress. Channel shear stress is another crucial factor that controls the sediment transport and erosion process (Krause, 2010). It is vital to determine the channel's sediment transport at a bankfull discharge as it is considered the channel-forming discharge (Krause, 2010). Channel shear stress is proportionately related to the hydraulic radius and energy gradient slope of a channel (Brunner, 2016). In this study, the site-specific distribution of channel shear stress showed a gradual downward transition from the multi-threaded site-4 to the channelized site-8 for the post-disturbance scenario discharge (32.21 m^3/s); as a result of decreasing energy gradient slope (Figure 23b, 28). In addition, the hydraulic radius was almost the same as the hydraulic depth of the channel (Figure 24). In the post-disturbance scenario, the maximum shear stress (around 98.71 N/m^2) was found in site 4 (Figure 23b). However, the energy gradient slope and hydraulic radius of site-5 were higher than site-4 (Figure 28). A pool effect was responsible for the higher shear stress of site-4. The water surface elevation of site-4 was 1.55 m for the post-disturbance period, which was estimated at 1.28 m at site-5 (Appendix H-4, H-5). Due to this higher depth, the shear stress of site-4 was higher than site-5. No significant change was observed in the total shear stress due to the conversion of hardwood forest dominated to shortleaf pine-dominated forest condition (Figure 23b). However, in the post-disturbance scenario, a significant change in shear stress was found in the single-channel compared to the multi-threaded channels of the study stream. In the post-disturbance scenario, the shear stress site-7 was around 13 times higher compared to the pre-settlement forest cover and good soil condition (Figure 23b).

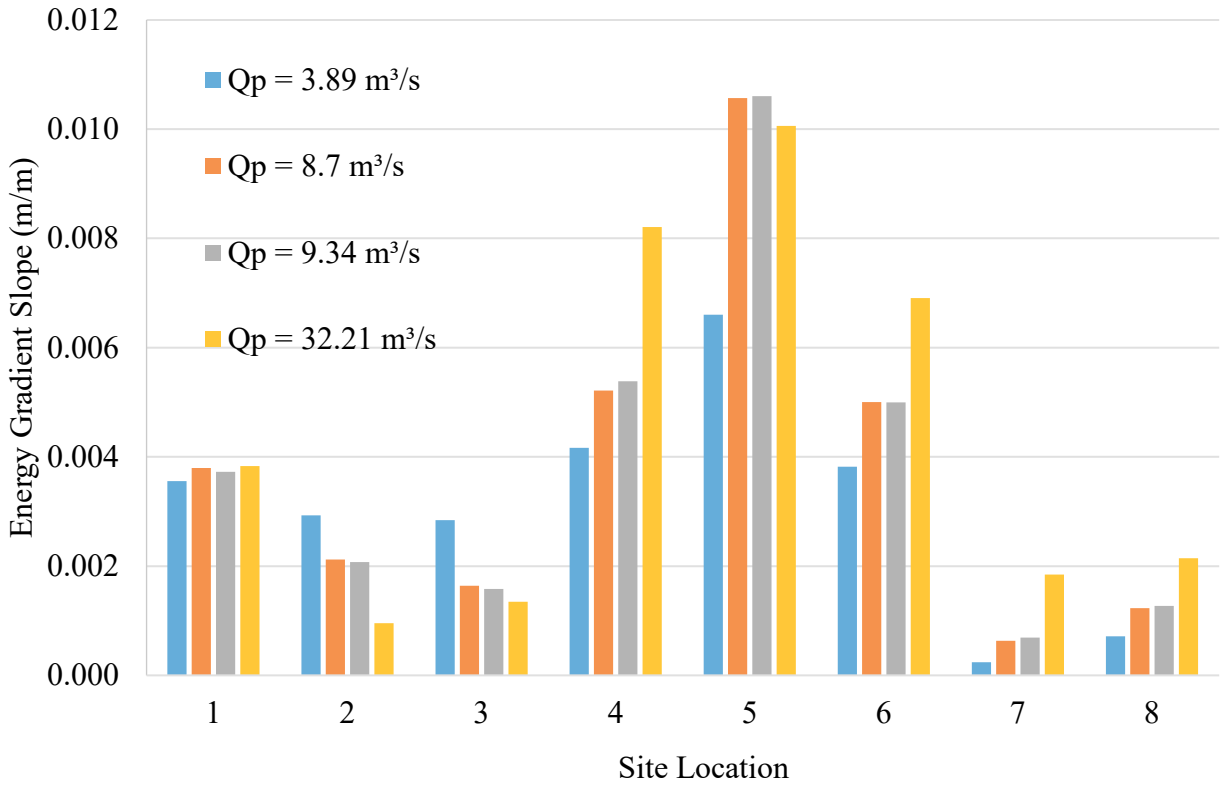

Figure 28. Energy gradient slopes for different discharges.

In this study, the HEC-RAS simulated shear stress and their associated moveable maximum sediment diameter were compared with the channel types and field measured grain size distribution. The simulated shear stress (around 99 N/m^2) of site-4 for the post-disturbance discharge was enough to move sediment with a maximum diameter of 167 mm (large cobble) (Figure 29). The pebble count survey result showed that this site's maximum observed pebble diameter was 90 mm, and D50 was 22.6 (Figure 29). Thus, the post-disturbance discharge could significantly alter the bed form and sediment transport of site-4. A similar finding was also found at site-1, where the post-disturbance discharge generated shear stress could transport a 63 mm sediment that was higher than the observed maximum pebble diameter (32 mm) (Figure 29). However, a different scenario was observed for the remaining four sites. On these sites, the post-

disturbance discharge generated shear stress was able to transport sediments that were lower than the observed maximum sediment diameter (Figure 29). In general, in the multi-threaded segments, the shear stress of all the scenarios could transport sediments that were higher than the observed D50, which caused more channel erosion during the simulation periods of the segment (Figure 29). On the other hand, site-7 and 8 were found comparatively stable where the pre-settlement and present-day shear stress could transport sediments that were lower than the observed D50 (Figure 29).

The overall shear stress distribution of the entire study stream showed that during the pre-settlement forest cover and good soil condition (Q = 3.89 m^3/s), the average shear stress of the multi-threaded segment was 19 N/m^2, which was calculated 33 N/m^2 in the channelized segment (Appendix I-1). The average shear stress of the incised and single-channel was estimated at 58 N/m^2 for the discharge of 3.89 m^3/s (Appendix I-1). In the present-day scenario, the average shear stress of the incised single channel was considerably higher compared to other scenarios. In the present day, the average shear stress of this segment was estimated at 105 $N/m^{2,}$ and a maximum of 307 N/m^2 was calculated at the headcut location that causing more channel incisions by increasing erosion and sediment supply. Channel incision occurs when a stream is affected by huge imbalances between upstream sediment supply and respective transporting power due to anthropogenic and natural disturbances (Simon and Rinaldi, 2006). It happens more where degradation starts without widening the channel with maximum boundary shear stress and unit stream power (Simon and Thorne, 1996). The lower w/d ratio (< 10) upstream to site-7 is crucial for increasing the incised channel and headcut migration. From this headcut location to site-7, the total shear stress dropped 307 to 10 N/m^2 (Appendix I-3). This condition had made this site-7 a depositional zone that obtained sediment from the headcut erosion.

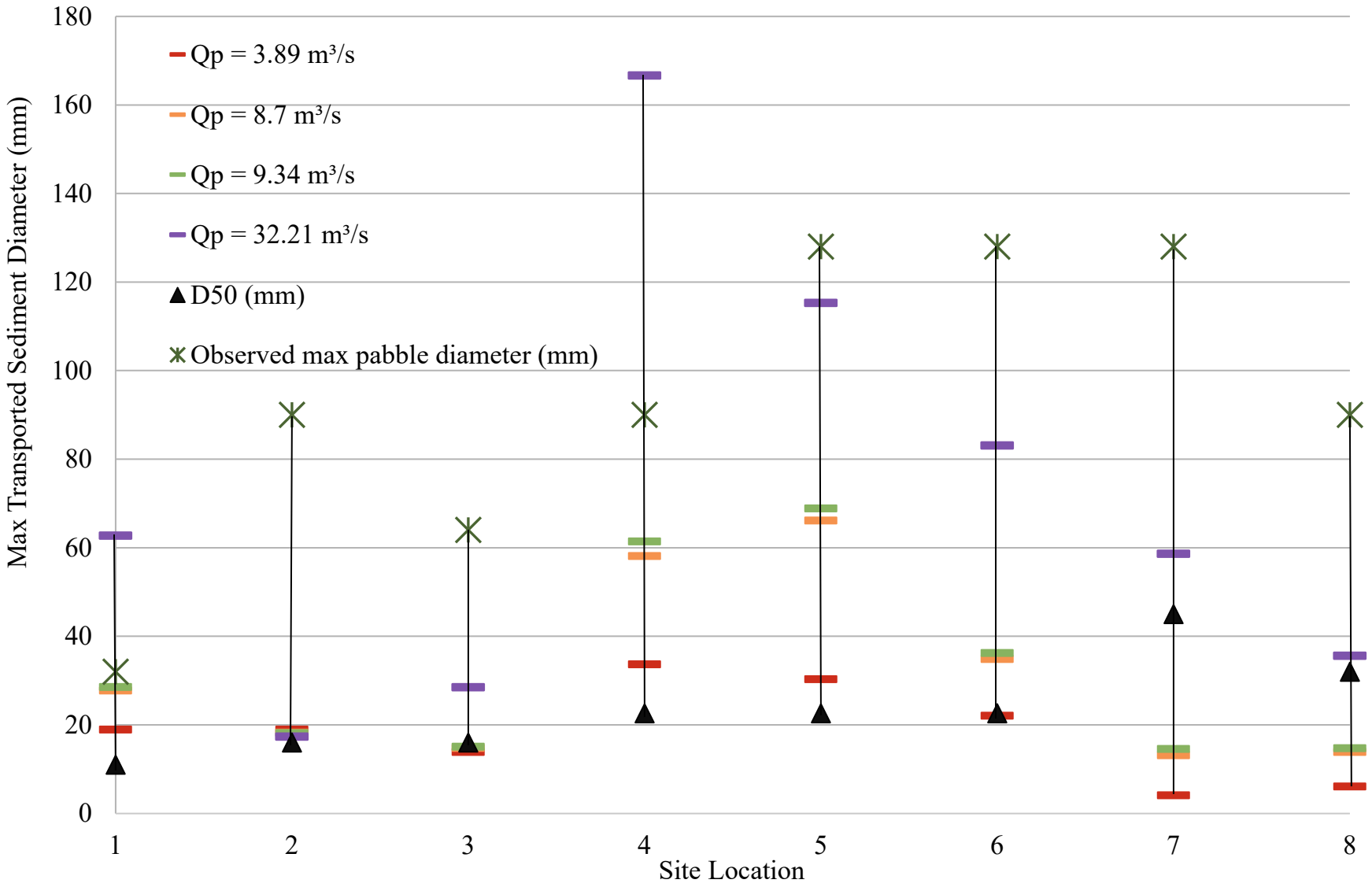

Figure 29. Maximum moveable sediment diameter for different peak discharges.

Channel Stream Power. Stream power is an important hydraulic parameter that can cause channel erosion in an increased peak discharge (Simon, 1989; Magilligan, 1992; Merritt and Wohl, 2003; Simon and Rinaldi, 2006; Surian and Cisotto, 2007; Ortega and Garzón Heydt, 2009; Yochum et al., 2017). The aggradation and degradation of the channel are related to the low and high channel's stream power (Simon, 1994). Then total stream power showed a decreasing trend for the present-day bankfull discharge (9.34 m^3/s) from site-6 to site-8 because of the downward energy gradient slope (Figure 23c, 28). In contrast, the unit stream power showed an increasing trend from site-4 to site-7 (Figure 23d). In the post-disturbance scenario, the total stream power of site-7 was increased by 34 times compared to the pre-settlement discharge of 3.89 m^3/s. However, maximum total stream power (32 W/m) was estimated at site-6. In the present-day and pre-settlement scenario discharges, maximum total stream power was estimated at site-5 (Figure 23c).

The entire study stream's overall total stream power distribution scenario showed a higher value ranging from 3.47 to 473 W/m in the incised and channelized segments for the present-day bankfull discharge (9.34 m^3/s) (Appendix J-3). During the pre-settlement discharge (3.89 m^3/s), the total stream power of this segment was between the range from 0.54 to 264 W/m (Appendix J-1). However, the increasing w/d ratio and decreasing energy gradient slope reduced the total stream power to a range of 18 to 87 W/m in the channelized segment for the post-disturbance discharge 32.21 m^3/s (Appendix J-4). At present-day discharge, the total stream power of the multi-threaded segment ranged from 2.24 to 27 W/m, which was calculated between the range 0.83 to 450 W/m in the channelized segment (Appendix J-3)

CONCLUSIONS

While headwater streams are vital components of a watershed, their hydrological responses to human and natural factors remain understudied (Kleelamp, 2016). Headwater stream channels are the conduits that disperse the effects of watershed disturbances, excessive runoff, and eroded sediment downstream and therefore are important for understanding the influence of human modifications on drainage networks (Macdonald and Coe, 2007). In the Ozark Highlands previous studies have focused on the larger alluvial channels downstream, with few studies of smaller headwater streams like Big Barren Creek (Kleekamp, 2016; Nickolotsky, 2005; Shepherd et al., 2010; Thies, 2017). This study aimed to understand the hydrologic and geomorphic alterations of the MBBC watershed due to anthropogenic disturbances including exploitive logging between 1890 and 1910. Using HEC-HMS simulations, hydrologic changes in a flood hydrograph were compared between the present-day hardwood-dominated watershed and several different historical land-use scenarios including a pine-dominated forest prior to Euro-american settlement. The present-day scenario was modeled in HEC-HMS using the most recent 2016 NLCD dataset, web soil survey data, meteorological parameters for the year 2018 to analyze a near-bankfull flood with a peak at 9.3 m^3/s produced by a 12.5 cm rainfall event during March 27-29, 2018. The historical land-use scenarios were generated by changing the forest species composition and soil/land-use characteristics based on published literaturature and land use records. In addition, the effects of different hydrologic senarios on channel hydraulics were assessed by comparing results from HEC-RAS modeling supported by channel morphology, channel substrate, and vegetation surveys for a main channel segment.

Importantly, model calibration was supported by actual discharge records from six continuous gaging stations located within Middle Big Barren watershed ranging in drainage area from 1.6 to 47.8 km^2. The calibration of the HEC-HMS model for 2018 conditions was performed by adjusting the curve number and maximum surface storage values and using flow data from a continuous stage gage network with calibrated rating curves. The average curve number (CN) of the MBBC watershed form the calibrated present-day model was 72. During the calibration process the model was found to be very sensitive to the curve number. For example, the reduction of only one unit from the calibrated CN value to indicate the better condition of the presettlement soils lowered the hydrograph discharge peak to zero for one sub-watershed in the gage network. Nevertheless, CN values used in this study were supported by measurements and assumptions reported by published studies. Through trial and error, the model was sufficiently calibrated with available data yielding a Nash-Sutcliffe Efficiency (NSE) coefficient of 0.85.

In the HEC-RAS simulation, Manning's roughness coefficients were evaluated during calibration to accurately indicate the water surface elevation (WSE) at the MBBC gage site. In this forested and rugged watershed, Manning's n values were estimated using the relative roughness of the channel and vegetation density on the floodplain. Roughness values were considered acceptable since the simulated WSE of the peak discharge (1.03 m) derived by the HEC-RAS simulation closely matched the field measured peak stage (1.01 m). The findings of this study will provide important insights to better understand the history of hydrologic changes and channel evolution in the watershed.

There are five key findings of this study:

1. Forest species composition has a significant impact on the runoff depth/rate and peak discharge of floods. In the present-day forest scenario, the observed runoff depth and peak

discharge of the MBBC watershed were 0.41 cm and 9.3 m^3/s, respectively. In comparision, forests in the pre-settlement period contained three times more shortleaf pine area with better soil conditions (i.e., CN reduced by 1) yielding a reduced runoff depth at 37% and peak discharge at 42% of the present-day condition. These findings suggest that shortleaf pine forest cover tended to increase the canopy interception and evapotranspiration, minimize rainfall throughfall, and reduced the total runoff and peak discharge. In general, the change from shortleaf pine to hardwood forest composition reduced canopy interception by 29% during an early spring rainstorm in the leaf-off season. Recent rainfall trends suggest larger rainfall events are occurring in the late winter-early spring prior to leaf-on conditions;

2. During the post-disturbance scenario, reduced forest cover and poorer soil/surface roughness conditions significantly increased the runoff depth and peak discharge to the highest levels assessed for this study. During the peak disturbance period defined as occuring prior to forest recovery with cut-over and shrub-dominated forest conditions, the runoff depth and peak discharge were estimated to be 1.2 cm and 32.2 m^3/s, respectively, with both about 2-times greater than under present-day conditions. During and after the peak logging period (1900-1930), higher runoff rates probably increased annual flood discharges, upland and channel erosion, suspended sediment yields, and channel size in headwater channel systems in MBBC;

3. Field data and Manning's n calculations indicated that channel roughness coefficients of the multi-threaded channel segments were higher compared to the single-channel segments. The average channel Manning's n value for multi-threaded segments was 0.13, 2-times higher than that of the single-channel segments. The average Manning's n value for the floodplain

along multi-threaded channels was 0.18, about 1.4-times higher than single-channel segments. The channel substrate composition for multi-threaded segments was typically fine-grained with more sand, fines, and organic matter/debris compared to single channel and human modified segments which contained more gravel, cobble, and boulders. Recall that in general, all streams in MBBC were ephemeral in nature so a variety of trees species were able to grow to maturity on the channel bed including pine, sycamore, oaks, and other hardwoods;

4. HEC-RAS modeling under different historical land-use scenarios showed that channel shear stress differed noticeably among the multi-threaded, single, and human-modified (i.e., channelized with built levees) channel segments in MBBC. Under present-day forest conditions, average shear stress values were 105 N/m^2 in single-channel reaches, 40 N/m^2 in channelized segments, and 25 N/m^2 in multi-threaded channel systems. Compared to pre-settlement forest cover with good soil conditions, present-day shear stress values increased by 29% in the multi-threaded channel, 59% in the single-channel, and 19% in the enlarged channelized segments. These findings suggest that increased shear stresses on channel beds due to higher runoff rates produced during past exploitive logging periods and, to a lesser degree, under recent land use management may have enlarged channels and transformed pre-historical multi-threaded systems into single-channel forms in some forested segments; and

5. Total stream power trends closely followed those for shear stress for present-day scenarios. Compared to the post-disturbance scenario, present-day stream power values were lower by 68% in multi-threaded segments, 23% in single-channels, and 14% in channelized segments. On the other hand, in the post-disturbance period, the unit stream power was higher by 23%

in multi-threaded segments (0.27 W/m^2), 73% lower in single channel (1.29 W/m^2), and 47% lower in channelized segment (0.87 W/m^2). In the post-disturbance period, the higher stage of the larger flood peak caused flow to spread out across the rough floodplain, thus reducing the unit stream power in the single-channel and channelized segments. It is apparent that pre-settlement channel widths were probably narrower than the present (Casagrand, 2021). This study suggests that higher shear stress and total stream power due to increased runoff was probably responsible causing channel scour and incision thus producing the wider channels observed in the forest today.

Using field surveys, geospatial analysis, and numerical modeling, this study evaluated the present-day and historical hydrology of the Big Barren Creek watershed. The change in forest composition from native pine to post-disturbance hardwoods triggered by exploitive logging from 1890-1910 appears to have been a main driver of hydrological change that continues to affect present-day channels. Exploitive logging of pine forests and, to a lesser extent, recent land use, resulted in widespread hardwood forest regeneration in Big Barren watershed. Therefore, reduced canopy interception rates, poorer soil infiltration, and lower evapotransipiration rates associated with historical logging practices and hardwood forest regeneration resulted in higher runoff rates which increased the magnitude and frequency of channel-forming floods in the leaf-off season whem nost flood-producing rains occur in the region. Subsequently, the energized hydrology probably resulted in the transformation of multi-threaded channel systems to single channel forms in many stream segments to create wider and deeper channels to contain the higher dicharges. The modeling approach used here can also be used to evaluate the effects of climate change on stream hydrology and channel response such as the effects of more intense

rainstorms and larger floods now being reported for the Ozark Highlands including several districts of Mark Twain National Forest.

REFERENCES

Abdelkarim, A., Gaber, A.F.D., Alkadi, I.I., Alogayell, H.M., 2019. Integrating remote sensing and hydrologic modeling to assess the impact of land-use changes on the increase of flood risk: A case study of the Riyadh-Dammam train track, Saudi Arabia. Sustain. 11, 1–32. https://doi.org/10.3390/su11216003

Ali, M., Khan, S.J., Aslam, I., Khan, Z., 2011. Simulation of the impacts of land-use change on surface runoff of Lai Nullah Basin in Islamabad, Pakistan. Landsc. Urban Plan. 102, 271–279. https://doi.org/10.1016/j.landurbplan.2011.05.006

Allen, R. G., Pereira, L.S., Raes, D., Smith, M., 1998. Crop evapotraspiration guidelines for computing crop water requirements., FAO Irrigation & drainage Paper 56. FAO, Food and Agriculture Organization of the United Nations,Roma.

Anderson, R.J., Bledsoe, B.P., Hession, W.C., 2004. Width of streams and rivers in response to vegetation, bank material, and other factors. J. Am. Water Resour. Assoc. 40, 1159–1172. https://doi.org/10.1111/j.1752-1688.2004.tb01576.x

Andresen, J., Hilberg, S., Kunkel, K., 2012. Historical climate and climate trends in the midwestern USA, U.S. National Climate Assessment Midwest Technical Input Report.

Andrews, E.D., Nankervis, J.M., 1995. Effective discharge and the design of channel maintenance flows for gravel-bed rivers 151–164. https://doi.org/10.1029/gm089p0151

Arcement, G.J., Schneider, V.R., 1993. Guide for selecting Manning's roughness coefficients for natural channels and flood plains, Anaesthesist. Denver, CO.

Bank, W., 2016. Five forest figures for the international day of forests. URL https://blogs.worldbank.org/opendata/five-forest-figures-international-day-forests

Barks, J.H., 1978. Water quality in the Ozark national scenic riverways, Missouri. Wasington D.C.

Beck, W.J., Moore, P.L., Schilling, K.E., Wolter, C.F., Isenhart, T.M., Cole, K.J., Tomer, M.D., 2019. Changes in lateral floodplain connectivity accompanying stream channel evolution: Implications for sediment and nutrient budgets. Sci. Total Environ. 660, 1015–1028. https://doi.org/10.1016/j.scitotenv.2019.01.038

Bhuiyan, H.A.K.M., McNairn, H., Powers, J., Merzouki, A., 2017. Application of HEC-HMS in a cold region watershed and use of RADARSAT-2 soil moisture in initializing the model. Hydrology 4, 1–19. https://doi.org/10.3390/hydrology4010009

Bizzi, S., Lerner, D.N., 2015. The use of stream power as an indicatior of channel sensitivity to erosion and deposition processes. River Res. Appl. 31, 16–27. https://doi.org/10.1002/rra

Bonan, G. B. (2008). Forests and climate change: forcings, feedbacks, and the climate benefits of forests. Science, 320 (5882), 1444–1449. doi:10.1126/science.1155121

Bosch, J.M. and Hewlett, J.D., 1982. A review of catchment experiments to determine the effect of vegetation changes on water yield and evapotranspiration. J. Hydrol. 55, 3–23.

Bradley, N.S., 2017. Geomorphic effects of logging railbeds on an Ozarks headwater stream, Mark Twain National.

Bradley, R., 2017. Geomorphic disturbance and anthropogenic modifications in Big Barren Creek , Mark Twain National Forest , Southeast Missouri. Missouri State University.

Brookes, A., Gregory, K.J., Dawson, F.H., 1983. an assessment of river channelization in England and Wales. Sci. Total Environ. 27, 97--111.

Brown, T.C., Hobbins, M.T., Ramirez, J.A., 2008. Spatial distribution of water supply in the coterminous United States. J. Am. Water Resour. Assoc. 44, 1474–1487. https://doi.org/10.1111/j.1752-1688.2008.00252.x

Brown, A. V., Lyttle, M.M., Brown, K.B., 1998. Impacts of gravel mining on gravel bed streams. Trans. Am. Fish. Soc. 127, 979–994. https://doi.org/10.1577/1548-8659(1998)127<0979:iogmog>2.0.co;2

Brunner, Gary W, 2016. HEC-RAS River Analysis System - Hydraulic reference manual, Version 5.0. US Army Corps of Engineers – Hydrologic Engineering Center 547.

Brunner, Gary W., 2016. HEC-RAS river analysis system hydraulic reference manual version 5.0, Hydrologic Engineering Center.

Carson, E.C., 2006. Hydrologic modeling of flood conveyance and impacts of historic overbank sedimentation on West Fork Black's Fork, Uinta Mountains, northeastern Utah, USA.

Geomorphology 75, 368–383. https://doi.org/10.1016/j.geomorph.2005.07.022

Casagrand, S.N., 2021. Historical changes of channel width in a headwater steram system, Mark Twain National Forest, Missouri. Unpublished thesis in Natural and Applied Science, Department of Geography, Geology, and Planning, Missouri State University.

Chen, Y., Xu, Y., Yin, Y., 2009. Impacts of land use change scenarios on storm-runoff generation in Xitiaoxi basin, China. Quat. Int. 208, 121–128. https://doi.org/10.1016/j.quaint.2008.12.014

Cluer, B., Thorne, C., 2014. A stream evolution model integrating habitat and ecosystem benefits. River Res. Appl. 30, 135–154. https://doi.org/10.1002/rra

Corbari, C., Ravazzani, G., Galvagno, M., Cremonese, E., Mancini, M., 2017. Assessing crop coefficients for natural vegetated areas using satellite data and eddy covariance stations. Sensors (Switzerland) 17. https://doi.org/10.3390/s17112664

Cunningham, R.J., 2007. Historical and social factors affecting pine management in the Ozarks during the Late 1800s through 1940. In: Kabrick JM, Dey DC, Gwaze D, editors. Shortleaf pine restoration and ecology in the Ozarks: proceedings of a symposium; 2006, Newtown Sq. ed, shortleaf pine restoration and ecology in the Ozarks: Proceedings of a symposium. Springfield (MO).

Cydzik, K., Hogue, T.S., 2009. Modeling postfire response and recovery using the hydrologic engineering center hydrologic modeling system (HEC-HMS). J. Am. Water Resour. Assoc. 45, 702–714. https://doi.org/10.1111/j.1752-1688.2009.00317.x

Dasanto, B.D., Pramudya, B., Boer, R., Suharnoto, Y., 2014. Effects of forest cover change on flood characteristics in the Upper Citarum Watershed. J. Manaj. Hutan Trop. (Journal Trop. For. Manag. 20, 141–149. https://doi.org/10.7226/jtfm.20.3.141

Davis, J. V, Petersen, J.C., Adamski, J.C., Freiwald, D.A., 1996. Water-quality assessment of the Ozark Plateaus study init, Arkansas, Kansas, Missouri, and Oklahoma-analysis of information in nutrients, suspended sediment, and suspended solids, 1970-92: Water-Resources Investigations Report 96-4003.

De Groot, R., Brander, L., van der Ploeg, S., Costanza, R., Bernard, F., Braat, L., Christie, M., Crossman, N., Ghermandi, A., Hein, L., Hussain, S., Kumar, P., McVittie, A., Portela, R., Rodriguez, L.C., ten Brink, P., van Beukering, P., 2012. Global estimates of the value of ecosystems and their services in monetary units. Ecosyst. Serv. 1, 50–61.

https://doi.org/10.1016/j.ecoser.2012.07.005

Dempsey, E.C., 2012. Geoarchaeology in the Current River valley, Ozarks national scenic riverways, Southeast Missouri. University of Kansas.

Easterling, D., Karl, T., 2000. Climate change impacts on the United States, The potential consequences of climate variation and change; Chapter 6: Midwest.

Elmore, A.J., Kaushal, S.S., 2008. Disappearing headwaters: Patterns of stream burial due to urbanization. Front. Ecol. Environ. 6, 308–312. https://doi.org/10.1890/070101

FEMA, 2002. HEC-RAS Procedures for HEC-2 Modelers. Washington DC.

Fitzpatrick, F.A., Knox, J.C., Whitman, H.E., 1999. Effects of historical land-cover changes on flooding and sedimentation, North Fish Creek, Wisconsin.

Fletcher, P.W., McDermott, R.E., 1957. Influence of geologic parent material and climate on distribution of shortleaf pine in Missouri. Colombia, MO.

Florsheim, J.L., Mount, J.F., Rutten, L.T., 2001. Effect of baselevel change on floodplain and fan sediment storage and ephemeral tributary channel morphology, Navarro River, California. Earth Surf. Process. Landforms 26, 219–232. https://doi.org/10.1002/1096-9837(200102)26:2<219::AID-ESP169>3.0.CO;2-0

Furniss, M.J., Staab, B.P., Hazelhurst, S., F, C.C., Roby, K.B., Ilhadrt, B.L., Larry, E.B., Todd, A.H., Reid, L.M., Hines, S.J., Bennett, K.A., Luce, C.H., Edwards, P.J., 2010. Water, climate change, and forests: Watershed stewardship for a changing climate, e. Gen. Tech. Rep. PNW-GTR-812PNW-GTR-812. Portland, OR.

Gilvear, D.J., Winterbottom, S.J., 1992. Channel change and flood events since 1783 on the regulated river tay, Scotland: Implications for flood hazard management. Regul. Rivers Res. Manag. 7, 247–260. https://doi.org/10.1002/rrr.3450070304

Gomi, T., Sidle, R.C., Richardson, J.S., 2002. Understanding processes and downstream linkages of headwater systems. Bioscience 52, 905–916. https://doi.org/10.1641/0006-3568(2002)052[0905:UPADLO]2.0.CO;2

Gott, J.D., 1975. Soil survey of Mark Twain National Forest area, Missouri (parts of Carter,

Oregon, Ripley and Shannon Counties).

Groisman, P.Y., Easterling, D.R., 1994. Variability and trends of total precipitation and snowfall over the United States and Canada. J. Clim. 7, 184–205. https://doi.org/10.1175/1520-0442(1994)007<0184:VATOTP>2.0.CO;2

Guyette, R., Larsen, D., 2000. A history of anthropogenic and natural disturbances in the area of the Missouri Ozark Forest Ecosystem Project in Schifley, S.R., and Brookshire, B.L., eds., Missouri Forest Ecosystem Project: Site History, Soils, Landforms, Woody and Herbaceous Vegetatio.

Guyette, R.P., Muzika, R.M., Voelker, S.L., 2007. The historical ecology of fire, climate and decline of shortleaf pine in the Missouri Ozarks. In: Kabrick JM, Dey DC, Gwaze D, eds. Shortleaf pine restoration and ecology in the Ozarks: proceedings of a symposium; 2006, Gen. Tech. ed. Springfield, MO.

Hadadin, N., 2010. Theoretical and analytical approaches for investigating the relations between sediment transport and channel shape. World Acad. Sci. Eng. Technol. 72, 156–161.

Harr, R.D., Harper, W.C., Krygier, T., Et, H., Forest, A.L., 1975. Changes in storm hydrographs after road building and clear-cutting in the Oregon Coast Range. Water Resour. Res. 11, 436–444.

Harvel, A., 2015. Hydrologic and hydraulic response to wildfires in the upper cache La Poudre watershed using a swat and HEC-RAS model Cascade. Colorado State University. https://doi.org/10.5897/ERR2015

Heine, R.A., Pinter, N., 2011. Levee effects upon flood levels: an empirical assessment. Hydrol. Process. https://doi.org/10.1002/hyp.8261 Levee

Hodges, R.L., 2015. Bankfull geomorphic relationships and HEC- RAS assessment in small catchments of the Cumberland Plateau Ecoregion. University of Tennessee.

Hu, Q., Willson, G.D., Chen, X., Akyuz, A., 2005. Effects of climate and landcover change on stream discharge in the Ozark Highlands, USA. Environ. Model. Assess. 10, 9–19. https://doi.org/10.1007/s10666-004-4266-0

Hu, S., Shrestha, P., 2020. Examine the impact of land use and land cover changes on peak discharges of a watershed in the midwestern United States using the HEC-HMS model. Pap.

Appl. Geogr. 6, 101–118. https://doi.org/10.1080/23754931.2020.1732447

Humphrey, M., Beekwilder, N., Goodall, J.L., Ercan, M.B., 2012. Calibration of watershed models using cloud computing. 2012 IEEE 8th Int. Conf. E-Science, e-Science 2012. https://doi.org/10.1109/eScience.2012.6404420

Hupp, C.R., Pierce, A.R., Noe, G.B., 2009. Floodplain geomorphic processes and environmental impacts of human alteration along coastal plain rivers, USA. Wetlands 29, 413–429. https://doi.org/10.1672/08-169.1

Jacobson, R.B., 2004. Downstream effects of timber harvesting in the Ozarks of Missouri: USDA General Technical Report NC-239, USDA General Technical Report NC-239.

Jacobson, R.B., 1995. Spatial controls on patterns of land-use induced stream disturbance at the drainage-basin scale—An example from gravel-bed streams of the Ozark Plateaus, Missouri. Geomorphology 219–239. https://doi.org/10.1029/gm089p0219

Jacobson, R.B., Primm, A.T., 1997. Historical land-use changes and potential effects on stream disturbance in the Ozark Plateaus, Missouri, US Geological Survey Water Supply Paper.

Jacobson, R.B., Pugh, A.L., 1998. Riparian-vegetation controls on the spatial pattern of stream-channel instability, Little Piney Creek, Missouri. https://doi.org/10.3133/wsp2494

James, T., 2020. Surface water quality and modelling surface discharge in Beaver Creek Watershed , Northeast Tennessee and Southwest Virginia. East Tennessee State University.

Jobe, A., Kalra, A., Ibendahl, E., 2018. Conservation reserve program effects on floodplain land cover management. J. Environ. Manage. 214, 305–314. https://doi.org/10.1016/j.jenvman.2018.03.016

Johnson, E., 2015. Effects of hydrologic modifications on flooding in Bottomland Hardwoods (MS thesis), the school of Renewable Natural Resources, Louisiana State University.

Jones, J.A., 2000. Hydrologic processes and peak discharge response to forest removal, regrowth, and roads in 10 small, experimental basins, western Cascades, Oregon. Water Resour. Res. 36, 2621–2642. https://doi.org/10.1029/2000WR900105

Jones, J.A., Grant, G.E., 1996. Peak flow responses to clear-cutting and roads in small and large

basins, western Cascades, Oregon. Water Resour. Res. 32, 959–974. https://doi.org/10.1029/95WR03493

Kleekamp, E.R., 2016. Development of reference reaches for Missouri streams final report.

Knighton, D., 1984. Fluvial forms and processes. Routledge, London (UK).

Knox, J.C., 1977. Human impacts on wisconsin stream channels. Ann. Assoc. Am. Geogr. 67, 323–342. https://doi.org/10.1111/j.1467-8306.1977.tb01145.x

Kochenderfer, J.N., Edwards, P.J., Wood, F., 1997. Hydrologie impacts of logging an appalachian watershed using west virginia's best management practices. North. J. Appl. For. 14, 207–218. https://doi.org/10.1093/njaf/14.4.207

Kondolf, G.M., Piégay, H., Landon, N., 2002. Channel response to increased and decreased bedload supply from land use change: Contrasts between two catchments. Geomorphology 45, 35–51. https://doi.org/10.1016/S0169-555X(01)00188-X

Krause, A., 2010. Floodplain response to historical land use change on the Upper Baraboo River, Wisconsin.

Leigh, D.S., 2016. Multi-millennial record of erosion and fires in the southern Blue Ridge Mountains, USA. https://doi.org/10.1007/978-3-319-21527-3_8

Lenhart, C.F., Titov, M.L., Ulrich, J.S., Nieber, J.L., Suppes, B.J., 2013. The role of hydrologic alternation and riparian vegetation dynamics in channel evolution along the Lower Minnesota River. Am. Soc. Agric. Biol. Enrineers 56, 549–561.

Lewis, J., 1998. Evaluating the impacts of logging activities on erosion and suspended sediment transport in the Caspar Creek watersheds. Proc. Conf. Coast. Watersheds Caspar Creek Story 55–69.

Liming, F.G., 1946. The range and distribution of shortleaf pine in Missouri. Tech. Pap. 106, Columbus.

Lyons, J.K., Beschta, R.L., 1983. Land use, floods, and channel changes: Upper Middle Fork Willamette River, Oregon (1936–1980). Water Resour. Res. 19, 463–471. https://doi.org/10.1029/WR019i002p00463

MacDonald, L.H., Coe, D., 2007. Influence of headwater streams on downstream reaches in forested areas. For. Sci. 53, 148–168. https://doi.org/10.1093/forestscience/53.2.148

Magilligan, F.J., 1992. Thresholds and the spatial variability of flood power during extreme floods. Geomorphology 5, 373–390. https://doi.org/10.1016/0169-555X(92)90014-F

Magilligan, F.J., Stamp, M.L., 1997. Historical land-cover changes and hydrogeomorphic adjustment in a small Georgia watershed. Ann. Assoc. Am. Geogr. 87, 614–635. https://doi.org/10.1111/1467-8306.00070

Malmer, A., Grip, H., 1990. Soil disturbance and loss of infiltrability caused by mechanized and manual extraction of tropical rainforest in Sabah, Malaysia. For. Ecol. Manage. 38, 1–12. https://doi.org/10.1016/0378-1127(90)90081-L

Mao, D., Cherkauer, K.A., 2009. Impacts of land-use change on hydrologic responses in the Great Lakes region. J. Hydrol. 374, 71–82. https://doi.org/10.1016/j.jhydrol.2009.06.016

Martin, D., Pavlowsky, R., 2011. Spatial patterns of channel instability along an Ozark River, Southwest Missouri. Phys. Geogr. 32, 445–468. https://doi.org/10.2747/0272-3646.32.5.445

McEnroe, B.M., 2010. Guidelines for continuous simulation of streamflow in Johnson County , Kansas , with HEC-HMS, Simulation.

McKenney, R., Jacobson, R.B., Wertheimer, R.C., 1995. Woody vegetation and channel morphogenesis in low-gradient, gravel-bed streams in the Ozark Plateaus, Missouri and Arkansas. Geomorphology 13, 175–198. https://doi.org/10.1016/0169-555X(95)00034-3

MDC, 2020. Missouri Watershed Protection Practice.

Merritt, D.M., Wohl, E.E., 2003. Downstream hydraulic geometry and channel adjustment during a flood along an ephemeral, arid-region drainage. Geomorphology 52, 165–180. https://doi.org/10.1016/S0169-555X(02)00241-6

Miller, S.O., Ritter, D.F., Kochel, R.C., Miller, J.R., 1993. Fluvial responses to land-use changes and climatic variations within the Drury Creek watershed, southern Illinois. Geomorphology 6, 309–329. https://doi.org/10.1016/0169-555X(93)90053-5

Montgomery, D.R., Buffington, J.M., 1993. Channel classification, prediction of channel

response, and assessment of channel condition. Washingt. State Dep. Nat. Resour. Rep. 84.

Moriasi, D.N., Arnold, J.G., Liew, M.W. V., Bingner, R.L., Harmel, R.D., Veith, T.L., 2007. Model evaluation guidelines for systematic quantificaiton of accuracy in watershed simulations. Am. Soc. Agric. Biol. Enrineers 50, 885–990. https://doi.org/10.1234/590

Mosley, M.P., 1982. Analysis of the effect of changing discharge on channel morphology and instream uses in a braided river, Ohau River, New Zealand. Water Resour. Res. 800–812.

Nadeau, T.L., Rains, M.C., 2007. Hydrological connectivity between headwater streams and downstream waters: How science can inform policy. J. Am. Water Resour. Assoc. 43, 118–133. https://doi.org/10.1111/j.1752-1688.2007.00010.x

Naiman, R.J., Décamps, H., McClain, M.E., Likens, G.E., 2005. Catchments and the physical template. Riparia 19–48. https://doi.org/10.1016/b978-012663315-3/50003-4

Nash, J.E., Sutcliffe, J. V., 1970. River flow forecasting through conceptual models part 1- A discussion of principles. J. Hydrol. 10, 282–290. https://doi.org/10.1080/00750770109555783

Nickolotsky, A.M., 2005. Step-pool morphology of a wilderness headwater stream of the Buffalo River, Arkansas. Missouri State University.

NRCS, 2010. National engineering handbook chapter 15, Time of Concentration. Washington, DC.

NRCS, 2007. Part 630 Hydrology national engineering handbook chapter 16 hydrographs, National Engineering Handbook. Washington DC.

NRCS, 1986. Urban hydrology for small watershed, Technical Release 55. Washington, DC.

Nunnally, N.R., Keller, E., 1979. Use of fluvial processes to minimize adverse effects of stream channelization. Water Resources Research Institute, The University of North Carolina, Chapel Hill, NC.

O'Neal, M.R., Nearing, M.A., Vining, R.C., Southworth, J., Pfeifer, R.A., 2005. Climate change impacts on soil erosion in midwest United States with changes in crop management. Catena 61, 165–184. https://doi.org/10.1016/j.catena.2005.03.003

Orndorff, A., 2017. Evaluating the effects of sedimentation from forest roads: a review. University of Florida.

Ortega, J.A., Garzón Heydt, G., 2009. Geomorphological and sedimentological analysis of flash-flood deposits. The case of the 1997 Rivillas flood (Spain). Geomorphology 112, 1–14. https://doi.org/10.1016/j.geomorph.2009.05.004

Owen, M., Pavlowsky, R., Womble, P., 2011. Historical disturbance and contemporary floodplain development along an Ozark River, Southwest Missouri. Phys. Geogr. 32, 423–444. https://doi.org/10.2747/0272-3646.32.5.423

Owen, M.R., Ahmed, S., Pavlowsky, R.T., 2021. Gaging station report for : hydrological monitoring of the Big Barren Creek Watershed , Mark Twain National Forest , Southeast Missouri. Springfield, MO.

Owen, M.R., Thies, M.S., Geier, K.M., Oavlowsky, R.T., 2018. Stream Crossing Inventory and Evaluation , Upper Big Barren Creek Watershed, Southeast Missouri.

Pavlowsky, R.T., Owen, M.R., Bradley, R.A., 2016. Historical rainfall analysis for the Big Barren Creek Watershed , Southeast Missouri (1955-2015).

Piest, R.F., Elliott, L.S., Spomer, R.G., 1976. Erosion of the Tarkio drainage system, 1845-1976. Pap. - Am. Soc. Agric. Eng. 2, 485–488. https://doi.org/10.13031/2013.35583

Pryor, S.C., Scavia, D., Downer, C., Gaden, M., Iverson, L., Nordstrom, R., Patz, J., Roberson, G.P., 2014. Ch. 18: Midwest., Climate change impacts in the United States: The third national climate assessment. https://doi.org/10.7930/J0J1012N.On

Reminga, K.N., 2019. Historical land use influence on fine-grained sedimentation in channel and floodplain deposits in a forested Missouri Ozark Watershed (MS thesis). Department of Geography, Geology, and Planning, Missouri State University, Springfield, MO.

Richardson, J.S., Danehy, R.J., 2007. A synthesis of the ecology of headwater streams and their riparian zones in temperate forests. For. Sci. 53, 131–147. https://doi.org/10.1093/forestscience/53.2.131

Roberts, R.G., Church, M., 1986. The sediment budget in severly disturbed watershed, Queen Charlotte Ranges, British Columbia. Can. J. For. Resour. 16, 1092–1106.

Robles, M.D., Marshall, R.M., O'Donnell, F., Smith, E.B., Haney, J.A., Gori, D.F., 2014. Effects of climate variability and accelerated forest thinning on watershed-scale runoff in southwestern USA ponderosa pine forests. PLoS One 9. https://doi.org/10.1371/journal.pone.0111092

Roman, G., Pavlowsky, R., Owen, M., 2019. Soil and vegetation monitoring to evaluate hydrological effects of prescribed burning in Big Barren Creek Watershed, Mark Twain National Forest, SE Missouri. Springfield (MO).

Roman, G.F., 2019. Geomorphic and land use controls on headwater channel morphology in Mark Twain National Forest (MS thesis), Department of Geography, Geology, and Planning, Missouri State University, Springfield, MO.

Rosgen, D., 2001. A stream channel stability assessment methodology, in: 7th Federal Interagency Sedimentation Conference. Reno, NV.

Rosgen, DL., 1996. Applied river morphology. Wildland hydrology, Pagosa Springs (CO).

Safeeq, M., Grant, G.E., Lewis, S.L., Hayes, S.K., 2020. Disentangling effects of forest harvest on long-term hydrologic and sediment dynamics, western Cascades, Oregon. J. Hydrol. 580, 124259. https://doi.org/10.1016/j.jhydrol.2019.124259

Scharffenberg, W., 2016. Hydrologic modeling system HEC-HMS user's manual CPD-74A.

Shepherd, S.L., Dixon, J.. C., Davis, R.K., Feinstein, R., 2010. The effect of land use on channel geometry and sediment distribution in gravel mantled bedrock streams, Illinois River watershed, Arkansas. River Res. Appl. 132–133. https://doi.org/10.1002/rra.1401

Simmons, C.E., 1993. Sediment characteristics of North Carolina streams, 1970-79, US Geological Survey Water-Supply Paper.

Simon, A., 1994. Gradation processes and channel evolution in modified west Tennessee streams: process, response, and form., US Geological Survey Professional Paper. https://doi.org/10.3133/pp1470

Simon, A., 1989. A model of channel response in disturbed alluvial channels. Earth Surf. Process. Landforms 14, 11–26. https://doi.org/10.1002/esp.3290140103

Simon, A., Rinaldi, M., 2006. Disturbance, stream incision, and channel evolution: The roles of excess transport capacity and boundary materials in controlling channel response. Geomorphology 79, 361–383. https://doi.org/10.1016/j.geomorph.2006.06.037

Simon, A., Rinaldi, M., 2000. Channel instability in the loess area of the midwestern United States. J. Am. Water Resour. Assoc. 36, 133–150. https://doi.org/10.1111/j.1752-1688.2000.tb04255.x

Simon, A., Thorne, C.R., 1996. Channel adjustment of an unstable coarse-grained stream: Opposing trends of boundary and critical shear stress, and the applicability of extremal hypotheses. Earth Surf. Process. Landforms 21, 155–180. https://doi.org/10.1002/(SICI)1096-9837(199602)21:2<155::AID-ESP610>3.0.CO;2-5

Singh, V.P., 2004. On the theories of hydraulic geometry. Int. J. 18, 196–218.

Sterling, E.A., Schoenfelder, C., 2010. Lake Samish Comprehensive Stormwater Plan – Hydrologic Modeling because.

Storck, P., Bowling, L., Wetherbee, P., Lettenmaier, D., 1998. Application of a GIS-based distributed hydrology model for prediction of forest harvest effects on peak stream flow in the Pacific Northwest. Hydrol. Process. 12, 889–904. https://doi.org/10.1002/(SICI)1099-1085(199805)12:6<889::AID-HYP661>3.0.CO;2-P

Sun, G., Vose, J.M., 2016. Forest management challenges for sustainingwater resources in the Anthropocene. Forests 7, 1–13. https://doi.org/10.3390/f7030068

Surian, N., Cisotto, A., 2007. Channel adjustments, bedload transport and sediment sources in a gravel-bed river, Brenta River, Italy. Earth Surf. Process. Landforms 32, 641–656. https://doi.org/10.1002/esp

Suryatmojo, H., 2015. Rainfall-runoff investigation of pine forest plantation in the Upstream area of Gajah Mungkur reservoir. Procedia Environ. Sci. 28, 307–314. https://doi.org/10.1016/j.proenv.2015.07.039

Tedela, N.H., McCutcheon, S.C., Rasmussen, T.C., Hawkins, R.H., Swank, W.T., Campbell, J.L., Adams, M.B., Jackson, C.R., Tollner, E.W., 2012. Runoff curve numbers for 10 small forested watersheds in the mountains of the Eastern United States. J. Hydrol. Eng. 17, 1188–1198. https://doi.org/10.1061/(ASCE)HE

Thies, M.S., 2017. Geomorphic characteristics and sediment transport in natural and channelized reaches of Big Barren Creek, Southeast Missouri (MS thesis), Department of Geography, Geology, and Planning, Missouri State University, Springfield, MO.

Tobin, G.A., 1995. the Levee Love Affair: a Stormy Relationship? JAWRA J. Am. Water Resour. Assoc. 31, 359–367. https://doi.org/10.1111/j.1752-1688.1995.tb04025.x

Toman, E., 2004. Forest Road Hydrology : The Influence of forest roads on stream flow at stream crossings. Oregon State University.

Trimble, S.W., Lund, S.W., 1982. Soil conservation and the reduction of erosion and sedimentation in the Coon Creek Basin, Wisconsin. Geol. Surv. Prof. Pap. (United States).

USDA, NRCS, 2006. Land resource regions and major land resource areas of the United States, the Caribbean, and the Pacific Basin, United States Department of Agriculture Handbook.

Vanacker, V., Molina, A., Govers, G., Poesen, J., Dercon, G., Deckers, S., 2005. River channel response to short-term human-induced change in landscape connectivity in Andean ecosystems. Geomorphology 72, 340–353. https://doi.org/10.1016/j.geomorph.2005.05.013

Voelker, S.T., 2004. Causes of forest decline and consequences for oak-pine stand dynamics in Southereastern Missouri. University of Missouri.

Walter, R.C., Merritts, D.J., 2008. Natural streams and the legacy of water-powered mills. Science (80-.). 319, 299–304. https://doi.org/10.1126/science.1151716

Ward, A.D., Trimble, S.W., 1995. Environmental hydrology, Second. ed. Lewis Publishing.

Wayne Martin, C., Hornbeck, J.W., Likens, G.E., Buso, D.C., 2000. Impacts of intensive harvesting on hydrology and nutrient dynamics of northern hardwood forests. Can. J. Fish. Aquat. Sci. 57, 19–29. https://doi.org/10.1139/f00-106

Weary, D.J., Harrison, R.W., Orndorff, R.C., Weems, R.E., Schindler, J.S., Repetski, J.E., Pierce, H.A., 2014. Bedrock geologic map of the Spring Valley, West Plains, and Parts of the Piedmont and Poplar Bluff 30’ × 60’ Quadrangles, Missouri, Including the Upper Current River and Eleven Point River Drainage Basins: U.S. Geological Survey Scientific Investigations .

Weary, D.J., Schindler, J.., 2004. Geologic map of the Van Buren South quadrangle, Carter County, Missouri.

Wehmeyer, L.L., Weirich, F.H., Cuffney, T.F., 2011. Effect of land cover change on runoff curve number estimation in Iowa, 1832-2001. Ecohydrology 4, 315–321. https://doi.org/10.1002/eco

Whiting, P.J., Bradley, J.B., 1993. A process-based classification system for headwater streams. Earth Surf. Process. Landforms 18, 603–612. https://doi.org/10.1002/esp.3290180704

Wigmosta, M.S., Perkins, W.A., 2011. Simulating the effects of forest roads on watershed hydrology 127–143. https://doi.org/10.1029/ws002p0127

Winkler, J.A., Andresen, J.A., Hatfield, J.L., Bidwell, D., Brown, D., 2014. Climate change in the midwest: A synthesis report for the national climate assessment, Tropical Forestry Handbook. Washington DC. https://doi.org/10.1007/978-3-642-41554-8_42-1

Winterbottom, S.J., 2000. Medium and short-term channel planform changes on the Rivers Tay and Tummel, Scotland. Geomorphology 34, 195–208. https://doi.org/10.1016/S0169-555X(00)00007-6

Yang, C.T., Stall, J.B., 1974. Unit stream power for sediment transport in natural rivers. Report No. 88. Water Resources Center, University Of Illinois at Urbana-Champaign.

Yochum, S.E., Sholtes, J.S., Scott, J.A., Bledsoe, B.P., 2017. Stream power framework for predicting geomorphic change: The 2013 Colorado Front Range flood. Geomorphology 292, 178–192. https://doi.org/10.1016/j.geomorph.2017.03.004

Zhang, H.L., Wang, Y.J., Wang, Y.Q., Li, D.X., Wang, X.K., 2013. The effect of watershed scale on HEC-HMS calibrated parameters: A case study in the Clear Creek watershed in Iowa, US. Hydrol. Earth Syst. Sci. 17, 2735–2745. https://doi.org/10.5194/hess-17-2735-2013

APPENDICES

Appendix A. Parameters for the reach routing method

Reach Number	Length (feet)	Slope (ft/ft)	Manning's N, channel	Index Flow (CFS)	Manning's N, Left Bank	Manning's N, Right Bank
R1	1165.17	0.0014	0.08	2035	0.16	0.16
R2	2509.28	0.003	0.07	2035	0.16	0.16
R3	2006	0.001	0.05	2040	0.15	0.15
R4	1571.27	0.001	0.034	2035	0.16	0.16
R5	1770.22	0.002	0.034	2035	0.16	0.16
R6	669.15	0.003	0.08	2035	0.16	0.16
R7	1023.71	0.002	0.035	2035	0.16	0.16
R8	2125.31	0.001	0.08	2035	0.16	0.16
R9	3736	0.001	0.05	2035	0.15	0.15
R10 (Channelized)	2133.45	0.002	0.035	2035	0.16	0.16
R11	5296.98	0.002	0.08	2035	0.16	0.16
R12 (Channelized)	1079.95	0.001	0.035	2035	0.16	0.16
R13	3985.45	0.001	0.07	2035	0.16	0.16
R14 (Channelized)	2144.13	0.002	0.035	2035	0.16	0.16
R15	1073.44	0.007	0.07	2035	0.15	0.15
R16	1747.06	0.002	0.128	2035	0.16	0.16
R17	1394.23	0.002	0.06	2035	0.15	0.15
R18 (Channelized)	592.94	0.002	0.035	2035	0.16	0.16
R19	2154.27	0.0012	0.06	2035	0.15	0.15
R20	772.54	0.004	0.07	2035	0.16	0.16
R21	1188.94	0.003	0.07	2035	0.16	0.16
R22 (Channelized)	708.44	0.003	0.035	2035	0.16	0.16
R23	420.12	0.0004	0.05	2035	0.15	0.15
R24 (Channelized)	519.4	0.002	0.035	2035	0.16	0.16

R25 (Channelized)	641.19	0.002	0.035	2035	0.16	0.16
R26 (Channelized)	1053.84	0.002	0.035	2035	0.16	0.16
R27 (Channelized)	1613.61	0.001	0.035	2035	0.15	0.15
R28 (Channelized)	1692.23	0.0025	0.035	2035	0.15	0.15
R29 (Channelized)	2976	0.002	0.035	2035	0.16	0.16
R30	2183.8	0.0008	0.06	2035	0.15	0.15
R31	2006	0.001	0.05	2035	0.15	0.15

Appendix B. Comparison between field survey and LiDAR extracted cross-sections.

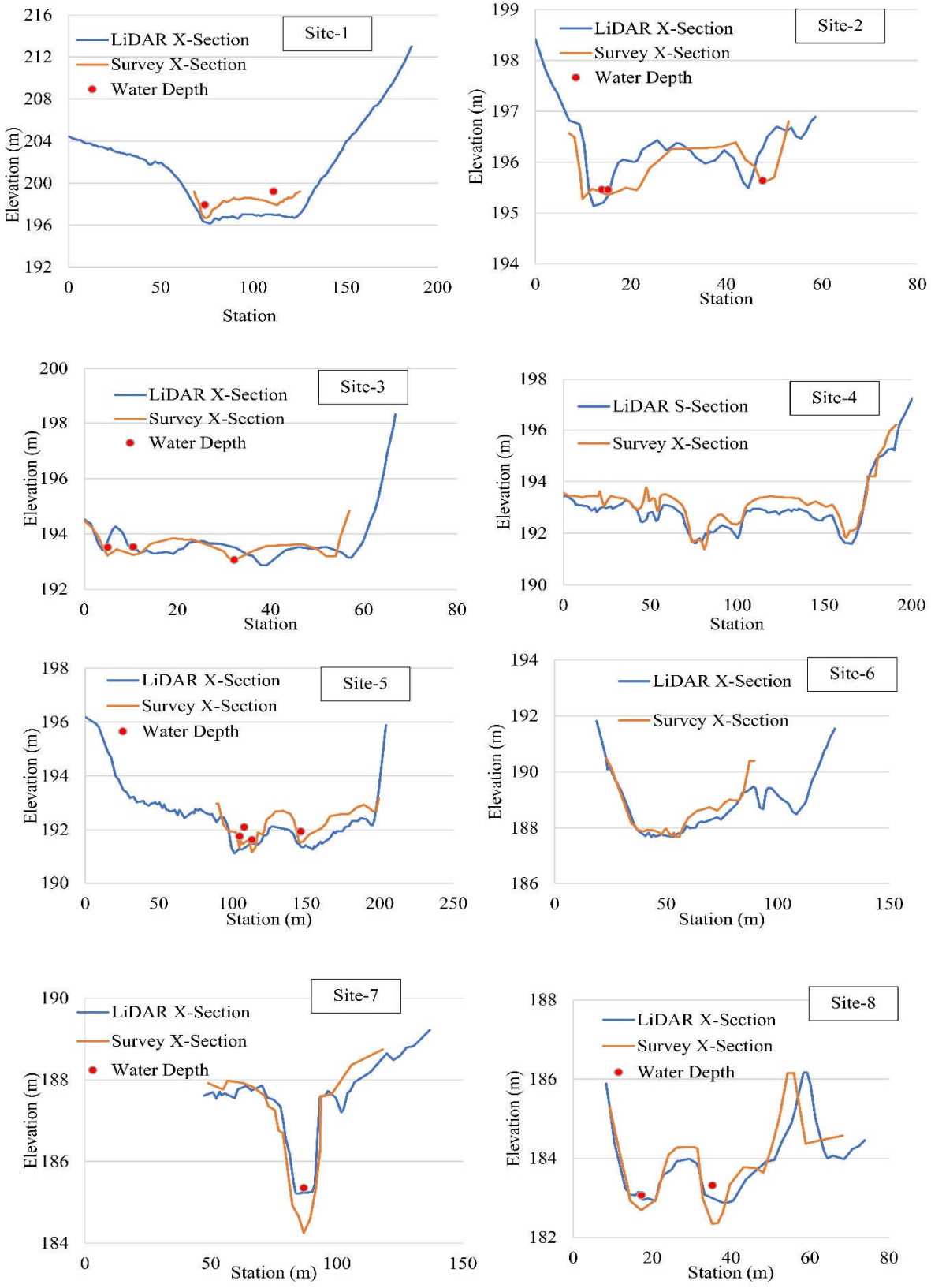

Appendix C. Present day (2016) HEC-HMS simulation and observed data (Rainfall amount =12.48 cm).

Parameters		TH	UBB	UBT	WP	PC	MBB
Area (sq. km.)		1.59	2.51	4.18	5.12	6.19	47.77
Flow Duration (hr.)	Observed	19.75	25.75	12.75	19.66	23.83	22.83
	Simulated	12.25	20.75	16.00	16.25	17.00	25.25
	RPD (+/-)	**46.88**	**21.51**	**-22.61**	**18.99**	**33.46**	**-10.07**
Avg. Discharge (cms)	Observed	0.57	0.80	1.98	0.29	0.25	2.03
	Simulated	0.97	0.74	2.03	0.30	0.34	2.03
	RPD (+/-)	**-51.95**	**7.79**	**-2.49**	**-3.39**	**-30.51**	**0.00**
Runoff Depth (cm)	Observed	2.74	3.02	2.18	0.48	0.33	0.41
	Simulated	2.92	3.22	2.79	0.40	0.43	0.41
	RPD (+/-)	**-6.36**	**-6.41**	**-24.55**	**18.18**	**-26.32**	**0.00**
Peak Discharge (cms), time	Observed	2.30	3.83	5.81	1.43	1.81	9.34
	Observed Time	11:30 (am)	12:30 (am)	14:00 (pm)	15:00 (pm)	14:15 (pm)	18:30 pm
	Simulated	2.28	3.59	5.43	1.46	1.79	9.34
	Simulated Time	10:15 (am)	12:30 (am)	12:30 (pm)	14:30 (pm)	14:30 (pm)	18:30 pm
	RPD (+/-)	**0.87**	**6.47**	**6.76**	**-2.08**	**1.11**	**0.00**
Lag Time (hr.)	Observed	3.05	4.05	5.55	6.55	5.80	10.05
	Simulated	1.83	4.05	4.08	6.08	6.08	10.05
	RPD (+/-)	**50.00**	**0.00**	**30.53**	**7.44**	**-4.71**	**0.00**

Appendix D. Detail analysis of the HEC-HMS pre-settlement scenario generation (Shortleaf pine-dominated forest).

Parameters		TH	UBB	UBT	WP	PC	MBB
Area (sq. km.)		1.59	2.51	4.18	5.12	6.19	47.77
Flow Duration (hr)	Present Simulation	12.25	20.75	16.00	16.25	17.00	25.25
	Pre-Settlement Simulated	21.00	25.75	16.00	16.26	17.00	27.50
	RPD (+/-)	-52.63	**-21.51**	0.00	**-0.06**	0.00	-8.53
Avg. Discharge (cms)	Present Simulation	0.97	0.74	2.03	0.30	0.34	2.03
	Pre-Settlement Simulated	0.53	0.79	2.02	0.29	0.40	1.68
	RPD (+/-)	58.67	-6.54	0.49	3.39	-16.22	18.87
Runoff Depth (cm)	Present Simulation	2.92	3.22	2.79	0.40	0.43	0.41
	Pre-Settlement Simulated	2.79	3.23	2.77	0.40	0.43	0.35
	RPD (+/-)	4.55	-0.31	0.72	0.00	0.00	15.79
Peak Discharge (cms)	Present Simulation	2.28	3.28	5.43	1.46	1.79	9.34
	Pre-Settlement Simulated	2.18	3.27	5.40	1.37	1.85	8.70
	RPD (+/-)	4.48	0.31	0.55	6.36	-3.30	7.10
Lag Time (hr)	Present Simulation	1.83	4.05	4.08	6.08	6.08	10.05
	Pre-Settlement Simulated	5.05	4.05	4.08	6.08	6.08	10.05
	RPD (+/-)	-93.60	0.00	0.00	0.00	0.00	0.00

Appendix E. HEC-HMS pre-settlement scenario generation (Shortleaf pine-dominated forest and CN reduced by 1).

Parameters		TH	UBB	UBT	WP	PC	MBB
Area (sq. km.)		1.59	2.51	4.18	5.12	6.19	47.77
Flow Duration (hr)	Present Simulation	12.25	20.75	16.00	16.25	17.00	25.25
	Pre-Settlement Simulated	21.00	19.00	15.50	---	10.25	13.75
	RPD (+/-)	**-52.63**	**8.81**	**3.17**	**---**	**49.54**	**58.97**
Avg. Discharge (cms)	Present Simulation	0.97	0.74	2.03	0.30	0.34	2.03
	Pre-Settlement Simulated	0.53	0.51	1.04	---	0.31	1.48
	RPD (+/-)	**58.67**	**36.80**	**64.50**	**---**	**9.23**	**31.34**
Runoff Depth (cm)	Present Simulation	2.92	3.22	2.79	0.40	0.43	0.41
	Pre-Settlement Simulated	2.33	2.81	1.90	---	0.18	0.15
	RPD (+/-)	**22.48**	**13.60**	**37.95**	**---**	**81.97**	**92.86**
Peak Discharge (cms)	Present Simulation	2.28	3.28	5.43	1.46	1.79	9.34
	Pre-Settlement Simulated	2.13	3.00	4.15	---	0.91	3.89
	RPD (+/-)	**6.80**	**8.92**	**26.72**	**---**	**65.19**	**82.39**
Lag Time (hr)	Present Simulation	1.83	4.05	4.08	6.08	6.08	10.05
	Pre-Settlement Simulated	5.08	6.08	6.08	---	6.08	11.08
	RPD (+/-)	**-94.07**	**-40.08**	**-39.37**	**---**	**0.00**	**-9.75**

Appendix F. HEC-HMS Post-Disturbance scenario generation (Shrubs cover and CN increased by 3).

Parameters		TH	UBB	UBT	WP	PC	MBB
Area (sq. km.)		1.59	2.51	4.18	5.12	6.19	47.77
Flow Duration (hr)	Present Simulation	12.25	20.75	16.00	16.25	17.00	25.25
	Post-Disturbance Simulation	21.00	17.50	17.50	16.25	17.00	27.25
	RPD (+/-)	**-52.63**	**16.99**	**-8.96**	**0.00**	**0.00**	**-7.62**
Avg. Discharge (cms)	Present Simulation	0.97	0.74	2.03	0.30	0.34	2.03
	Post-Disturbance Simulation	1.52	1.52	2.51	1.14	1.88	6.07
	RPD (+/-)	**-44.18**	**-69.03**	**-21.15**	**-116.67**	**-138.74**	**-99.75**
Runoff Depth (cm)	Present Simulation	2.92	3.22	2.79	0.40	0.43	0.41
	Post-Disturbance Simulation	4.27	4.57	3.76	1.57	1.88	1.24
	RPD (+/-)	**-37.55**	**-34.66**	**-29.62**	**-118.78**	**-125.54**	**-100.61**
Peak Discharge (cms)	Present Simulation	2.28	3.28	5.43	1.46	1.79	9.34
	Post-Disturbance Simulation	3.43	4.14	6.36	4.71	6.46	32.21
	RPD (+/-)	**-40.28**	**-23.18**	**-15.78**	**-105.35**	**-113.21**	**-110.08**
Lag Time (hr)	Present Simulation	1.83	4.05	4.08	6.08	6.08	10.05
	Post-Disturbance Simulation	1.58	1.58	3.58	5.58	5.58	8.33
	RPD (+/-)	**14.66**	**87.74**	**13.05**	**8.58**	**8.58**	**18.72**

Appendix G. Channel velocity distribution.

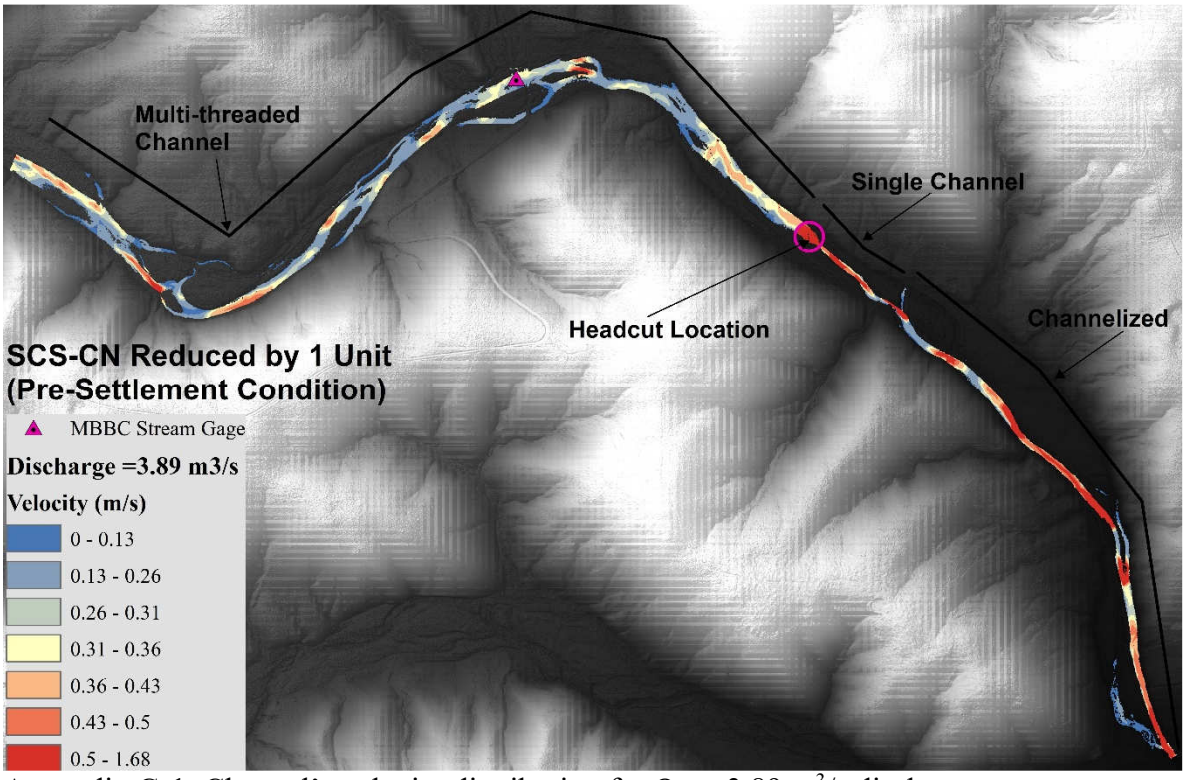

Appendix G-1: Channel's velocity distribution for Qp = 3.89 m^3/s discharge

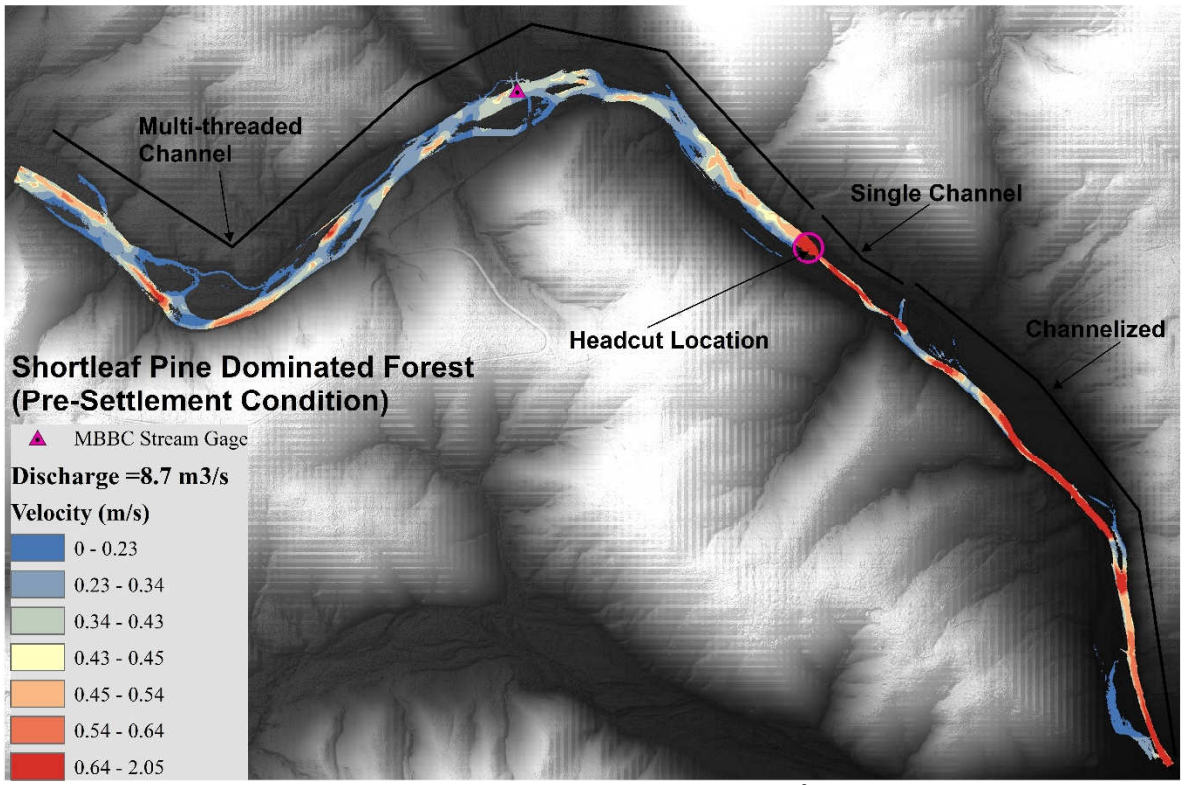

Appendix G-2: Channel's velocity distribution for Qp = 8.7 m^3/s discharge

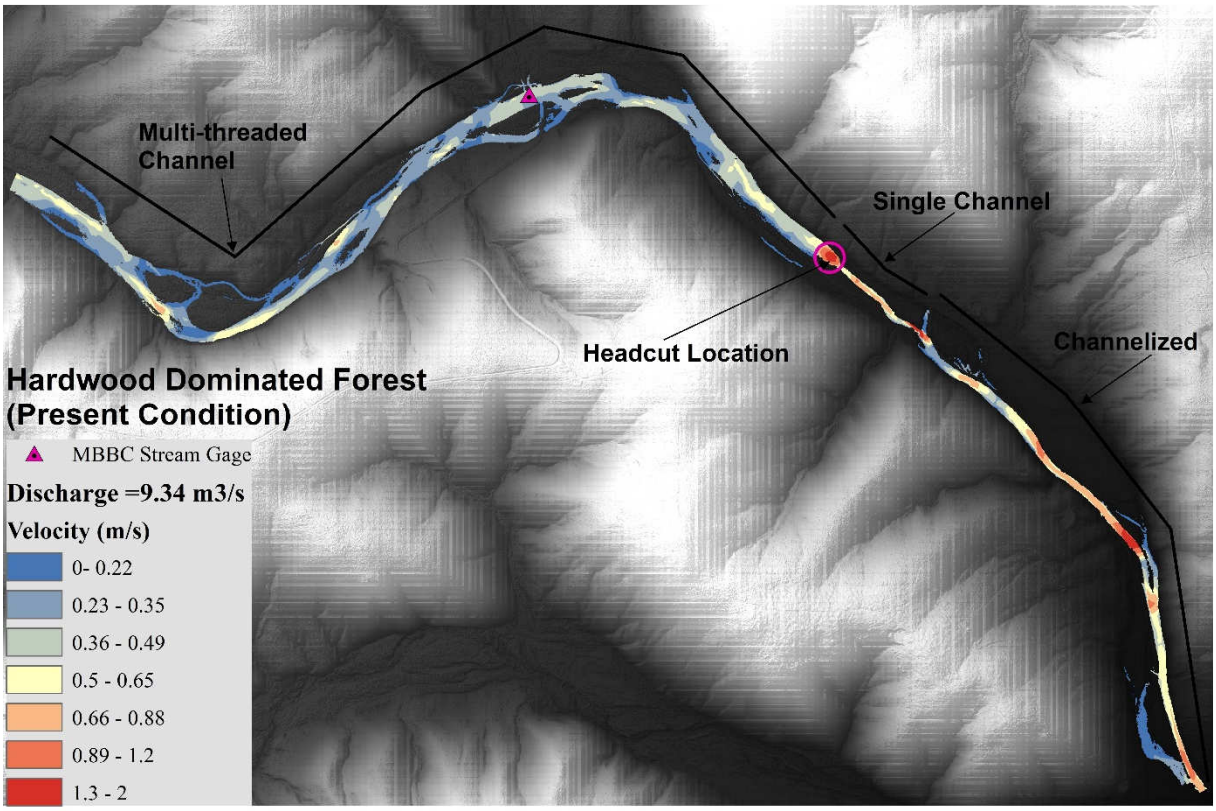

Appendix G-3: Channel's velocity distribution for Qp = 9.34 m^3/s discharge

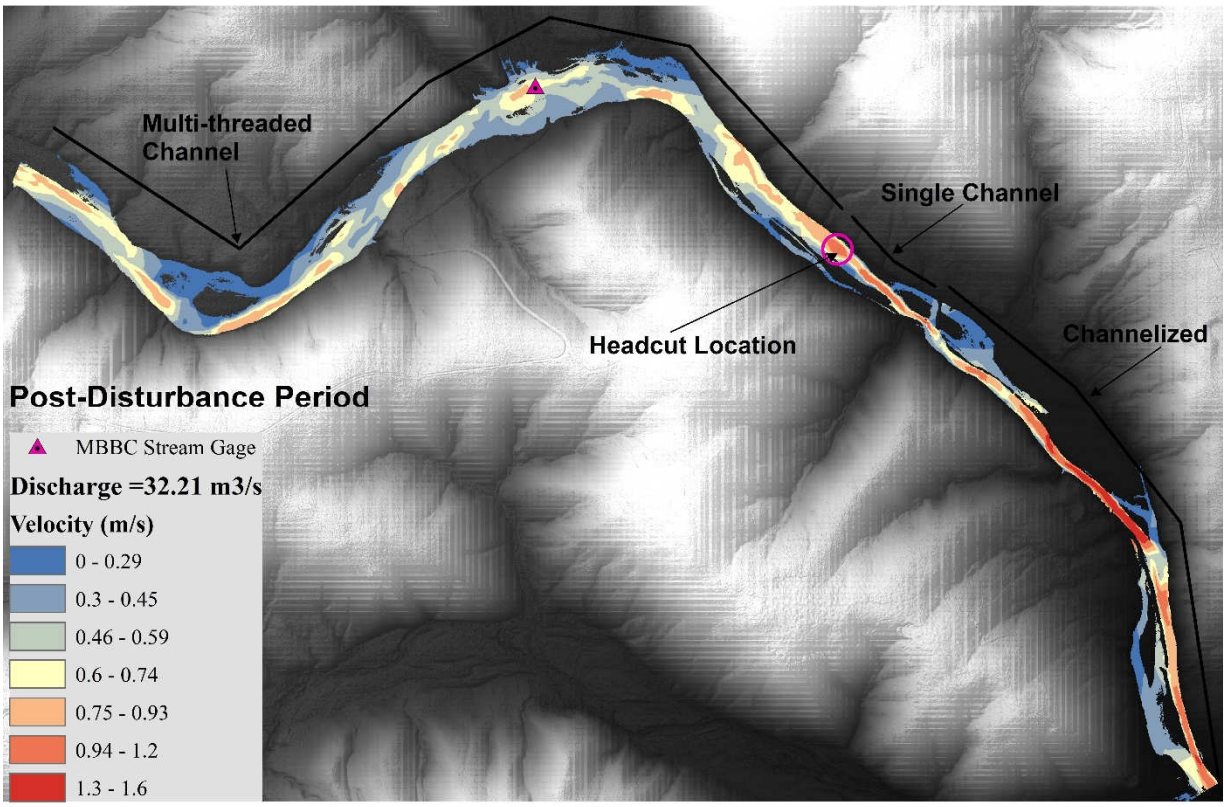

Appendix G-4: Channel's velocity distribution for Qp = 32.21 m^3/s discharge

Appendix H. Water surface elevations for the simulated discharges.

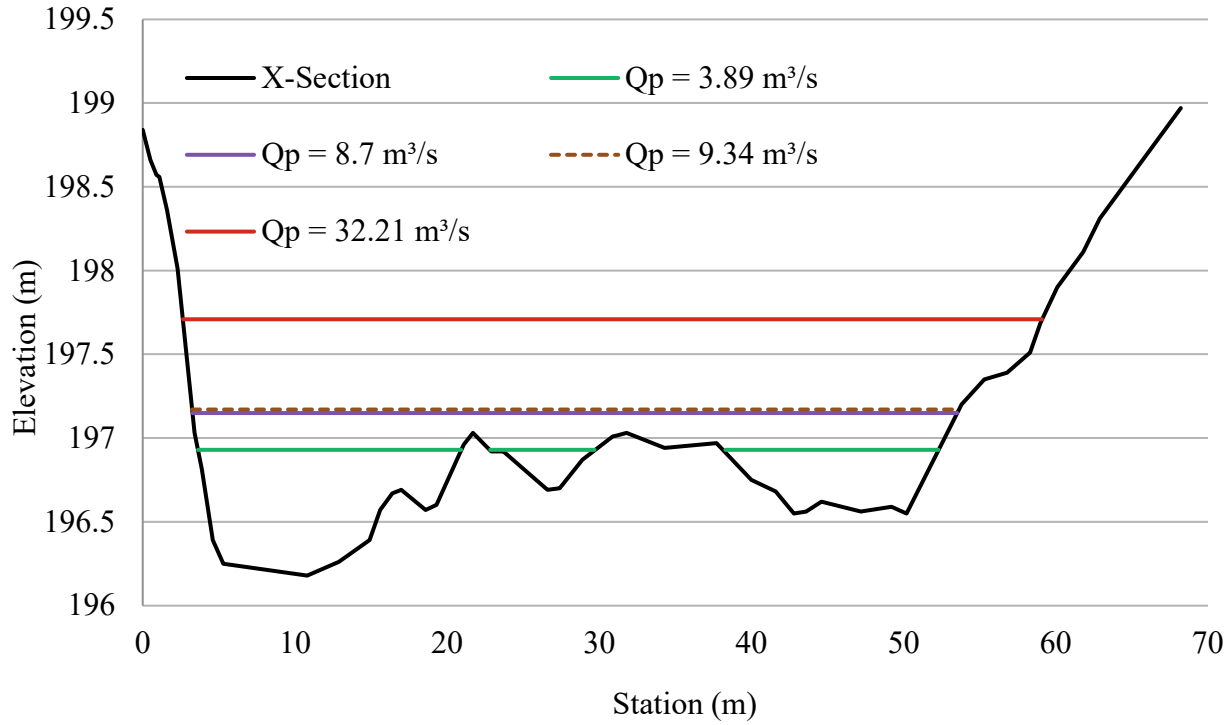

Appendix H-1. Water surface elevations at site-1 at different peak discharge.

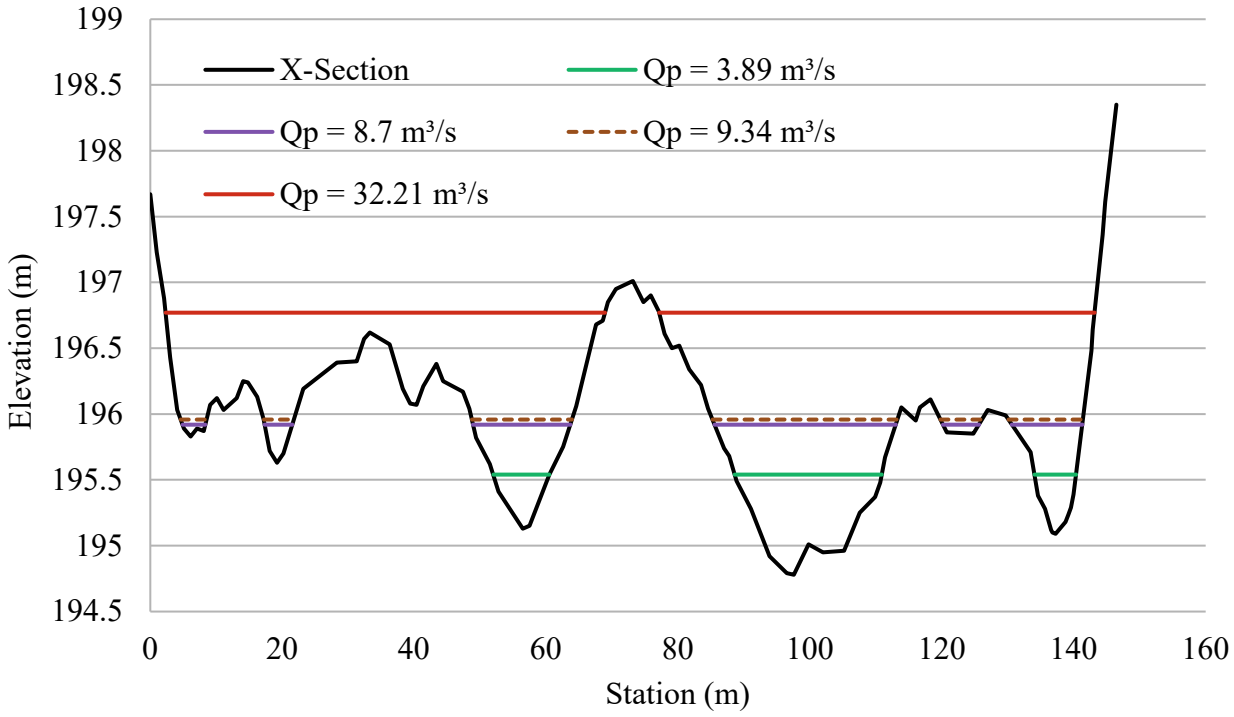

Appendix H-2. Water surface elevations at site-2 at different peak discharge.

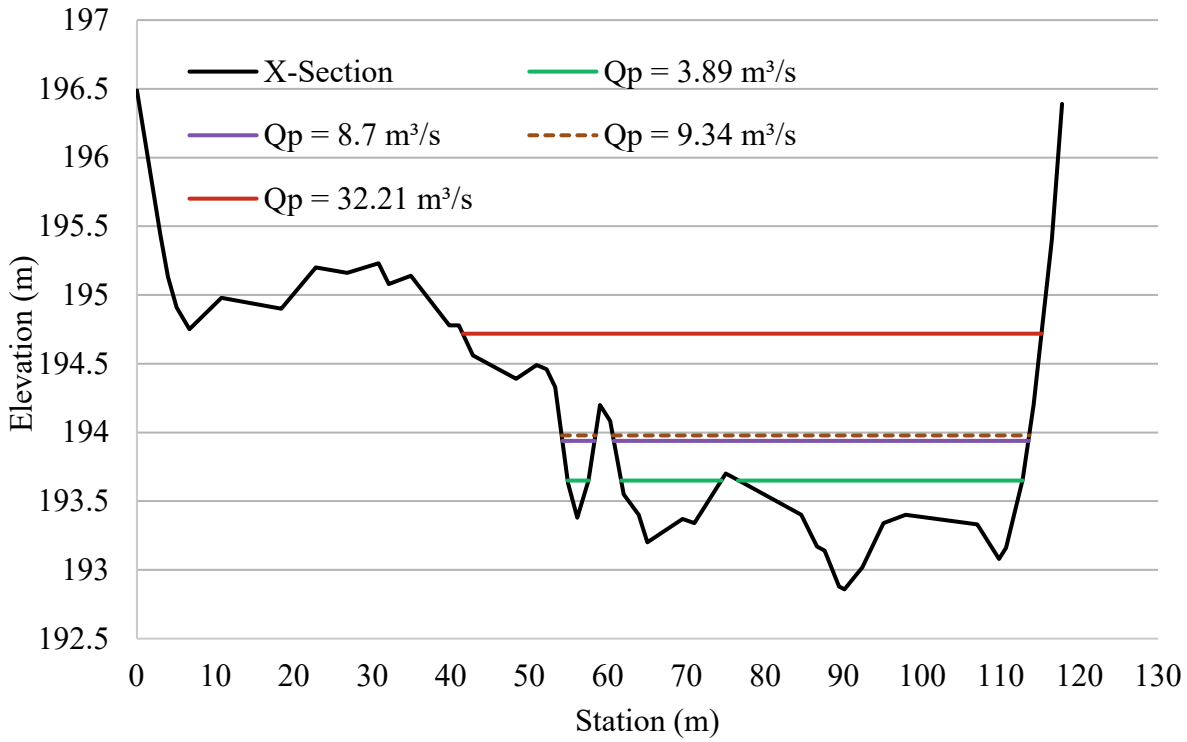

Appendix H-3. Water surface elevations at site-3 at different peak discharge.

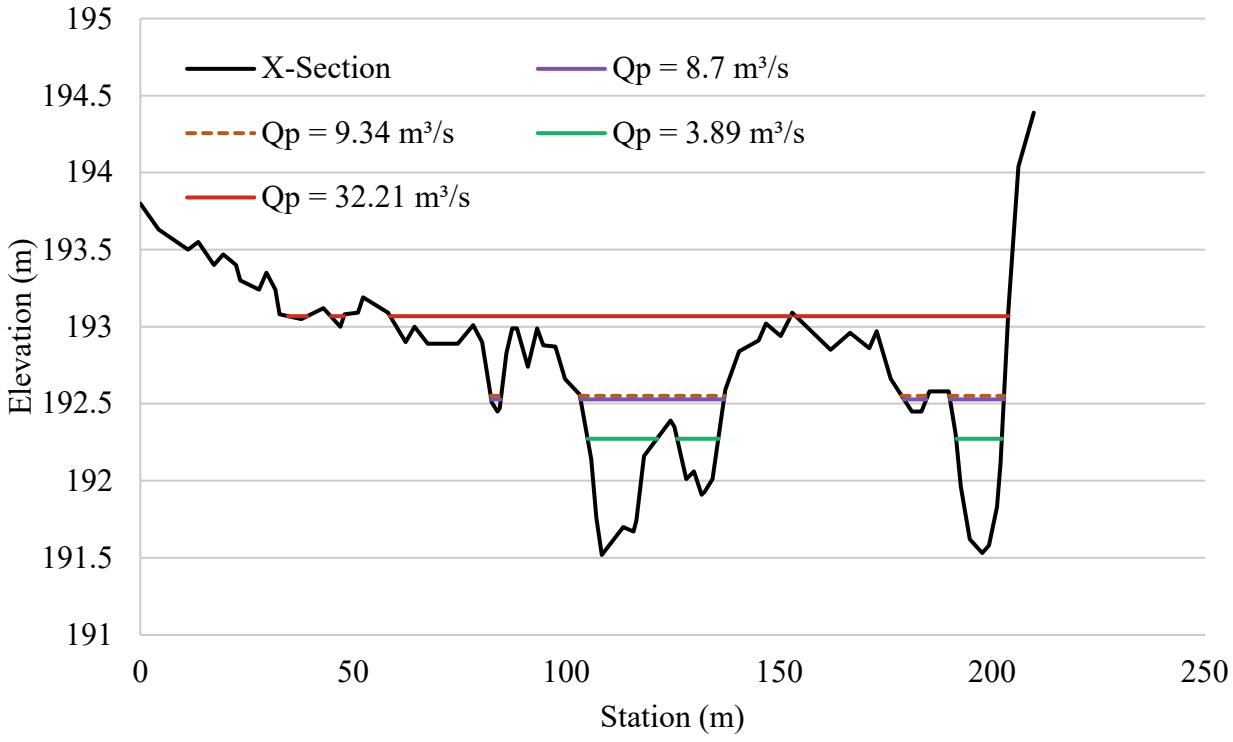

Appendix H-4. Water surface elevations at site-4 at different peak discharge.

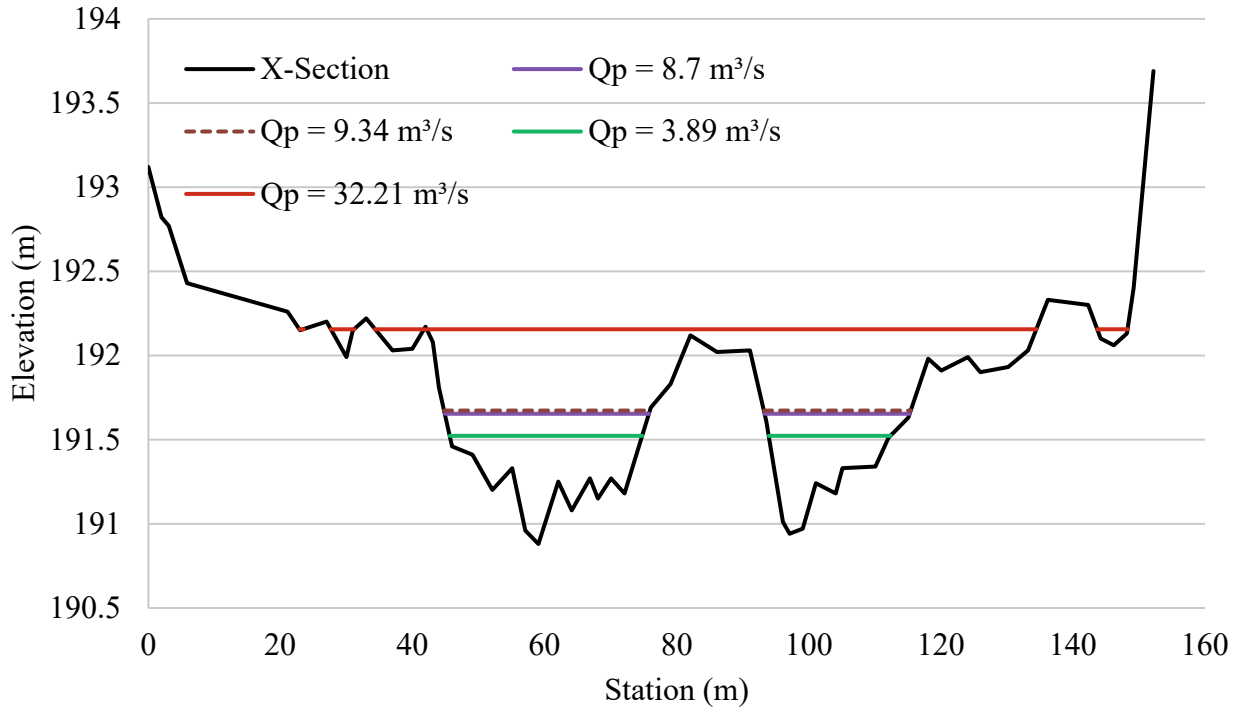

s

Appendix H-5. Water surface elevations at site-5 at different peak discharge.

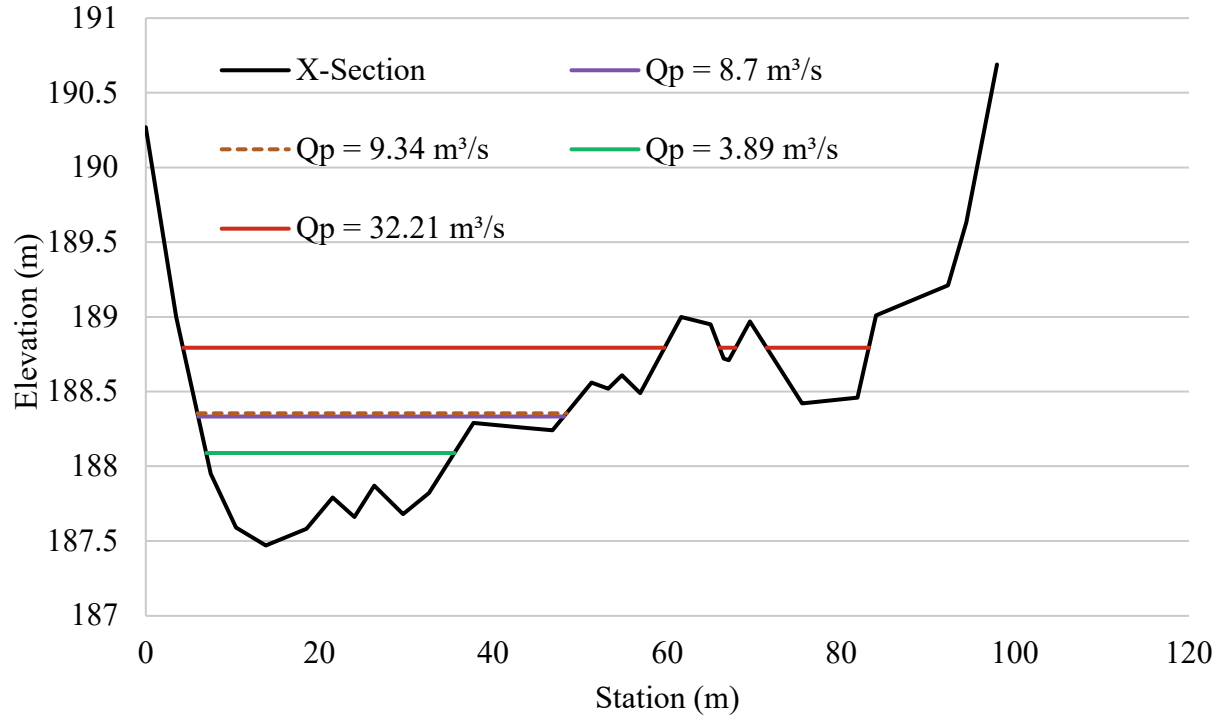

Appendix H-6. Water surface elevations at site-6 at different peak discharge.

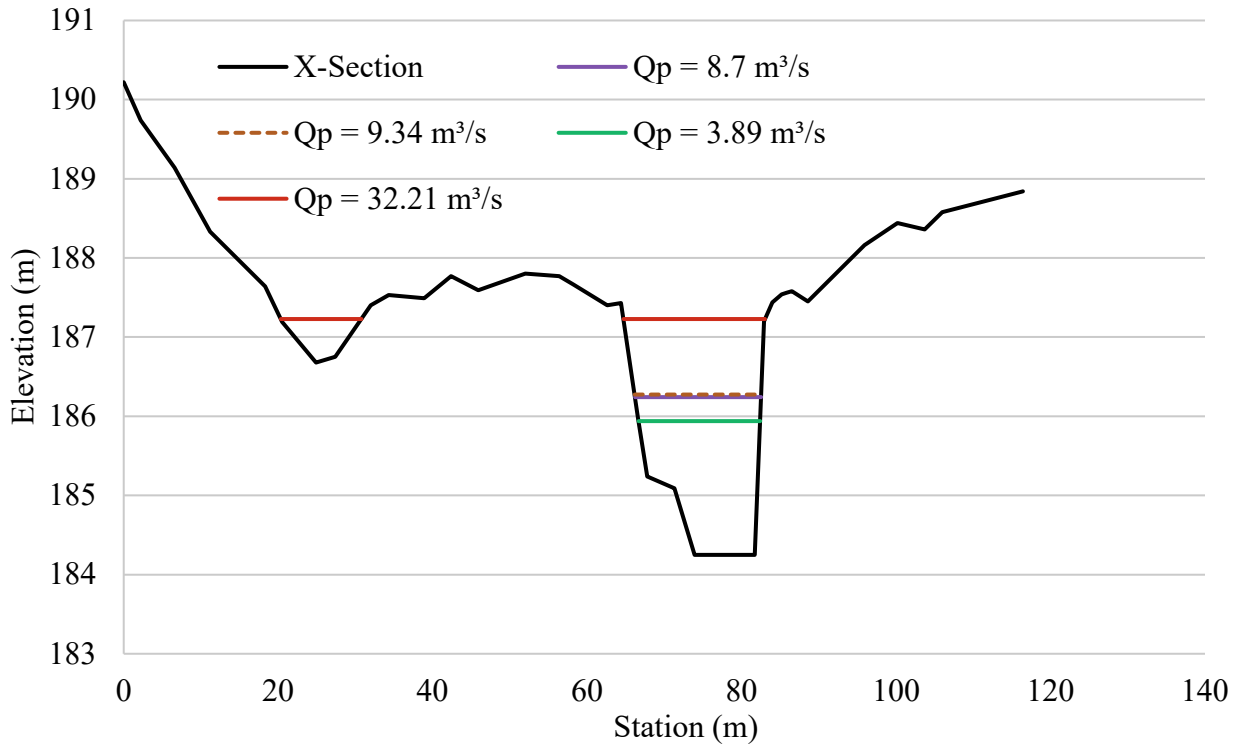

Appendix H-7. Water surface elevations at site-7 at different peak discharge.

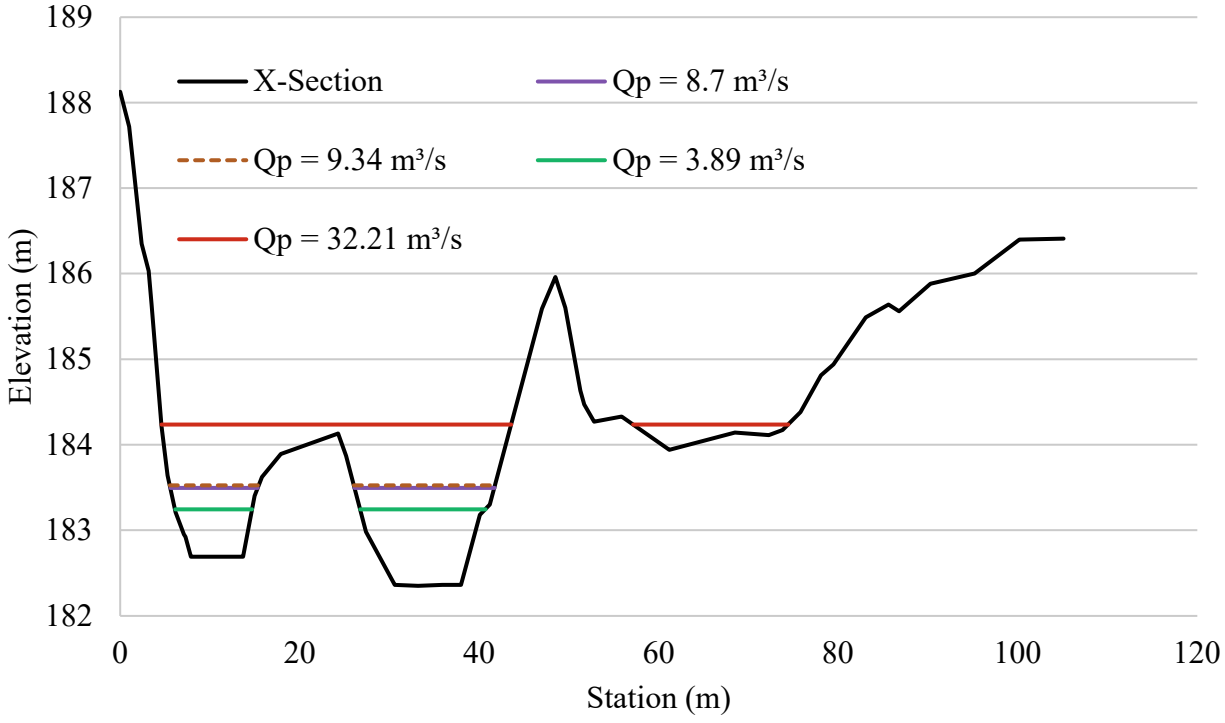

Appendix H-8. Water surface elevations at site-8 at different peak discharge.

Appendix I. Channel total shear stress distribution.

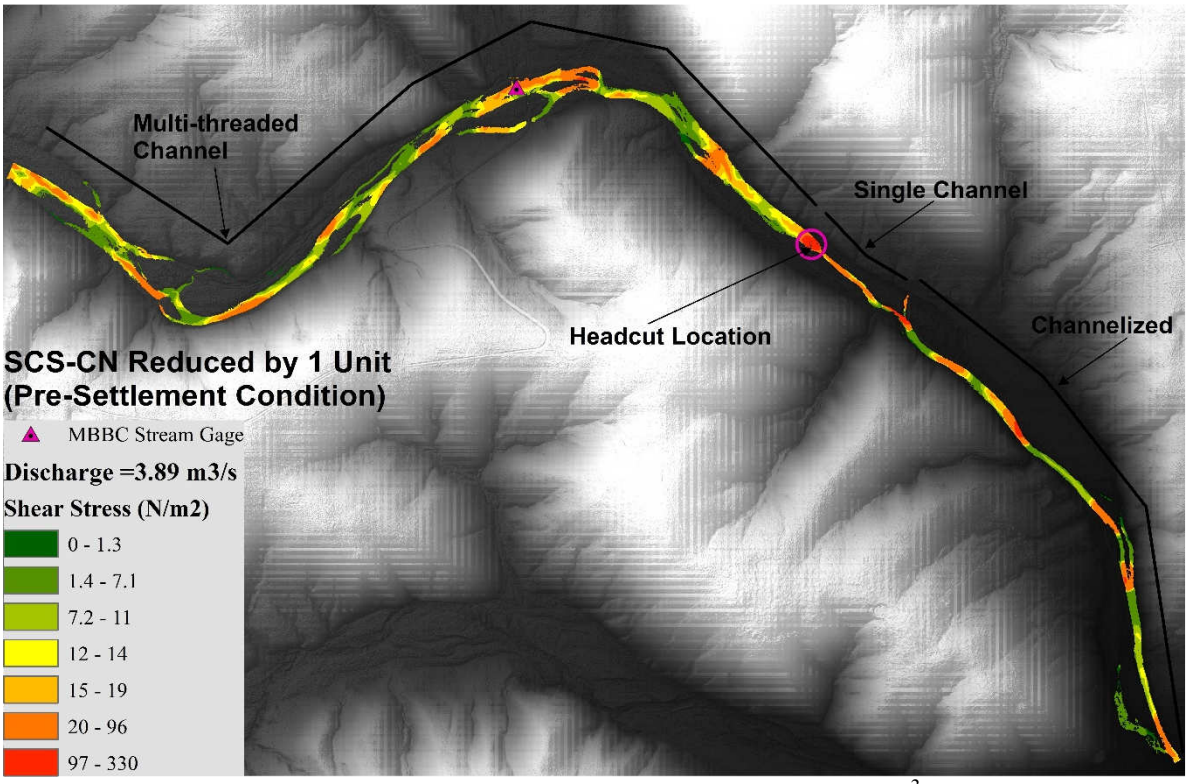

Appendix I-1. Channel's total shear stress distribution for Qp = 3.89 m^3/s discharge.

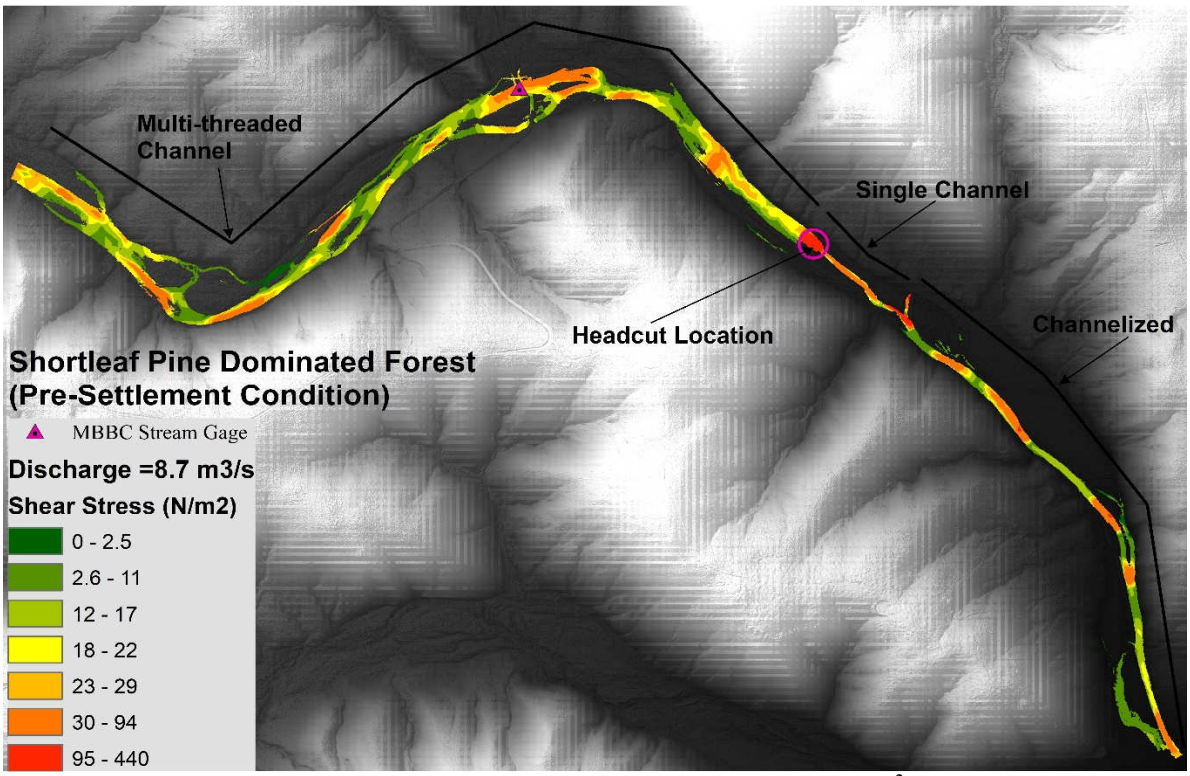

Appendix I-2. Channel's total shear stress distribution for Qp = 8.7 m^3/s discharge.

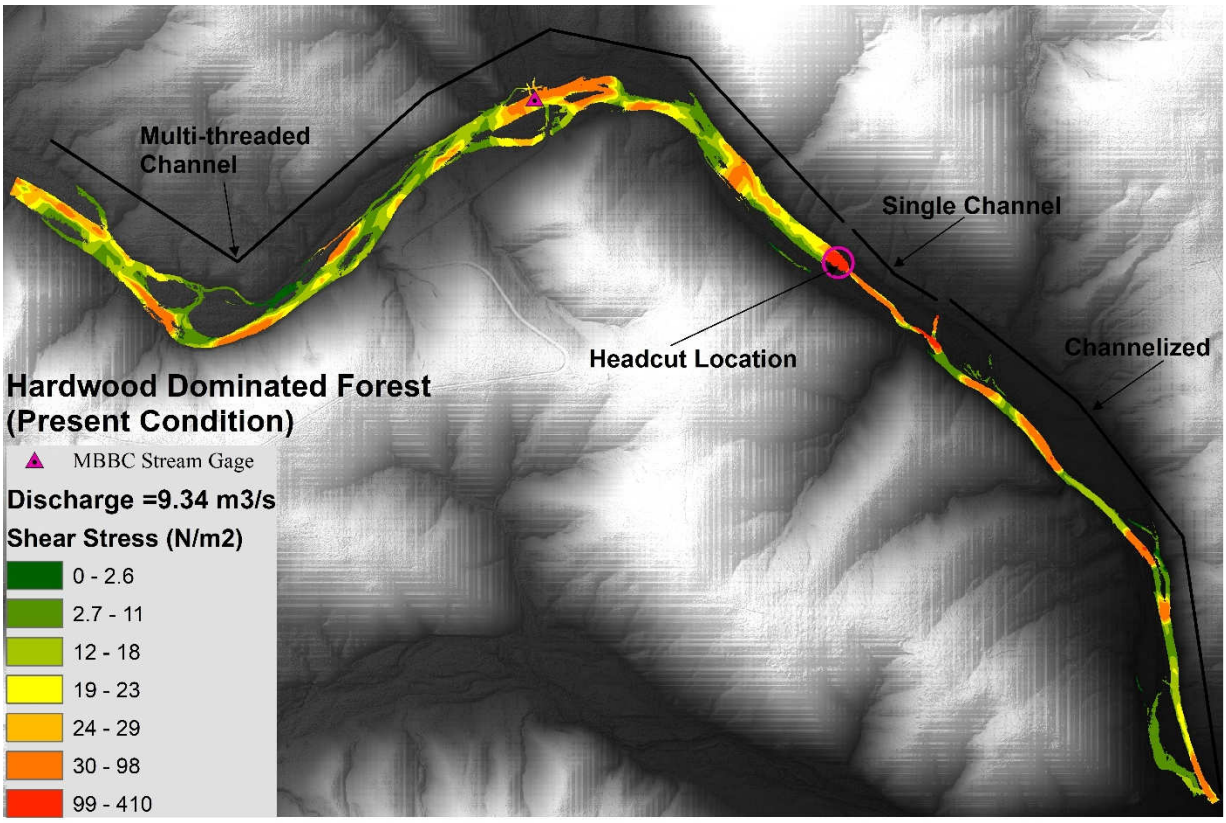

Appendix I-3. Channel's total shear stress distribution for Qp = 9.34 m^3/s discharge.

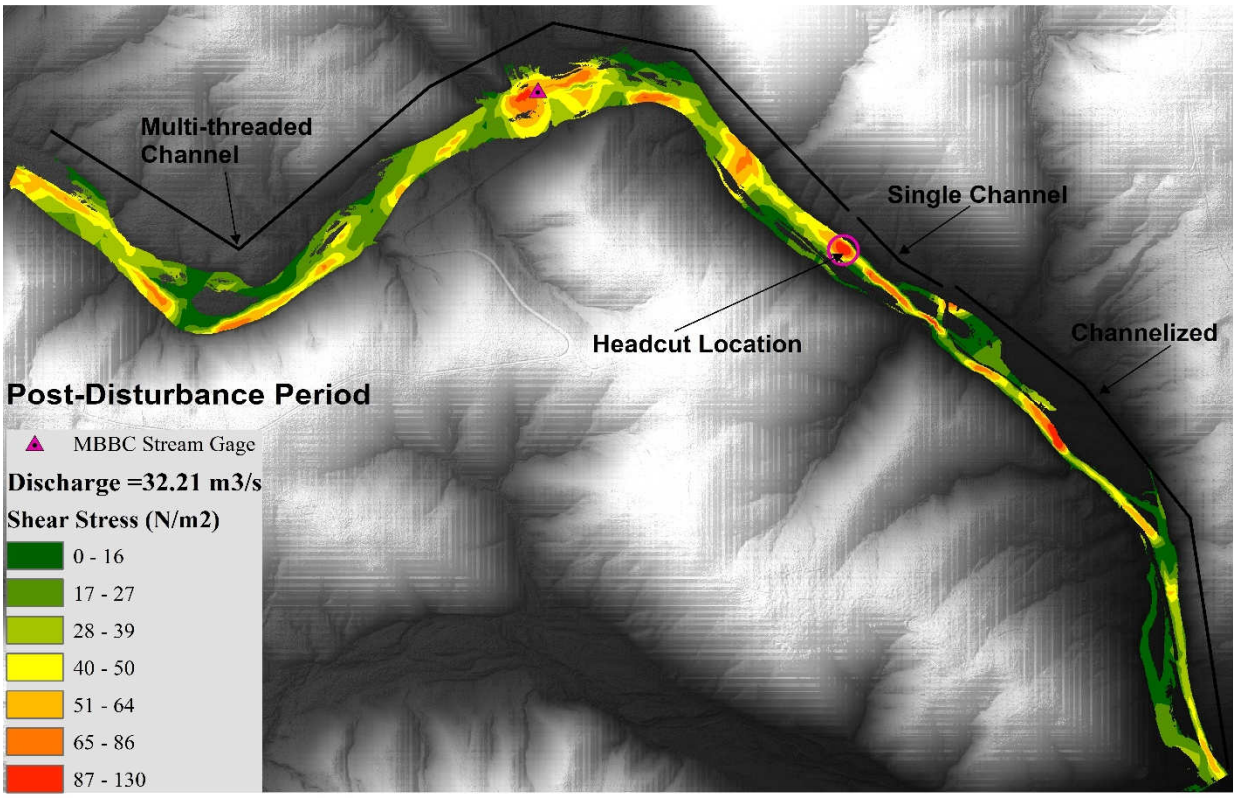

Appendix I-4. Channel's total shear stress distribution for Qp = 32.21 m^3/s discharge.

Appendix J. Channel total stream power distribution.

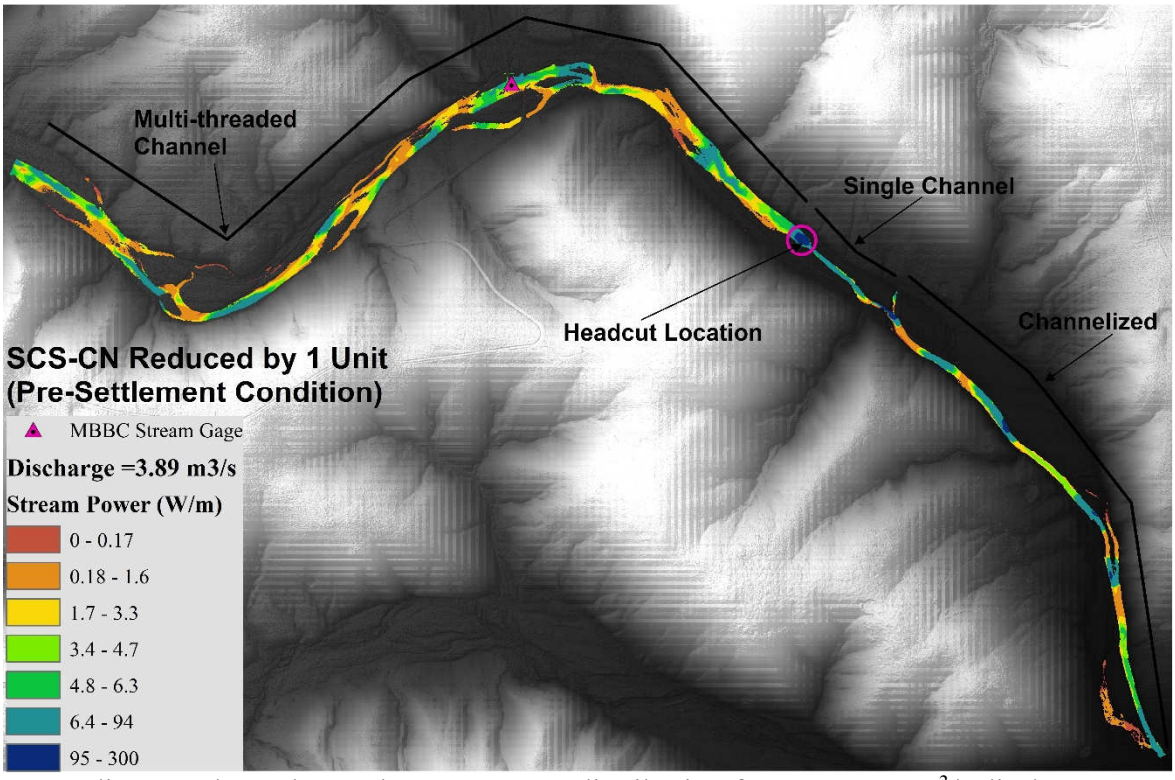

Appendix J-1. Channel's total stream power distribution for Qp = 3.89 m^3/s discharge.

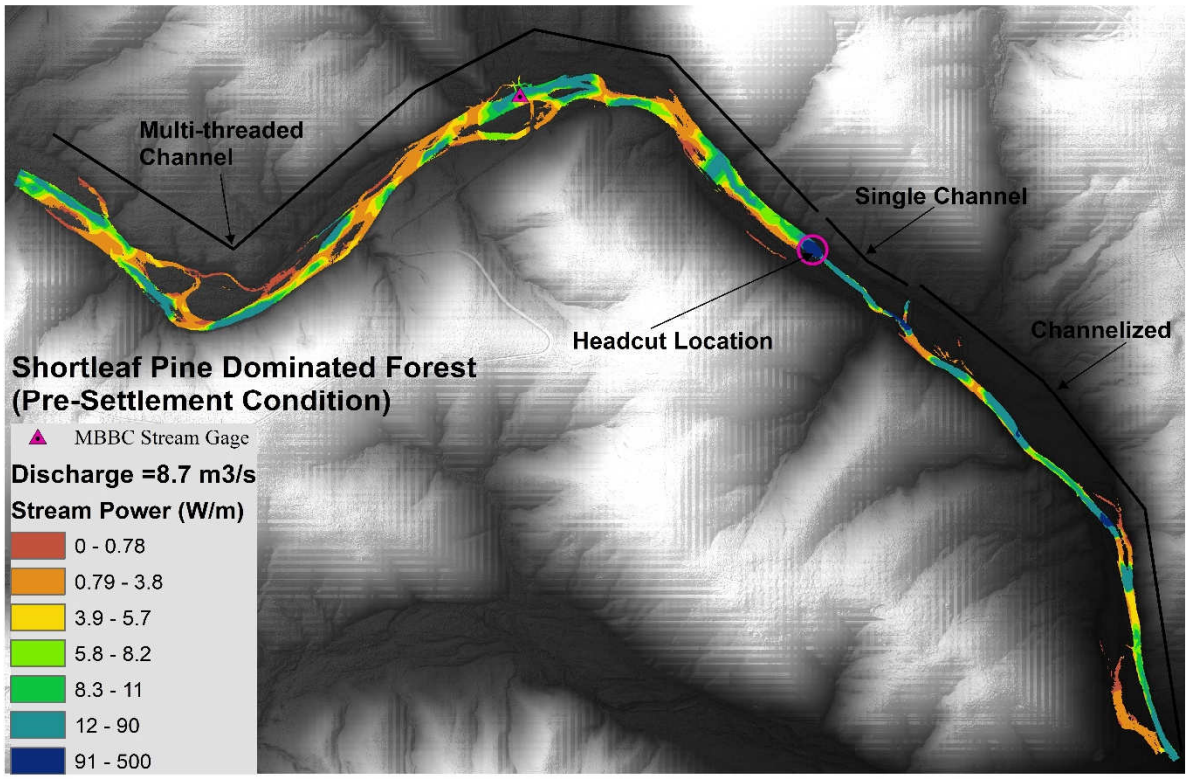

Appendix J-2. Channel's total stream power distribution for Qp = 8.7 m^3/s discharge.

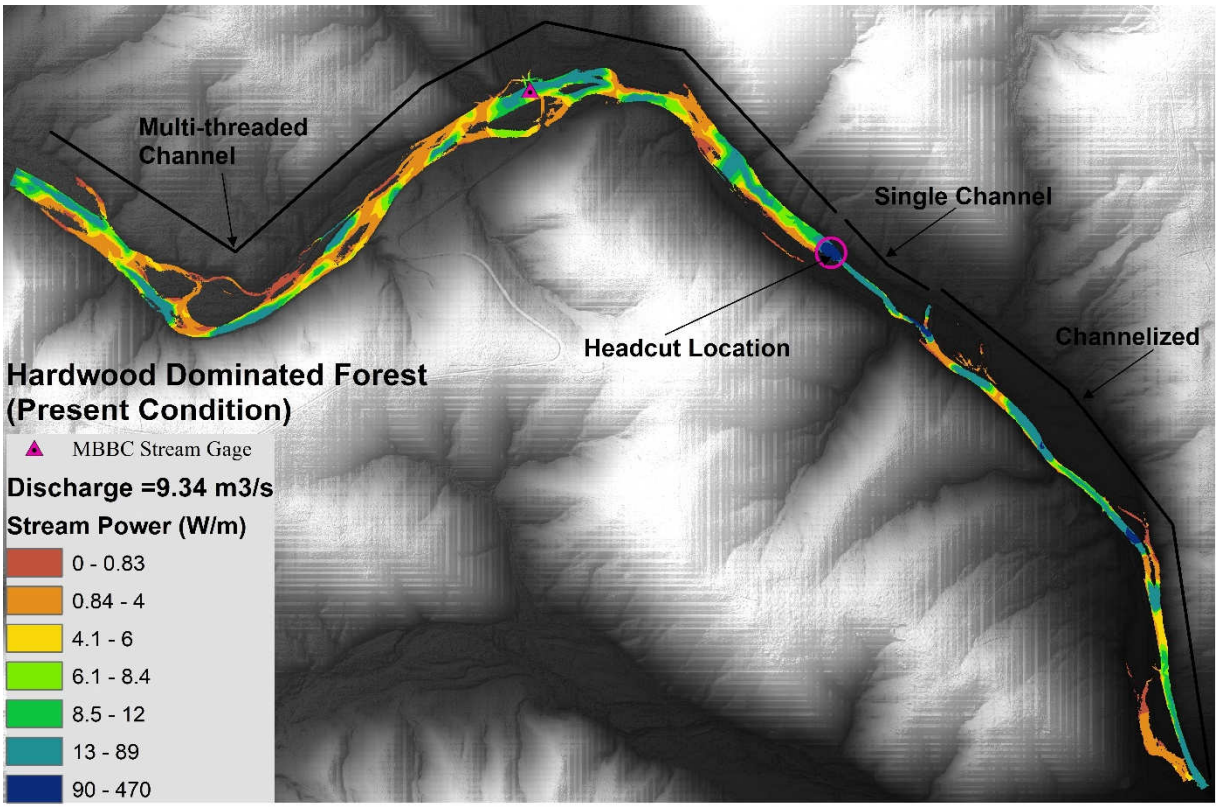

Appendix J-3. Channel's total stream power distribution for Qp = 9.34 m^3/s discharge.

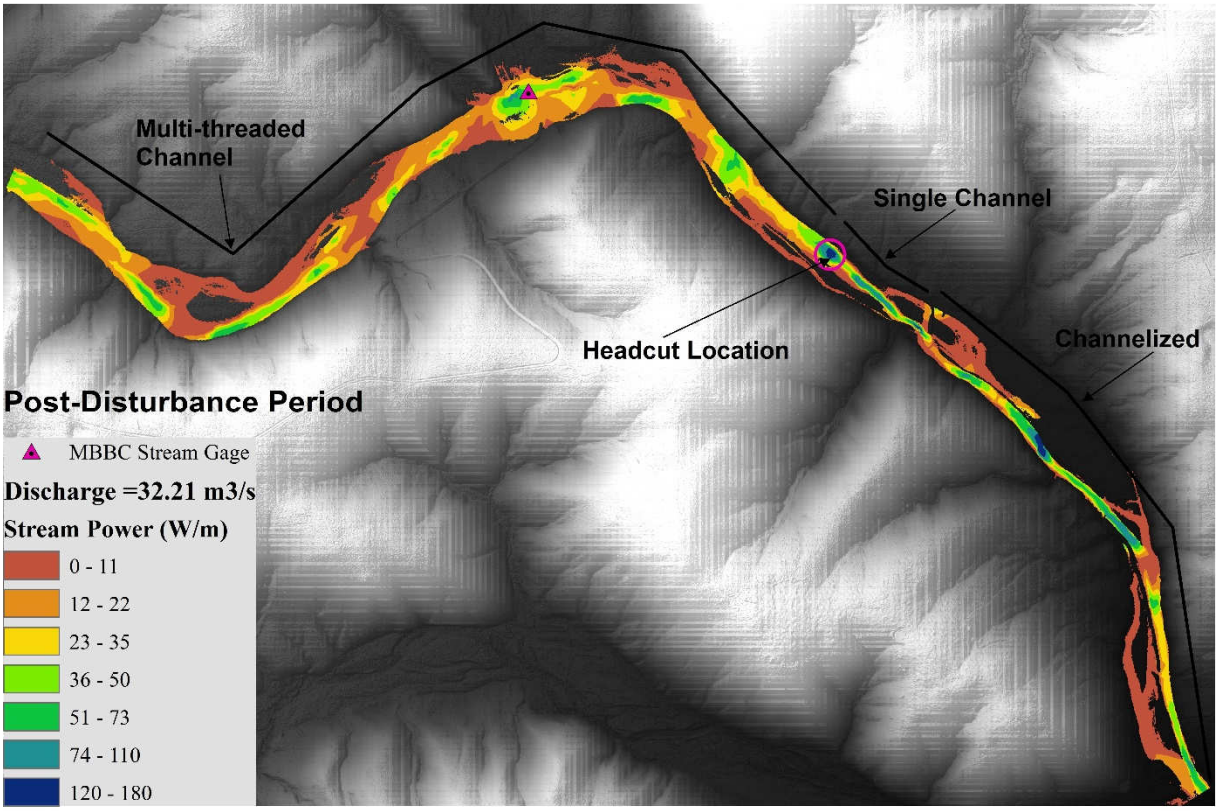

Appendix J-4. Channel's total stream power distribution for Qp = 32.21 m^3/s discharge.